

AD-A065 164

GEORGIA INST OF TECH ATLANTA ENGINEERING EXPERIMENT --ETC F/G 6/18
IN-VIVO DETERMINATION OF ENERGY ABSORPTION IN BIOLOGICAL TISSUE--ETC(U)
JAN 79 E C BURDETTE, F L CAIN, J SEALS

DAA629-75-6-0182

UNCLASSIFIED

ARO-13231.1-L

NL

1 OF 2
ADA
065164



DDC FILE COPY

ADA065164

FINAL TECHNICAL REPORT

PROJECT A-1755

LEVEL II

9
6.5

IN-VIVO DETERMINATION OF ENERGY
ABSORPTION IN BIOLOGICAL TISSUE

By

E. C. Burdette, F. L. Cain, and J. Seals

Prepared for

U. S. ARMY RESEARCH OFFICE

P. O. BOX 12211

RESEARCH TRIANGLE PARK, NORTH CAROLINA 27709

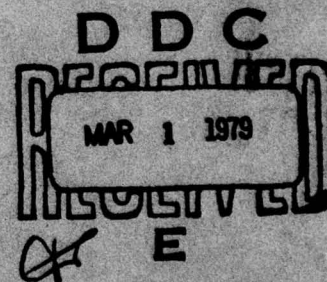
GRANT NO. DAAG29-75-G-0182

Submitted by

BIOMEDICAL GROUP

ELECTROMAGNETIC EFFECTIVENESS DIVISION

SYSTEMS AND TECHNIQUES LABORATORY



January 1979

GEORGIA INSTITUTE OF TECHNOLOGY

Engineering Experiment Station

Atlanta, Georgia 30332



DISTRIBUTION STATEMENT A

Approved for public release;
Distribution Unlimited

79 02 27 008

| REPORT DOCUMENTATION PAGE | | READ INSTRUCTIONS BEFORE COMPLETING FORM |
|---|---------------------------------|---|
| 1. REPORT NUMBER 13231.1-L | 2. GOVT ACCESSION NO. 18 ARO | 3. RECIPIENT'S CATALOG NUMBER 9 |
| 4. TITLE (and Subtitle) IN-VIVO Determination of Energy Absorption in Biological Tissue | | 5. TYPE OF REPORT & PERIOD COVERED Final Report 30 Jun 75 - 31 Dec 78 |
| 6. AUTHOR(s) E. C./Burdette, Fred E./Cain J./Seals | | 7. PERFORMING ORG. REPORT NUMBER |
| 8. CONTRACT OR GRANT NUMBER(s) 15 DAAG29-75-G-0182 | | 9. PROGRAM ELEMENT, PROJECT, TASK AREA & WORK UNIT NUMBERS |
| 10. CONTROLLING OFFICE NAME AND ADDRESS U. S. Army Research Office P. O. Box 12211 Research Triangle Park, NC 27709 | | 11. REPORT DATE 11 Jan 79 |
| 12. MONITORING AGENCY NAME & ADDRESS (if different from Controlling Office) 12 1040 | | 13. NUMBER OF PAGES 91 |
| 14. DISTRIBUTION STATEMENT (of this Report) Approved for public release; distribution unlimited. | | 15. SECURITY CLASS. (of this report) Unclassified |
| 15a. DECLASSIFICATION/DOWNGRADING SCHEDULE | | |
| 16. DISTRIBUTION STATEMENT (of the abstract entered in Block 20, if different from Report) | | |
| 17. SUPPLEMENTARY NOTES The view, opinions, and/or findings contained in this report are those of the author(s) and should not be construed as an official Department of the Army position, policy, or decision, unless so designated by other documentation. | | |
| 18. KEY WORDS (Continue on reverse side if necessary and identify by block number) Biological Tissue Energy Absorption Dielectric Properties IN VIVO Tissue Electrical Properties Electromagnetic Energy Radiation Hazards Living Tissues Living Tissue Power Absorption | | |
| 19. ABSTRACT (Continue on reverse side if necessary and identify by block number) The research efforts performed during this three-phase program have been successfully completed. Two different <u>in-vivo</u> probe techniques and their associated instrumentation were studied, the accuracy and repeatability of these techniques were evaluated, and a semi-automated data acquisition/data processing system was developed. One technique considered involved needle-like monopole probes of different lengths, and the second technique involved a dual-probe (two closely-spaced probes with extended center conductors) configuration. | | |

Mr. F
Engin
Georg
Atlan

PROGRESS REPORT

1. ARO PROPOSAL NUMBER: P-13231-L
2. PERIOD COVERED BY REPORT: 30 June 1975 through 30 December 1978
3. TITLE OF PROPOSAL: IN-VIVO Determination of Energy Absorption in
Biological Tissue
4. CONTRACT OR GRANT NUMBER: DAAG29-75-G-0182
5. NAME OF INSTITUTION: Georgia Institute of Technology
6. AUTHOR(S) OF REPORT: F.L. Cain, E.C. Burdette, and J. Seals
7. LIST OF MANUSCRIPTS SUBMITTED OR PUBLISHED UNDER ARO SPONSORSHIP DURING THIS PERIOD, INCLUDING JOURNAL REFERENCES:
Burdette, E.C., Seals, J., Toler, J.C., and Cain, F.L., "Preliminary In-Vivo Probe Measurements of Electrical Properties of Tumors in Mice," 1977 IEEE MTT-S International Microwave Symposium Digest, San Diego, California, June 1977, pp. 344-347.
Abstract of this paper was included as an appendix in the Second Annual Technical Report.
8. SCIENTIFIC PERSONNEL SUPPORTED BY THIS PROJECT AND DEGREES AWARDED DURING THIS REPORTING PERIOD:
- | | |
|---------------|--------------------------|
| F.L. Cain | V.E. Bernard |
| E.C. Burdette | A.S. Murray |
| J. Seals | J.A. Fay |
| H.A. Ecker | W.H. Warden |
| A.L. Stanford | A. Gonzalez |
| C.P. Burns | |
| M.L. Studwell | |
| E.S. Lowe | No degrees were awarded. |
| L.G. McKee | |
| J.R. Jones | |

Mr. Fred L. Cain
Engineering Experiment Station
Georgia Institute of Technology
Atlanta, GA 30332

13231-L

| | |
|---------------------------------|---|
| ACCESSION for | |
| NTIS | White Section <input checked="" type="checkbox"/> |
| DDC | Buff Section <input type="checkbox"/> |
| UNANNOUNCED | <input type="checkbox"/> |
| JUSTIFICATION..... | |
| BY..... | |
| DISTRIBUTION/AVAILABILITY CODES | |
| Dist. | AVAIL. and/or SPECIAL |
| A | |

79 02 27 038

FINAL TECHNICAL REPORT

PROJECT A-1755

IN-VIVO DETERMINATION OF ENERGY ABSORPTION
IN BIOLOGICAL TISSUE

BY

E.C. Burdette, F.L. Cain, and J. Seals

Biomedical Group
Electromagnetic Effectiveness Division
Systems and Techniques Laboratory
Engineering Experiment Station
Georgia Institute of Technology
Atlanta, Georgia 30332

Grant No. DAAG29-75-G-0182

January 1979

Prepared For

U.S. Army Research Office
P.O. Box 12211
Research Triangle Park, North Carolina 27709

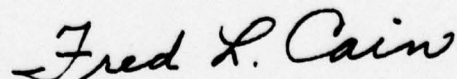
FOREWORD

The research on this three-phase program was carried out by personnel of the Biomedical Group of the Electromagnetic Effectiveness Division of the Systems and Techniques Laboratory of the Engineering Experiment Station at the Georgia Institute of Technology, Atlanta, Georgia 30332. Mr. F.L. Cain served as Principal Investigator. The program, which was sponsored by the U.S. Army Research Office (ARO), Research Triangle Park, North Carolina 27709, under Grant No. DAAG29-75-G-0182, was designated by Georgia Tech as Project A-1755.

This Final Technical Report covers the work which was performed from 30 June 1975 through 31 December 1978. As requested by the Chief of the Information Office at ARO, two comprehensive annual reports on results obtained during the first two phases of the this three-phase program were previously submitted. The results of those two reports are also summarized in this Final Technical Report; in addition, specific details are presented where appropriate.

This work was made possible through the combined efforts of many people at the U.S. Army Research Office, at the Medical College of Georgia, at the Emory University School of Medicine, and at the Georgia Institute of Technology. The authors would especially like to thank Dr. F.W. Morthland at ARO, Dr. A.M. Karow at the Medical College of Georgia, Mr. E.J. Malveaux at the Emory University School of Medicine, and Mr. J.R. Jones at Georgia Tech, all of whom contributed to the success of this research program.

Respectfully submitted,



Fred L. Cain
Principal Investigator

TABLE OF CONTENTS

| <u>Section</u> | <u>Page</u> |
|---|-------------|
| I. INTRODUCTION. | 1 |
| A. Research Objectives. | 2 |
| B. Summary of Phase I Efforts | 3 |
| C. Summary of Phase II Efforts. | 4 |
| D. Summary Phase III Efforts. | 5 |
| II. PROBE MEASUREMENT SYSTEM DEVELOPMENT. | 8 |
| A. Review of Dielectric Characteristics and Measurement Techniques | 8 |
| B. Theoretical Basis. | 10 |
| C. Measurement System | 12 |
| D. Microwave Measurement Error Correction and Calibration. | 16 |
| E. Probe Fabrication. | 20 |
| III. SEMI-AUTOMATED DATA ACQUISITION/DATA PROCESSING DEVELOPMENT AND TESTING | 23 |
| A. System Design Concept. | 23 |
| B. Hardware Selection | 25 |
| C. Hardware Interconnection and Operation | 28 |
| D. Evaluation of Accuracy and Speed of Hardware in the SDADP System | 32 |
| E. Software Development | 35 |
| 1. Initialization Subroutine | 36 |
| 2. Data Acquisition Subroutine | 38 |
| 3. Error Correction Subroutine | 40 |
| 4. Preliminary Test Results. | 40 |
| IV. SUMMARY OF EXPERIMENTAL RESULTS | 46 |
| A. Measurements of Standard Dielectric Materials. | 47 |
| 1. Sample-Size Effects | 48 |
| 2. Error Correction Model. | 52 |
| B. Investigation of Temperature and Drug Effects on Measured Dielectric Properties | 62 |
| C. Summary of In-Vivo Tissue Measurements | 75 |
| V. CONCLUSIONS | 84 |
| VI. RECOMMENDATIONS | 88 |
| VII. REFERENCES. | 89 |

LIST OF FIGURES

| <u>Figure</u> | | <u>Page</u> |
|---------------|--|-------------|
| 1. | Two configurations of the infinitesimal probe. | 14 |
| 2. | Block diagram of <u>In-vivo</u> Dielectric Property Measurement System consisting of probe, network analyzer, and associated instrumentation | 15 |
| 3. | Error models used for test set/connection errors | 18 |
| 4. | Calibration conditions used to determine directivity, source match, and frequency tracking errors. | 19 |
| 5. | Diagram of <u>in-vivo</u> measurement probe | 21 |
| 6. | Block diagram of prototype semi-automated data acquisition/data processing system | 27 |
| 7. | Flow chart of operational sequence of SDADP system | 29 |
| 8. | Interconnection diagram for components in SDADP system | 30 |
| 9. | Overall flow chart of software routines for semi-automated data acquisition/data processing system. | 37 |
| 10. | Theoretical linear relationship between frequency of signal from sweep generator and SWEEPOUT levels. | 39 |
| 11. | Unprocessed measured reflection coefficient amplitude data for deionized water at 23°C over the 2.0 - 4.0 GHz frequency range. | 53 |
| 12. | Unprocessed measured reflection coefficient phase data for deionized water at 23°C over the 2.0 - 4.0 GHz frequency range. | 54 |
| 13. | Measured reflection coefficient amplitude data for open circuit, short circuit, and three matched load terminations over the 2.0 - 4.0 GHz frequency range. | 56 |
| 14. | Measured reflection coefficient phase data for open circuit, short circuit, and three matched load terminations over the 2.0 - 4.0 GHz frequency range. | 57 |
| 15. | Printout of computed error correction terms and corrected water reflection coefficient data for FORTRAN program. | 58 |
| 16. | Relative dielectric constant of deionized water computed from corrected and uncorrected probe measurements compared to the range of dielectric constant data from reference sources. | 59 |
| 17. | Conductivity of deionized water computed from corrected and uncorrected probe measurements compared to the range of conductivity data from reference sources. | 60 |

| <u>Figure</u> | <u>Page</u> |
|---|-------------|
| 18. Measured relative dielectric constant of rat platelets in 20% plasma-RCD. | 64 |
| 19. Measured conductivity of rat platelets in 20% plasma-RCD | 65 |
| 20. Loss tangent of rat platelets in 20% plasma-RCD. | 66 |
| 21. Measured relative dielectric constant of human platelets in 20% plasma-RCD. | 67 |
| 22. Measured conductivity of human platelets in 20% plasma-RCD | 68 |
| 23. Loss tangent of human platelets in 20% plasma-RCD | 69 |
| 24. Measured reflection coefficient, (a) amplitude and (b) phase, of serially diluted concentrations of <u>E. coli</u> bacteria in distilled water over the 1.63 - 1.67 GHz frequency range | 73 |
| 25. Measured reflection coefficient (a) amplitude and (b) phase, of serially diluted concentrations of <u>E. coli</u> bacteria in distilled water over the 3.98 - 4.00 GHz frequency range | 74 |
| 26. Experimentally determined relative dielectric constant of <u>in-vivo</u> rat muscle and canine muscle compared to reference data [34]. | 77 |
| 27. Experimentally determined conductivity of <u>in-vivo</u> rat muscle and canine muscle compared to reference data [34]. | 78 |
| 28. Experimentally determined relative dielectric constant and conductivity of <u>in-vivo</u> and <u>in-vitro</u> canine kidney cortex compared to reference data [34]. | 79 |
| 29. Experimentally determined relative dielectric constant and conductivity of <u>in-vivo</u> canine fat tissue at 37°C. | 80 |
| 30. Experimentally determined relative dielectric constant and conductivity of <u>in-vivo</u> rat brain at 32°C. | 81 |
| 31. Experimentally determined relative dielectric constant and conductivity of rat blood at 23°C. | 82 |

LIST OF TABLES

| <u>Table</u> | | <u>Page</u> |
|--------------|--|-------------|
| I. | RESULTS OF TEST TO DETERMINE THE ACCURACY OF THE SDADP IN MEASURING FREQUENCY. | 43 |
| II. | RESULTS OF TEST TO EVALUATE THE OPERATING SPEED OF THE DATA ACQUISITION PROCESS. | 45 |
| III. | SAMPLE SIZE EFFECTS ON DIELECTRIC PROPERTIES OF DEIONIZED WATER MEASURED WITH INFINITESIMAL PROBE | 50 |
| IV. | SAMPLE SIZE EFFECTS ON DIELECTRIC PROPERTIES OF METHANOL MEASURED WITH INFINITESIMAL PROBE | 51 |
| V. | RELATIVE DIELECTRIC CONSTANT AND CONDUCTIVITY (mmho/cm) OF WATER COMPUTED FROM CORRECTED MEASUREMENTS | 61 |
| VI. | SUMMARY OF Me ₂ SO EFFECTS ON THE DIELECTRIC CHARACTERISTICS OF CANINE KIDNEY CORTEX | 71 |

SECTION I

INTRODUCTION

The research presented in this Final Report is the conclusion of efforts initiated during the first two years of the program. Comprehensive annual reports [1,2] detailing the results of the investigations performed during the first two years were submitted previously; consequently, only those aspects of previously performed research pertinent for clearly illustrating current results will be included in this report. The basic purpose of the overall research investigation was to study and develop an in-vivo measurement technique for determining dielectric properties of living tissues over a wide range of frequencies from which power absorption may be calculated. The successful conclusion to this development is important because dosimetry that is based on an accurate knowledge of in-vivo tissue electrical properties is of paramount importance both in beneficial medical applications of electromagnetic (EM) energy [3-7] and in the determination of radiation hazards with respect to personnel safety [8,9].

Many attempts to determine power absorbed in living tissues have been made through the measurement of power entering and leaving an enclosed cavity in which an animal is placed as well as by implanting various types of probes in the animal (or tissue sample) either to measure the temperature of the tissue or to measure directly the internal field intensity. Although many techniques have been investigated, no one suitable well-accepted technique has been developed. The problem that plagues most investigators who attempt to use probes for direct internal field measurement is that of direct interaction with the applied EM field. Conventional thermocouples and thermistors have proven to be generally unusable [10], and although other probes have been developed which minimize the interaction with incident EM fields [11,12], their usefulness is not only confined to somewhat limited temperature ranges, they must also be calibrated before

each use. Further, only one of these probes is commercially available at this time.

Although direct minimally perturbing temperature and EM field measurement techniques are currently under investigation, another approach would be to develop a realistic analytical model capable of accurate dosimetry determination for complex and arbitrary geometries upon which arbitrary field configurations are incident [13]. Such a model would require extensive experimental validation, but once completed, the model could provide extremely useful data in a very short time period which would result in a significant savings over the costs in time and equipment to obtain the same information experimentally. However, the most important factor both in direct field and temperature measurements and in analytical modelling is a knowledge of the in-vivo electrical properties of the tissues under study. Because the power absorption associated with electromagnetic exposure of tissue depends on the electrical properties of the tissue, it is important that these properties be known in-vivo rather than in-vitro and over a wide range of frequencies rather than at a few "spot" frequencies.

A. Research Objectives

The objectives of this research program are to investigate and develop a simple, flexible, and accurate method for determining the dielectric properties and power absorption of living tissues over a wide frequency range extending from the VHF region well into the microwave region (≤ 10 GHz) and to use this method to obtain basic data for various tissues over this wide frequency range. The efforts in this program are directed toward the analysis and development of a suitable probe for performing in-vivo dielectric measurements over the frequency range from 100 MHz to 10 GHz or above, which in turn will permit the calculation of microwave absorption characteristics of various tissues. Specific areas of investigation include (1) extension of the frequency range of the probe, (2) elimination of sample volume effects on measured data, (3) development of swept frequency measurement techniques which permit performing rapid measurements, (4) determination of probe accuracy, (5) development of a simple measurement procedure, and (6) determination of

the in-vivo electrical properties of various tissues. A long term objective would be to utilize these results in the detection and treatment of cancer, in the establishment of an electromagnetic radiation safety level with respect to personnel, and in the eventual development of a radiation simulator with direct readout of power absorption.

B. Summary of Phase I Efforts

The investigations performed under Phase I were carried out during the first year of this research program and are detailed in the first Annual Report [1]. The primary tasks performed during the first year of the program were (1) mathematical investigations to confirm the validity of existing equations, (2) extension of the theoretical aspects of the single monopole probe technique to the microwave frequency range, (3) limited measurements on standard materials and in-vitro tissues, and (4) limited investigation of a needle-like dual probe technique for power absorption measurement. Once the validity of the antenna modeling theorem upon which the probe development is based was confirmed, a series of single (needle-like) monopole probes were fabricated and tested at UHF and microwave frequencies. Since the validity of the probe impedance expression was dependent upon both the probe length as it appears in the medium and the probe's length to diameter ratio, it was found that even probes as short as 0.49 cm were limited to an upper useful frequency of approximately 1.0 GHz in tissue. This led to the initial development of an infinitesimal monopole probe which has an impedance which is entirely capacitive. This probe was used for measurements of certain standard dielectric materials at frequencies up to 4.0 GHz and in-vivo canine kidney tissue up to 2.0 GHz. A second probe measurement technique which could possibly be used for direct power absorption measurements was also briefly investigated. This dual probe technique employed two needle-like probes, tightly coupled electrically, one of which is used for transmitting and one for receiving. The results obtained using both probe measurement techniques for measurements of standard dielectric materials and in-vitro tissue were extremely encouraging.

C. Summary of Phase II Efforts

The investigations performed under Phase II were carried out during the second year of the program and are detailed in the second Annual Report [2]. The primary research efforts performed during the second year were directed toward (1) further development of the in-vivo infinitesimal monopole measurement probe and instrumentation, (2) frequency extension to 10 GHz or higher, (3) determination of the measurement accuracy of the probe/instrumentation through detailed measurements of standard dielectric materials, and (4) in-vivo measurements of a number of tissue types including muscle, kidney, brain, and blood as well as six malignant tumor lines. Further development of the infinitesimal monopole measurement probe included (1) the verification of the analytical treatment of the probe in which it was viewed essentially as an open-circuited coaxial line whose impedance is totally reactive and (2) the determination of the radiation conductance fringing field of the probe. The effects of sample size variation were also investigated, and it was determined that even very small sample volumes of 0.03 in^3 (0.5 cm^3) could be accurately measured because the fringing field from the small 0.085-inch diameter probe placed against lossy tissue was essentially negligible.

Investigations were also conducted to extend the usable frequency range of the probe above that achieved in the first year's efforts and to initiate the development of swept-frequency measurement techniques. These efforts resulted in the extension of the usable frequency range of the probe to above 10 GHz and in improvements in the measurement instrumentation and in the data processing techniques. Sources of measurement errors at microwave frequencies were analyzed, and through a first iteration, the instrumentation was improved to minimize these errors.

The accuracy of the in-vivo electrical property measurement system, consisting of the infinitesimal monopole probe and the impedance measurement instrumentation, was determined over the 100 MHz to 10 GHz frequency range through a series of measurements using standard

dielectric materials. These materials included water, methanol, ethylene glycol, and two different saline solutions. Not only were the results good, but the repeatability of these measurements was also determined with a resulting standard-error-of-the-mean (SEM) of only a few percent over the entire frequency range.

Finally, both the in-vitro and in-vivo measurements of several tissues were also performed. These included in-vitro and in-vivo canine kidney tissue measurements, in-vivo canine muscle and fat measurements, in-vivo rat muscle, brain, and blood measurements, and measurements of six strains of subcutaneously transplanted tumors (mammary, glioma, carcinoma -- two types of each) in mice. These measurements have yielded data that heretofore have been unavailable.

D. Summary Phase III Efforts

The overall research program under this grant was initiated as a three-phase, three-year program. However, the third phase of the research was extended an additional six months through a no-cost time extension to permit the study and design of a semi-automated data acquisition and processing system to be used in conjunction with the in-vivo probe measurement technique. The tasks performed during the third phase of the grant include the implementation of a microprocessor-based data acquisition/data processing system, the investigation of microwave measurement error correction techniques suitable for use with the probe measurement system, investigation of probe design factors which limit measurement accuracy, and further probe dielectric measurements. These efforts are summarized below.

An investigation of the problems associated with data acquisition and processing of in-vivo probe measurements led to the conclusion that a microprocessor-based, automated or semi-automated system was needed to increase the speed and to minimize the human involvement in the data collection process. In Phases I and II, data resulting from in-vivo probe measurements were obtained either by recording the information from a network analyzer phase/magnitude display or by extracting the experimental values from swept-frequency X-Y recordings. Both of these

data collection processes are tedious, time-consuming, and vulnerable to human error.

Because of these limitations with manual data collection and processing, a semi-automated data collection and processing system was designed around a Commodore PET computer which uses a MOSTEK 6502 microprocessor. This data acquisition system permits rapid, accurate, data collection and at the same time also permits correction of the inherent directivity, source match, and frequency tracking microwave measurement errors present in the measured data. The system automatically collects measured reflection coefficient data from the probe, processes these data, and outputs computed dielectric property data. Measurements are made over swept-frequency bands of 0.1 to 1 GHz, 1 to 2 GHz, 2 to 4 GHz, 4 to 6 GHz, 6 to 9 GHz, and 9 to 12 GHz. The semi-automated data acquisition system samples swept measurements at 10 to 20 discrete frequencies per sweep band and records the resulting dielectric data on magnetic tape. Manual data collection required pulling points from a graph by hand, and typically, data were processed for only 5 to 8 frequencies per band. The resolution of the semi-automated system exceeds that attainable by reading points off graphs. The present data acquisition system measures the amplitude of the reflection coefficient to within about 0.04 dB and phase to within about 0.2 degrees. Further, the system is automated to the extent that the only human involvement is in the initializing of parameters, the interchanging of program and data tapes, and the handling of probes, calibration terminations, and test samples.

In addition to the implementation of computerized data acquisition techniques, efforts were directed toward minimizing the effects of residual microwave measurement errors associated with the network analyzer measurement system. An error correction model which reduces microwave measurement errors (directivity, source match, frequency tracking) associated with reflection measurements was developed and added to the microprocessor-based semi-automated system. The data processing is performed in two steps. First, the calibration/error correction algorithm involves measurements of terminations (short

circuits, open circuits, and matched loads) for which the reflection coefficients are known. From these data, the error correction model computes the different measurement error terms and then uses these terms to correct the raw data by solving for the value of the reflection coefficient which would have been measured had none of the errors been present. Second, the corrected experimental data are processed by an algorithm which computes the dielectric properties of the sample under test. Both the error correction terms and computed dielectric properties are displayed on the CRT and can be stored on magnetic tape for later retrieval.

During Phase III, attention has also been given to probe design factors and fabrication techniques. Probe fabrication techniques are extremely important in the overall probe design. Errors in measurement accuracy have resulted from factors such as imperfect attachment of connectors and even from minor variations in the materials used for the probe itself. These factors have also resulted in limitations on the useful frequency range of several probe designs. In an effort to minimize degradation of probe performance, extreme care was taken during the fabrication process to ensure proper connector attachment, extremely smooth contact surfaces, and a number of other factors which are detailed in Section II. Gold and nickel plating were also employed to minimize possible probe/sample chemical interactions and to reduce possible electrode polarization effects at the lower frequencies.

Finally, additional measurements of lossy dielectric materials were performed as part of the investigation of probe design factors, fabrication techniques, and evaluation of the semi-automated data acquisition/data processing system. Probes of different sizes, including a probe having a diameter comparable to that of a No. 18 hypodermic needle, were evaluated via measurements of deionized water and other standard liquid dielectrics. A limited number of tissue measurements were performed, and these are summarized together with measurements performed during earlier phases in Section IV.

SECTION II

PROBE MEASUREMENT SYSTEM DEVELOPMENT

In this section, the development of the in-vivo dielectric property measurement system, consisting of the probe and the associated instrumentation, is discussed. First a brief review of different measurement techniques is presented. This is followed by a discussion of the theoretical basis of the in-vivo measurement probe and a description of microwave measurement errors associated with reflectometer measurements. A method for measurement error correction is presented, and finally, probe design factors and fabrication techniques are discussed.

A. Review of Dielectric Characteristics and Measurement Techniques

The interaction of EM fields with tissue is highly dependent upon the dielectric properties of the tissue. These properties are often expressed in terms of the complex permittivity, $\epsilon^* = \epsilon' - j\epsilon''$. This parameter is a complex mathematical quantity whose real part ϵ' is conventionally expressed relative to the permittivity of free space ϵ_0 by the ratio ϵ'/ϵ_0 , which is the relative dielectric constant K' . The imaginary part ϵ'' of the complex permittivity is the loss factor which is equal to the product $\epsilon'\tan\delta$, where $\tan\delta$ is defined to be the loss tangent of the material. It can be seen that $\tan\delta = \epsilon''/\epsilon'$. The conductivity σ of a material is usually defined as $\sigma = (2\pi f)\epsilon'\tan\delta$, where f is the frequency in hertz.

The relative dielectric constant of a material influences the velocity and the wavelength of an EM wave propagating through that material. It also influences the amount of energy that can be stored in a dielectric medium. The loss tangent ($\tan\delta$) influences the attenuation of an EM field propagating through that medium and is associated with the amount of energy that can be dissipated in a medium as heat [14]. The differences between the dielectric properties of free space and tissue can be attributed to the presence of various polarization mechanisms in the tissue. A large number of polarizable elements

results in a large dielectric constant and vice versa.

Measurement techniques that may be utilized to determine tissue dielectric properties are based upon measuring the effects of these polarization mechanisms at a specific frequency. Several standard techniques for measuring tissue dielectric properties utilize impedance bridges, resonant circuits, transmission lines/waveguides, and resonant cavities. A detailed analysis of these techniques [15,16] indicates that only transmission line/waveguide techniques can be utilized over a relatively wide band of frequencies for a single physical configuration. Most tissue measurements in the past have been performed using transmission line techniques.

Although the short-circuited coaxial transmission line and waveguide techniques have been the most widely used for tissue dielectric measurements, a number of features of these techniques make them less than optimal for determining the dielectric characteristics of tissues. First, standard methods require the excision of the tissue sample to be measured. Second, the exact dimensions of the sample are critical to the computation of correct dielectric information. In the case of waveguide measurements, the tissue samples are often diced, ground, chopped, etc., and then placed or even poured into the waveguide sample holder [17]. However, the accuracy of the measured data is affected by factors such as sample surface smoothness. Similar problems also exist for the case of coaxial transmission line measurements except that the sample size is often significantly smaller than that required for waveguide measurements. However, it is not possible to obtain in-vivo data using the above measurement techniques.

Recently, techniques suitable for in-vivo dielectric property measurements have been reported. Initial investigations at Georgia Tech [18] resulted in the investigation of an in-vivo measurement technique which is based upon an antenna modeling theorem. The measurement technique employed a monopole probe approximately one centimeter in length which appeared as an electrically-short antenna over the 0.01 - 0.1 GHz operating range of the measurement system. At higher frequencies, the technique was not suitable because the short monopole

impedance expression used to describe the terminal impedance of the antenna was no longer valid.

An additional technique which has been used for performing in-vivo measurements of skin is referred to as an "open transmission line resonator" and is based on changing the resonance of a stripline circuit by perturbing the fringing field of an open-ended transmission line [19]. This technique, however, is limited to measurements of tissues that contact the surface. Further, because the area occupied by the 1.5-cm diameter transmission line is so great, insertion into tissue is impossible. A truly in-vivo probe measurement technique capable of performing accurate dielectric measurements over a wide frequency range did not result until the work initiated under this ARO grant was performed.

B. Theoretical Basis

The theoretical basis of the in-vivo measurement probe stems from the application of an antenna modeling theorem to the characterization of unknown dielectric media [20]. For short monopole probes, the radiated power depends directly upon the extended length of the center conductor of the probe. When the length of the probe is approximately one-tenth wavelength, factors such as penetration depth in the medium under study at a given frequency must be considered along with other factors such as significant changes in relative probe length in high dielectric media, because the wavelength is smaller in media other than air. Further, care must be taken to ensure the validity of the analytical impedance expression for the probe when it is inserted into a lossy dielectric medium. When the length of the probe becomes infinitesimally short, the impedance becomes entirely reactive, and the above factors become less important because they do not cause a problem. In either case, the antenna modeling theorem is valid. In a non-magnetic medium where $\mu = \mu_0$, the antenna modeling theorem can be expressed mathematically as

$$\frac{Z(\omega, \epsilon^*)}{\eta} = \frac{Z(n\omega, \epsilon_0)}{\eta_0}, \quad (1)$$

results in a large dielectric constant and vice versa.

Measurement techniques that may be utilized to determine tissue dielectric properties are based upon measuring the effects of these polarization mechanisms at a specific frequency. Several standard techniques for measuring tissue dielectric properties utilize impedance bridges, resonant circuits, transmission lines/waveguides, and resonant cavities. A detailed analysis of these techniques [15,16] indicates that only transmission line/waveguide techniques can be utilized over a relatively wide band of frequencies for a single physical configuration. Most tissue measurements in the past have been performed using transmission line techniques.

Although the short-circuited coaxial transmission line and waveguide techniques have been the most widely used for tissue dielectric measurements, a number of features of these techniques make them less than optimal for determining the dielectric characteristics of tissues. First, standard methods require the excision of the tissue sample to be measured. Second, the exact dimensions of the sample are critical to the computation of correct dielectric information. In the case of waveguide measurements, the tissue samples are often diced, ground, chopped, etc., and then placed or even poured into the waveguide sample holder [17]. However, the accuracy of the measured data is affected by factors such as sample surface smoothness. Similar problems also exist for the case of coaxial transmission line measurements except that the sample size is often significantly smaller than that required for waveguide measurements. However, it is not possible to obtain in-vivo data using the above measurement techniques.

Recently, techniques suitable for in-vivo dielectric property measurements have been reported. Initial investigations at Georgia Tech [18] resulted in the investigation of an in-vivo measurement technique which is based upon an antenna modeling theorem. The measurement technique employed a monopole probe approximately one centimeter in length which appeared as an electrically-short antenna over the 0.01 - 0.1 GHz operating range of the measurement system. At higher frequencies, the technique was not suitable because the short monopole

where $\omega = 2\pi f$ = angular frequency (radians),

$\eta = \sqrt{\mu_0/\epsilon^*}$ = the complex intrinsic impedance of the dielectric medium,

$\eta_0 = \sqrt{\mu_0/\epsilon_0}$ = the intrinsic impedance of free space, and

$n = \sqrt{\epsilon^*/\epsilon_0}$ = the complex index of refraction of the medium relative to that of air.

This theorem is valid as long as the probe's field is contained completely within the medium and the analytical expression which describes the probe impedance is the same, in both the medium and free space. For a short monopole antenna, the impedance is given by [21]

$$Z = A\omega^2 + \frac{1}{jC\omega} \quad , \quad (2)$$

where A and C are physical constants determined by the probe dimensions. Utilizing the form of antenna impedance given in Equation (2) in the modeling theorem of Equation (1) and redefining the complex index of refraction n in terms of the loss tangent of the medium, it is possible to obtain a pair of equations in two unknowns which can be iteratively solved. This analysis is presented in detail in the first Annual Technical Report [1].

To determine the dielectric properties of small sample volumes, it is necessary to use a probe having very poor radiation efficiency. For the case of the infinitesimal probe where the extended length approaches zero, the impedance is a totally reactive complex capacitance. In that case, the radiation resistance R_r of the probe is zero and no power ($P_r = I_r^2 R_r$) is radiated. This is more clearly illustrated by examining the radiation resistance of the monopole expressed in terms of the length of the probe as

$$R_r \text{ (monopole)} = 40\pi^2 \left(\frac{\ell}{\lambda}\right)^2 \quad , \quad (3)$$

where λ is the wavelength and l is the length of the monopole [21]. By expressing the terminal impedance of the probe in the form

$$Z = R_r - jX, \quad (4)$$

it can be seen that as $R_r \rightarrow 0$, the probe impedance becomes

$$Z = -jX, \quad (5)$$

where Z is totally reactive (X is the reactance).

The infinitesimal monopole probe looks like an open-circuited coaxial line which has been previously analyzed [22-24]. The impedance of an open-circuited line is

$$Z = \frac{1}{j\omega C^*}, \quad (6)$$

where $C^* = \epsilon^*C$ and C is as defined in Equation (2). Expanding this impedance expression in the antenna modeling theorem yields the result

$$Z(\omega, \epsilon) = \frac{1}{j\omega C[K'(1 - j\tan\delta)]}, \quad (7)$$

which is the same expression as the imaginary part of Equation (5) in the First Annual Technical Report [1]. Therefore, for the case of an open-circuit transmission line, the antenna modeling theorem reduces to Equation (7). A somewhat more extensive treatment of the infinitesimal probe opening onto a ground plane is presented in the Second Annual Technical Report [2].

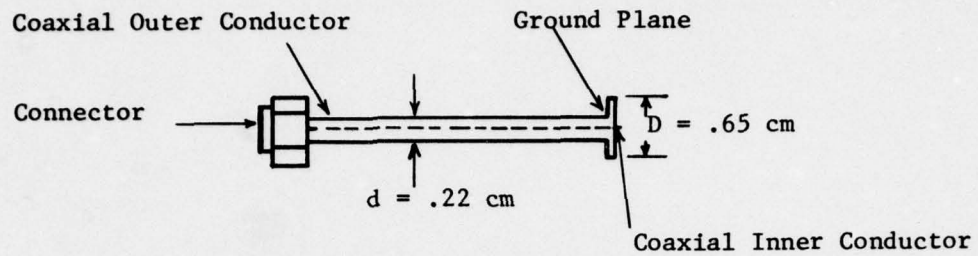
C. Measurement System

A number of probe configurations have been investigated during the course of this three-phase research program. These probes have ranged

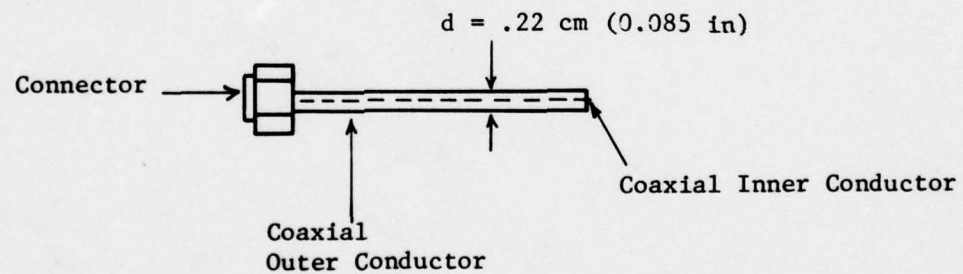
in length from infinitesimal probes of essentially zero length to probes 1 cm in length. Probes have been fabricated which range in diameter from the size of a #18 hypodermic needle to 0.141-inch diameter semi-rigid coaxial cable. Several infinitesimal monopole measurement probes have been fabricated from 0.085-inch diameter semi-rigid coaxial cable. The two basic probe configurations which have been used most extensively are schematically illustrated in Figure 1. Both probes are fabricated from 0.085-inch diameter semi-rigid coaxial cable which was disassembled, gold plated, and then reassembled. If a circular ground plane, such as the one illustrated in Figure 1(a), was attached to the probe, this was done before plating and reassembly. Probes of this type as well as probes which have smaller and larger diameters were used to perform in-vivo dielectric measurements of tissues.

The instrumentation used to measure the impedance of the measurement probe was identical to that described in the previous Annual Technical Reports [1,2]. The measurement system consists basically of a reflectometer and a network analyzer (Hewlett-Packard 8410B). The network analyzer measures the complex reflection coefficient data which are subsequently used as input data to a computer algorithm which computes the dielectric property information. During Phase III of the program, a semi-automated microcomputer-based data acquisition/data processing system was designed and implemented. The computer algorithm for computing dielectric properties from in-vivo probe measurements now resides in the microcomputer. An overall block diagram of the measurement system, including the data acquisition interface and microcomputer, is shown in Figure 2. The system operates as follows:

1. A sweep band is selected between 0.1 GHz and 10.0 GHz,
2. The endpoint frequencies are logged into the microcomputer,
3. The sweep is manually triggered and the data acquisition system samples the amplitude and phase of the reflection coefficient at any desired number (up to 40) of equally-spaced frequencies within the sweep band,
4. The measured data are stored temporarily in memory and from there are processed to yield dielectric property information, and
5. The results are displayed on a CRT screen and are stored on magnetic tape for later use.



(a) Monopole dielectric measurement probe with ground plane.



(b) Monopole dielectric measurement probe without ground plane.

Figure 1. Two configurations of the infinitesimal probe.

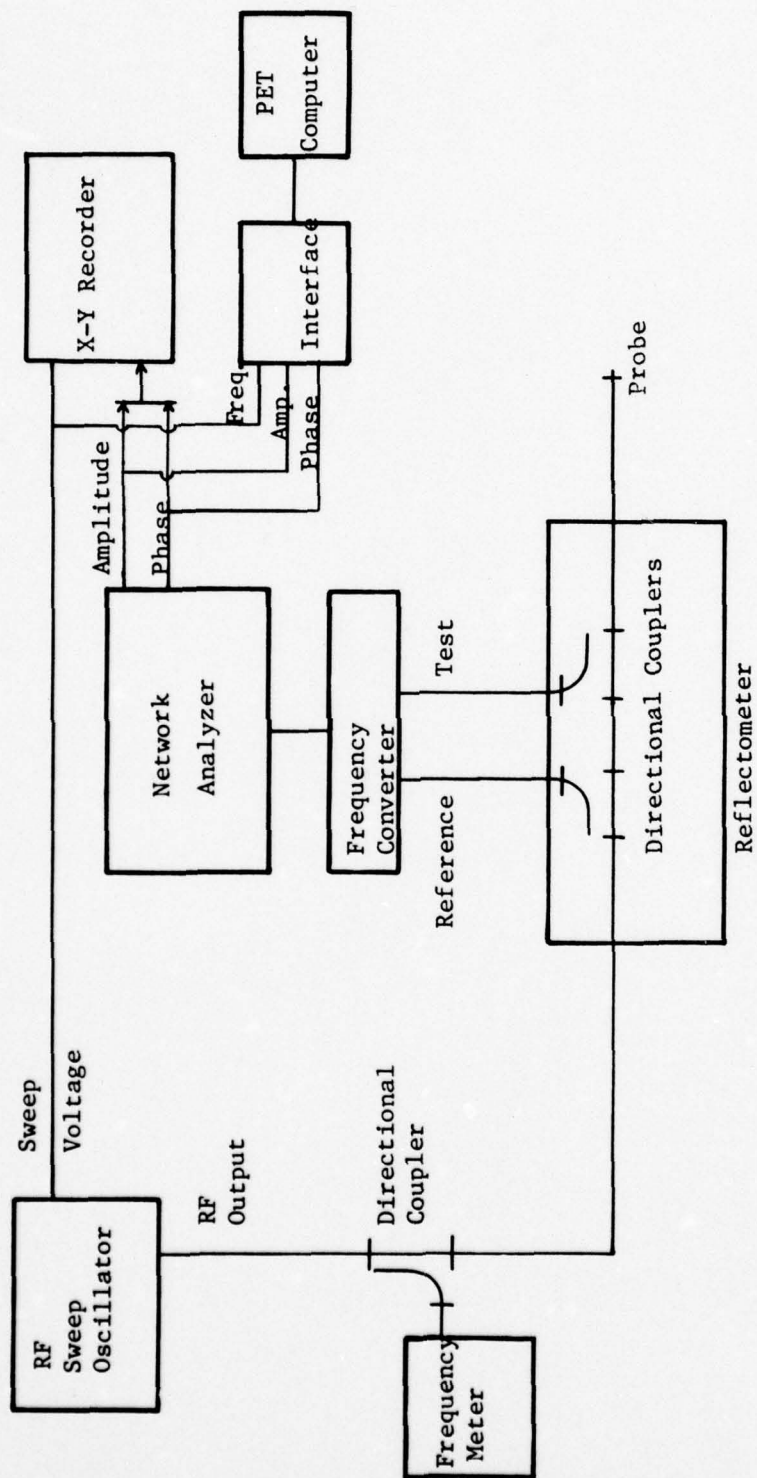


Figure 2. Block diagram of In-Vivo Dielectric Property Measurement System consisting of probe, network analyzer and associated instrumentation.

The data acquisition/data processing system is described in detail in the following section. However, at this point it should be noted that the data processing includes a calibration/error correction routine which takes into account and corrects for systemic measurement errors associated with the network analyzer system.

D. Microwave Measurement Error Correction and Calibration

As described in the Second Annual Technical Report [2], measurement errors associated with the network analyzer can be separated into two categories: instrument errors and test set/connection errors. Instrument errors are measurement variations due to noise, imperfect conversions in such equipment as the frequency converter, crosstalk, inaccurate logarithmic conversion, non-linearity in displays, and overall drift of the system. Test set/connection errors are due to the directional couplers in the reflectometer, imperfect cables, and the use of connector adapters. The instrument errors exhibited by the 8410B network analyzer are very small. Noise is specified to be less than -78 dBm equivalent input noise, and the isolation between channels is > 65 dB from 0.1 - 6.0 GHz and > 60 dB from 6.0 - 12.4 GHz. Reference and test channels track within ± 0.3 -dB amplitude and $\pm 1^\circ$ phase over any octave band from 0.1 GHz to 8.0 GHz with only a slight degradation at 12.4 GHz. Drift is specified to be within ± 0.05 dB/ $^\circ$ C and $\pm 0.1^\circ$ phase/ $^\circ$ C. The primary source of measurement uncertainty is due to test set/connectors at UHF and microwave frequencies. These uncertainties are quantified as directivity, source match, and frequency tracking errors.

During the second phase of the program, an effort was initiated to determine the cause of variations in the raw data which appeared as "ripples". In Phase III, an analytical model for correcting test set/correction errors was derived based on the model used by Hewlett-Packard for correcting reflectivity measurements on their semi-automatic network analyzer system [25]. This model accounts for directivity, frequency tracking, and source match errors. A detailed description of these systemic measurement errors is presented in the Second Annual Technical Report [2]. Here, the modeling efforts will be reported.

Each of the three types of test set/correction errors are shown schematically in Figure 3. The term S_{11m} is the measured reflection coefficient, and S_{11a} is the actual reflection coefficient. The directivity error E_{11} is due primarily to direct leakage of the incident signal into the reflected signal channel. The source match error E_{22} is caused by the re-reflection of the reflected signal back to the test port. $E_{21}E_{12}$, the frequency tracking error, is caused by small variations in gain and phase flatness between the test and reference channels of the analyzer as a function of frequency. If all of the three errors are known at each frequency, it is possible to remove them mathematically. These three error terms are determined by calibrating the system using three independent standard terminations whose actual reflection coefficient S_{11a} is known at all frequencies of interest. The measured reflection coefficient S_{11m} expressed as a function of the error terms and the actual reflection coefficient S_{11a} is

$$S_{11m} = E_{11} + \frac{S_{11a}(E_{21}E_{12})}{1 - E_{22}S_{11a}} \quad (8)$$

The calibration process is depicted in Figure 4. The directivity error E_{11} is determined by measuring a sliding matched load termination for a number of different path lengths. Because no matched load is truly perfectly matched, multiple load measurements are made. The loci of these points form a circle whose center is the true directivity error vector. The remaining error terms are determined in like manner through the solution of Equation (8). A short circuit and an open circuit termination provide the two necessary conditions for determining E_{22} and $E_{21}E_{12}$ (Figure 4). Once the measurement error terms are known at each frequency, S_{11a} can be determined from S_{11m} . Solving

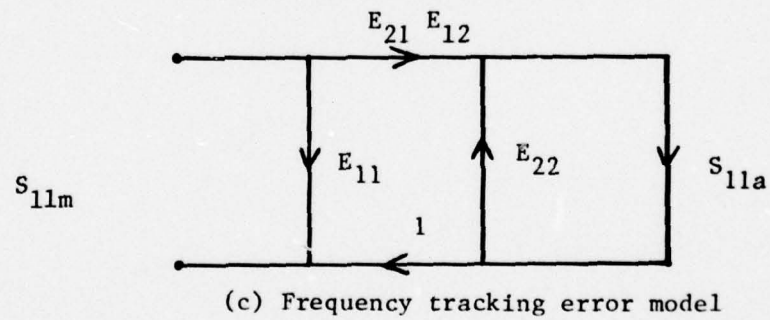
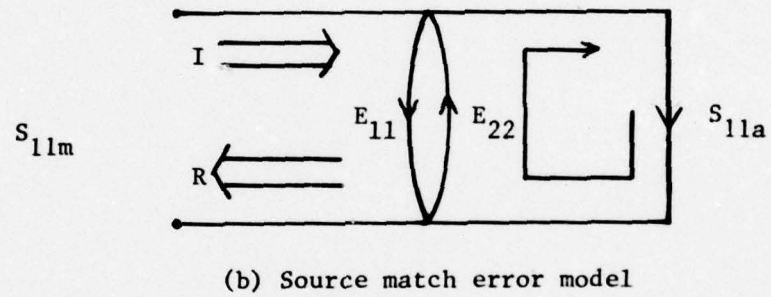
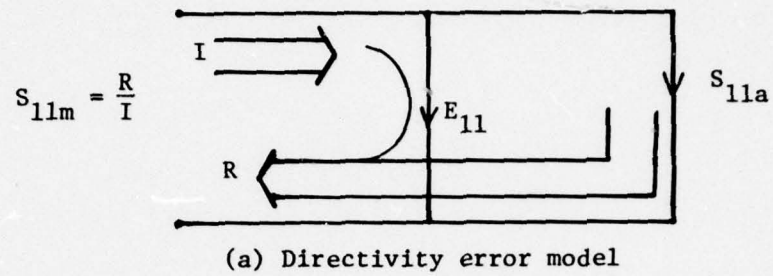
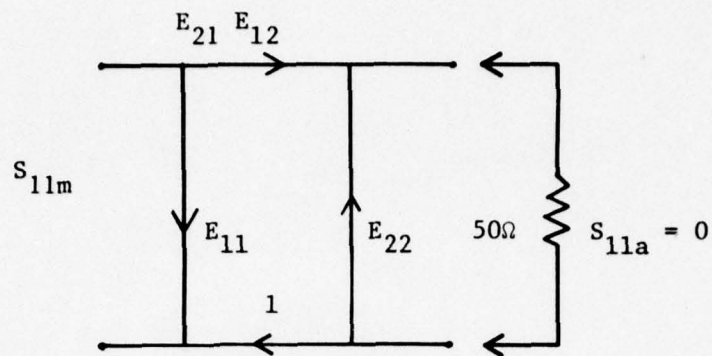
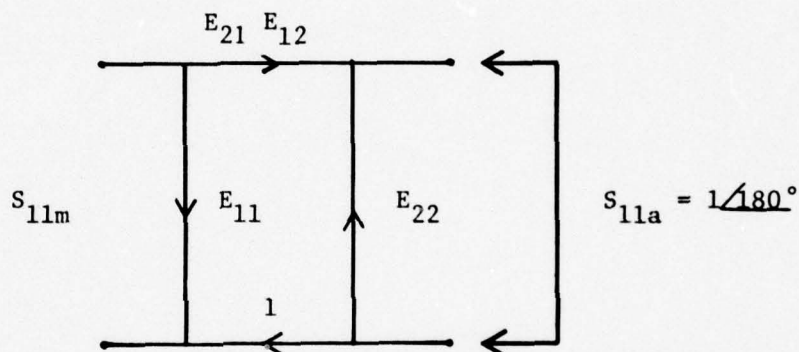


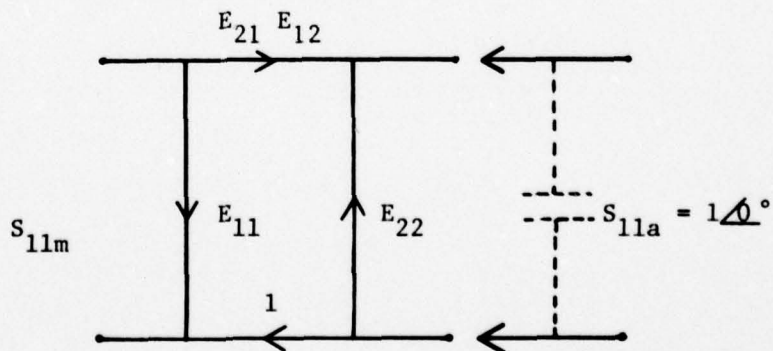
Figure 3. Error models used for test set/connection errors.



(a) Matched load calibration used for determination of Directivity error.



(b) Short circuit calibration condition used in determination of Source Match and Frequency Tracking errors.



(c) Open circuit calibration condition (with capacitance compensation) used in determination of Source Match and Frequency Tracking errors.

Figure 4. Calibration conditions used to determine directivity, source match, and frequency tracking errors.

Equation (8) for S_{11a} , one obtains

$$S_{11a} = \frac{S_{11m} - E_{11}}{E_{22}(S_{11m} - E_{11}) + E_{21}E_{12}} \quad (9)$$

Equation (9) is implemented in the error correction routine which is part of the data processing software on the microcomputer system. Once the measured data are corrected, the remaining data processing software computes the dielectric properties of the test material.

The error correction/calibration model was tested on deionized water data measured in the 2 to 4-GHz frequency range. The results of these tests are presented in Section IV.

E. Probe Fabrication

Methods for improved probe fabrication were also investigated during the third phase of the program. Laboratory measurements of standard liquid dielectric materials performed with different probes of similar design revealed that the measurement accuracy and frequency response of the probe are functions of how carefully and accurately the probe itself was fabricated. Therefore, a number of specific steps were taken to improve the repeatability of accurate probe fabrication.

A cutaway diagram of the in-vivo measurement probe is shown in Figure 5. The probe is fabricated from a section of open-ended semi-rigid coaxial cable with a slightly extended center conductor. The small circular ground plane minimizes fringing effects. The SMA connector is attached to the probe by first removing the center conductor and teflon dielectric material. The connector is then soldered to the outer conductor followed by reassembly of the probe using the center conductor as the center pin of the connector, thus avoiding additional soldering. In this manner, it is possible to attach the SMA connector without heating the teflon dielectric. While disassembled, the center and outer conductors of the probe are first

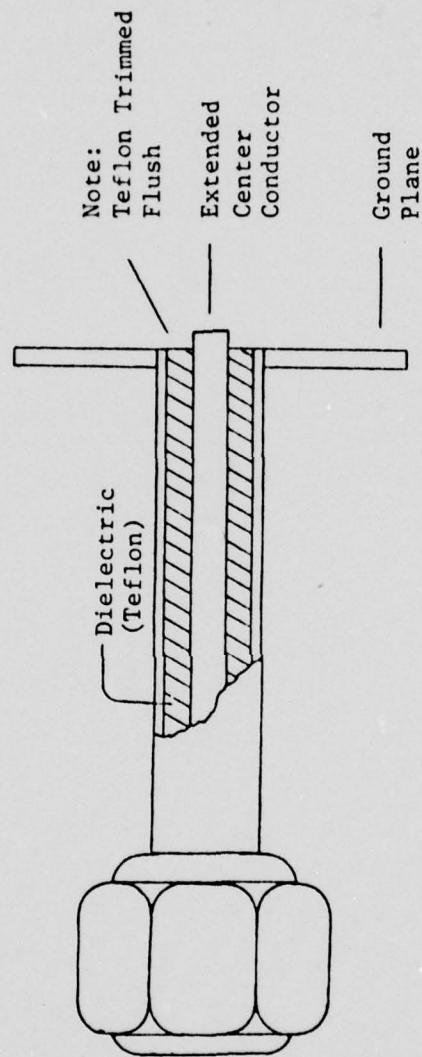


Figure 5. Diagram of in vivo measurement probe.

flashed with nickel plating and then gold plated. Plating the probe with an inert metal, such as gold, greatly reduces chemical reactions between the probe and the electrolyte in the tissue. This process virtually eliminates oxidation of the probe's metallic surfaces and helps to minimize electrode polarization effects at lower frequencies (0.01 - 0.05 GHz).

A probe fabrication method which has worked well is summarized in the following steps:

- Step 1. Remove the Teflon dielectric and center conductor from a short piece (approximately three centimeters length) of semi-rigid coaxial cable.
- Step 2. Silver solder a small circular disk to one end of the tube formed by the now-empty outer conductor. Machine the surface of this disk smooth.
- Step 3. Electroplate the resulting item and the center conductor that was previously removed. Use either nickel, gold, or platinum plating.
- Step 4. Solder a connector to the other end of the outer conductor tube.
- Step 5. Replace the Teflon dielectric and the plated center conductor, leaving the center conductor slightly extended.
- Step 6. Finally, trim any excess Teflon away from the extended center conductor.

SECTION III

SEMI-AUTOMATED DATA ACQUISITION/DATA PROCESSING SYSTEM DEVELOPMENT AND TESTING

A significant portion of the technical effort expended during the third year of this research program was directed toward the development of a prototype semi-automated data acquisition/data processing (SDADP) system. The decision to emphasize development of a SDADP system was made after it was observed that the existing manual technique for collecting and analyzing in-vivo probe data was tedious, time consuming, and hindering further advancement of the in-vivo probe concept. Construction of the prototype SDADP system was successfully completed, and preliminary tests have shown it to be capable of satisfactorily performing the data acquisition/data processing operations necessary for in-vivo probe measurements. The remainder of this section of the report details pertinent information about the prototype SDADP system including discussions of the overall system design concept, system development, and preliminary test results.

A. System Design Concept

Factors considered during the design of the semi-automated data acquisition/data processing (SDADP) system included the basic functions that the system would have to be able to perform and the shortcomings of the existing manual technique that would have to be eliminated. The basic performance function of the SDADP system is to accurately measure the parameters needed for computing the dielectric properties of the material being tested. These parameters are the frequency of the RF signal being employed and the amplitude and phase of the complex reflection coefficient of the in-vivo probe. The network analyzer system (see Figure 2) utilized to perform the in-vivo probe measurements provides the values of these unknown parameters through three signal ports: SWEEPOUT, AMP, and PHASE. The outputs of these three ports are DC voltages that are calibrated to be linearly proportional to the aforementioned frequency, amplitude, and phase

parameters, respectively. Therefore, it is necessary that the SDADP system be capable of accurately measuring and interpreting the information available at these ports.

Although measurements could be made with the existing manual technique, it had several shortcomings that made it cumbersome to use. One of its major drawbacks was the inordinately large amount of time required for the overall process of determining a material's dielectric properties. This fact limited the number of in-vivo probe measurements that could be made which in turn limited the time available for advancement and refinement of the in-vivo probe concept. Additional drawbacks of the manual technique included susceptibility to human errors in reading the recorded data and its inability to determine a material's dielectric properties on a real-time basis.

The following is a summary description of the manual technique. This description will aid one in identifying the causes of the manual-technique drawbacks as well as indicate some specific capabilities that must be incorporated into the SDADP to eliminate these drawbacks.

- (1) Initially, the measurement system must be set up. This involves tasks such as setting the endpoint frequencies on the sweep generator and selecting the appropriate calibration ranges on the X-Y recorder.
- (2) During the actual data acquisition process, the SWEEPOUT signal is used to drive the X channel (horizontal) on the X-Y recorder. The AMP and PHASE signals are used (on alternating frequency sweeps) to drive the corresponding Y channel (vertical) of the recorder. The resulting recordings represent plots of the amplitude and phase of the complex reflection coefficient as functions of frequency.
- (3) After all the required amplitude and phase plots are obtained, an architect's scale is used to manually extract the frequency, amplitude, and phase information, which is then tabulated.
- (4) The tabulated data are typed into a computer where it is used to compute the desired dielectric property information.

The majority of the time required when using the manual technique is expended in Items (1), (3), and (4), respectively, in setting up the measurement equipment, manually extracting and tabulating the data from

the X-Y recordings, and typing the tabulated data into the computer. However, only a small percentage of the time is expended by the actual data acquisition process, which does not depend on human performance. Also, questionable data often results because of the dependence of the operations on human performance, and as a result, rechecking and/or repeating the measurement process is often necessary in the manual mode.

Determination of the basic performance functions for the SDADP system were studied as well as the re-evaluation of the performance of the existing manual technique. This study led to the establishment of the following design guidelines for the SDADP system.

- (1) SDADP system accuracy must be comparable to or better than that obtained with the existing manual technique.
- (2) Set-up and calibration time for the equipment must be minimized.
- (3) Manual extraction, tabulation, and data typing must be eliminated in order to minimize measurement time, maximize data reliability, and increase data taking capacity.
- (4) SDADP system must be capable of performing dielectric property measurements on a real-time basis.

The primary improvement gained through the SDADP system, of course, is to minimize or eliminate human involvement in the in-vivo probe measurement process. The design concept that was chosen for the SDADP system from the preceding guidelines consists of a computer-controlled multiplexer, analog-to-digital converter unit, and a microprocessor based computer. The following subsections present details about the specific stages and components that comprise the SDADP system as well as the structure and philosophy of the software used for controlling the overall measurement process.

B. Hardware Selection

The selection of the hardware components to be utilized in implementing the SDADP system was based on two criteria: (1) the components would have to be able to operate within specified speed and accuracy limits and (2) the interfacing of these components (with each other and with the existing network analyzer system) should require

minimal effort. The major hardware components selected were a microprocessor-based desk-top computer (Commodore PET - Model 2001) and a subminiature multiplexer/analog-to-digital converter (Analogic-Model MP6812). Initially, some consideration was given to either purchasing a commercially available semi-automated network analyzer system (Hewlett Packard 8409A) or developing a dedicated microprocessor-based system from ground level. However, the tremendous cost and/or development time required for implementing either of these possibilities eliminated them from further consideration.

The Commodore PET is a complete stand-alone digital computer that has two I/O ports for interfacing with peripheral devices, a 1000 character CRT display, and built in cassette storage (for storing program or data files). It has a resident BASIC interpreter and can be alternatively programmed directly in machine code. It has a powerful feature that allows programming in mixed mode (i.e., a single program can contain both BASIC and machine language routines) when desired. The PET is a highly versatile instrument which can perform several functions in the SDADP system including control of other components, processing of all data, and data storage. The Analogic Model MP6812 unit is a microprocessor compatible combination multiplexer and analog-to-digital (A-D) converter unit. It can accept as many as 16 separate analog signals which can be individually multiplexed to a precision 12-bit A-D converter. The purpose of the MP6812 interface unit is to digitize the outputs of the SWEEPOUT, AMP, and PHASE signals from the network analyzer so that the parameter values can be accepted by the PET. A simplified diagram of the SDADP system is presented in Figure 6. The system operates in the following manner:

- (1) To initiate the measurement process, the PET sends out a pulse to the external trigger input of the sweep generator.
- (2) The PET then transmits a sequence of pulses to signal the MP6812 to begin sampling the SWEEPOUT signal.
- (3) The PET continuously samples the corresponding binary output of the MP6812 until it determines that the sweep generator is at the desired frequency.
- (4) Once the proper frequency is found, the PET sends out a different set of pulses to the MP6812 that signal it to

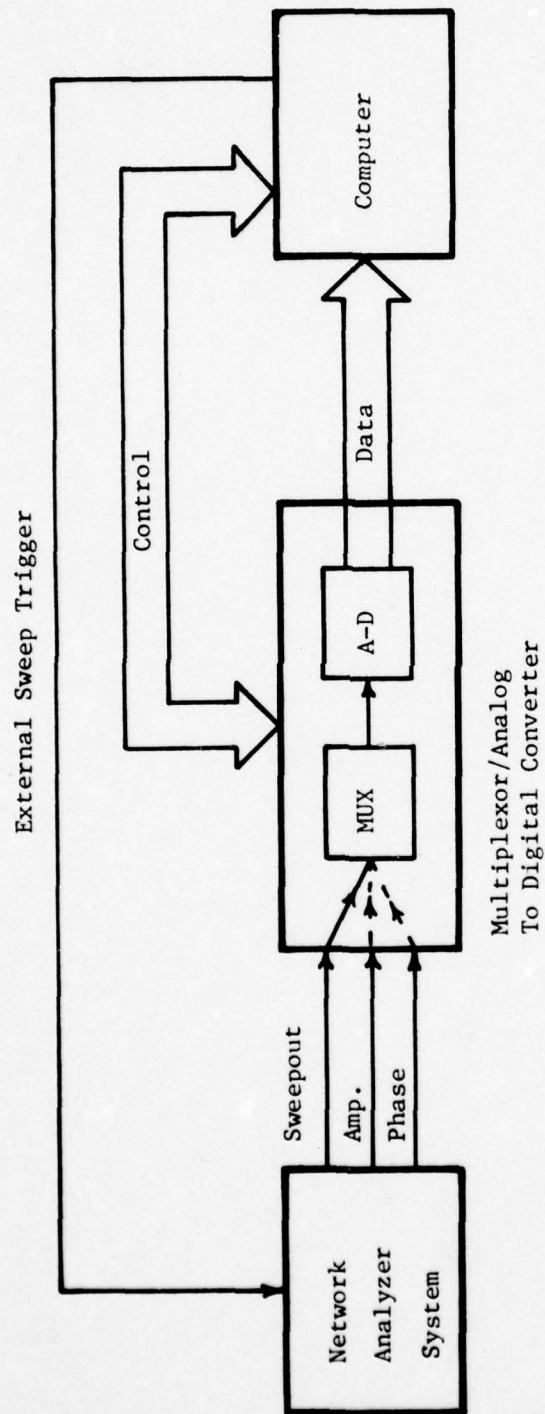


Figure 6. Block diagram of prototype semi-automated data acquisition/data processing system.

sequentially sample the signals from the SWEEPOUT, AMP and PHASE ports. The corresponding binary numbers are then stored in the PET computer.

- (5) Steps 2, 3, and 4 are then repeated until data have been obtained at all of the desired frequencies.
- (6) At the completion of a data run, the PET retrieves the frequency, amplitude, and phase data from its memory and uses it to compute the dielectric properties of the dielectric material being measured.
- (7) The computed dielectric properties are then displayed on the CRT as well as stored permanently on a cassette tape.

These steps are summarized by the flow chart in Figure 7. It should be noted that this is a highly simplified view of the measurement process, which does not include pertinent aspects of the measurement process such as initialization of the measurement equipment and computation of error correction terms. A more detailed explanation of the complete operation of the SDADP system is presented later in this section.

C. Hardware Interconnection and Operation

Although one of the reasons for selecting the PET and the MP6812 was their compatibility, interconnecting these devices required a considerable effort involving approximately 200 separate wiring connections (either wire-wrap or solder). In addition, various cable/connector assemblies were fabricated, and the MP6812, a triple D-C power supply, and various switches, connectors, etc. were mounted in an appropriate housing. The essential features of the SDADP system interconnections are presented in Figure 8. The analog signals from the network analyzer's SWEEPOUT, AMP, and PHASE ports are routed to the first three ANALOG INPUT channels (CH 0, CH 1, and CH 2, respectively) of the MP6812. A multiplexer (controlled by the PET) in the MP6812 selects one of the three channels and switches it to the internal precision (12-bit) A-D converter. The 12-bit binary output of the A-D is then fed to the PET through BINARY OUTPUT lines B1 through B12 where B1 represents the most significant bit (MSB) of the 12 bit word. The PET inputs the 12-bit binary word through two parallel I/O ports. The lower 8 bits are inputted through data lines DI01 through DI08 on the

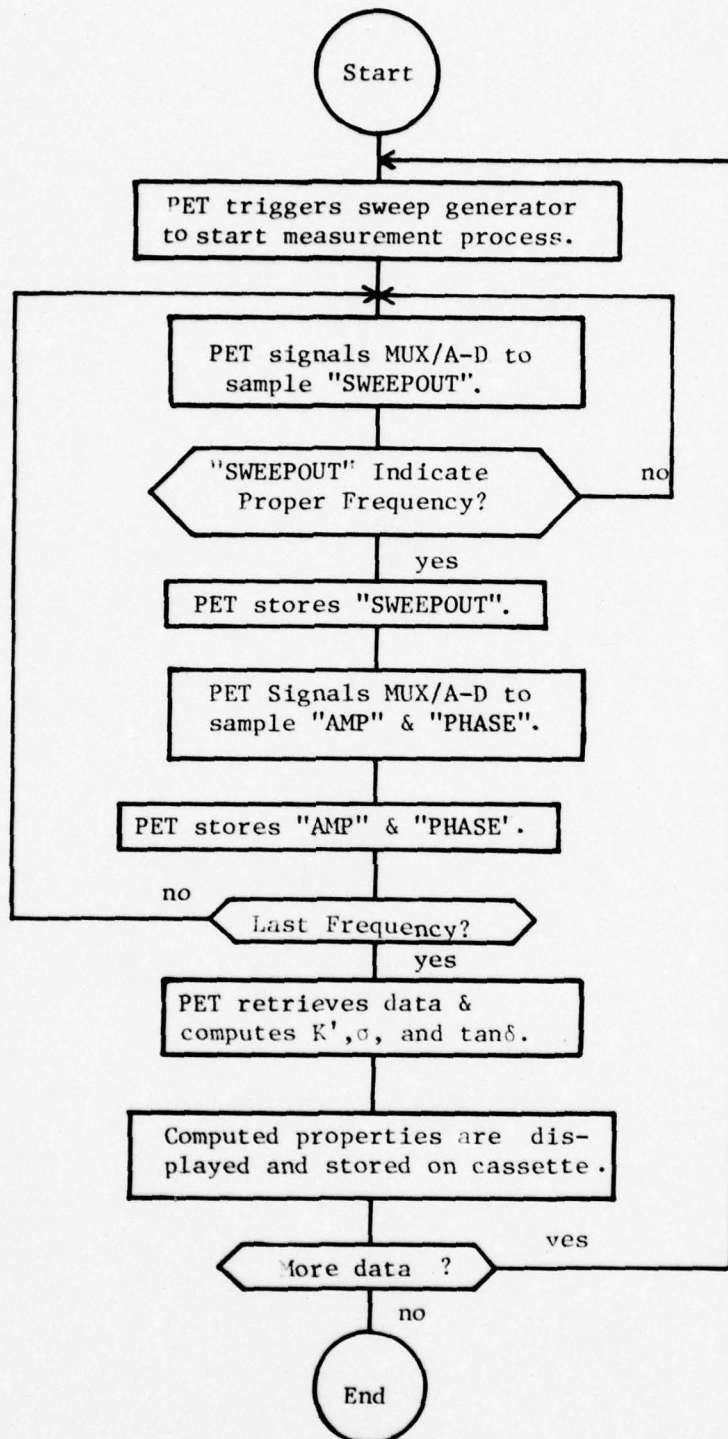


Figure 7. Flow chart of operational sequence of SDADP system

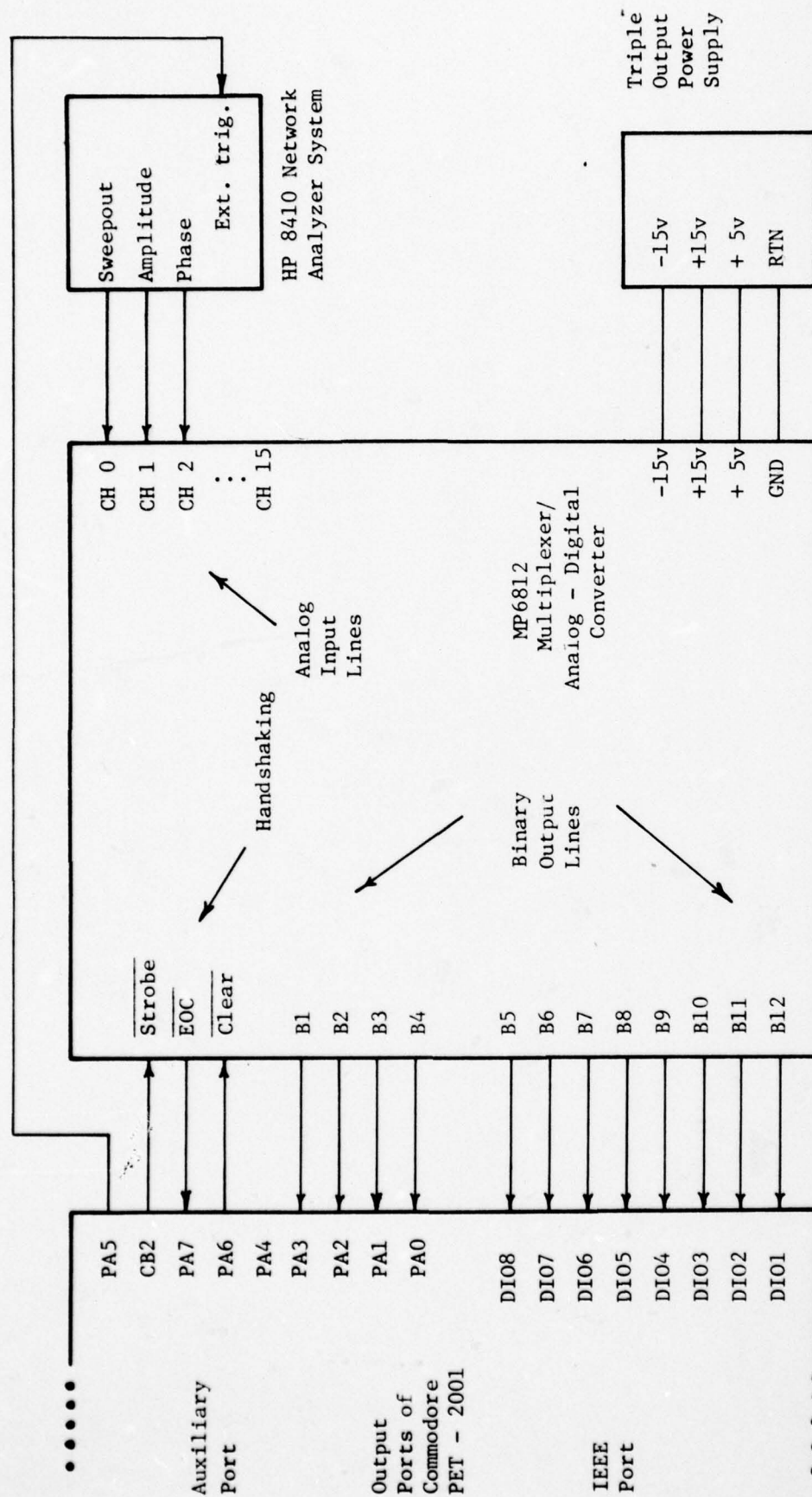


Figure 3. Interconnection diagram for components in SDADP system.

PET's IEEE Standard 488 interface port. The upper 4 bits are inputted through data lines PA0 through PA3 of the PET's auxiliary port. The two I/O ports are utilized because the microprocessor (MOS TECHNOLOGY 6502) in the PET microcomputer can only process 8-bit words, and therefore, each 12-bit data point must be converted to two 8-bit words for storage and processing.

The function of the lines indicated as HANDSHAKING is to provide the appropriate signals for synchronizing the operations of the PET, the MP6812, and the network analyzer system. The MP6812 will perform a measurement only when it receives a negative going pulse on its STROBE input. The PET is able to provide this signal through its CB2 handshaking line. CB2 can be initially setup so that it is normally in a "high" (or "logical 1") state. The peripheral interface adapter (a chip used for interfacing the microprocessor with peripheral devices) controlling CB2 can then be programmed so that CB2 generates the required negative going pulse whenever the microprocessor performs a "write" operation to the memory location corresponding to the peripheral interface adapter.

When the MP6812 receives a STROBE pulse and begins the analog-digital conversion process, it must signal the PET that it is currently "busy". This information is pertinent to the PET since the data on the MP6812's BINARY OUTPUT lines are not valid until the A-D conversion process has been completed. Also, it is undesirable to re-strobe the MP6812 while it is still busy from a previous strobe. The MP6812 accomplishes this signalling through its end of conversion (EOC) output which has two possible logic states. EOC is in a "low" (or "logical 0") state when the A-D converter is idle and in a "high" state when the A-D converter is operating. Therefore, before accepting data from or re-strobing the MP6812, the PET always checks the status of the EOC signal. If a "busy" is indicated, the PET will continuously recheck EOC until a "low" state is detected. It can be noted that the EOC signal is tied to the PA7 line (PA7 is one of the eight I/O lines, PA0 to PA7, through which 8-bit binary data is passed to and from the microprocessor in the PET) on the PET's auxiliary I/O port. PA7 was selected in order to make

use of the capability of the PET's microprocessor to perform branch instructions based on the current status of the flag bits comprising the microprocessor's condition code (CC) register. One of the flag bits (the "N" flag bit) is set or cleared depending on whether the last operation performed by the microprocessor resulted in a negative or positive value. Since PA7 represents the sign bit of the binary word present at the PET's auxiliary I/O port, the "N" flag will be set whenever EOC is high (A-D busy) or cleared whenever EOC is low (A-D idle). This enables the PET to check the status of EOC (and hence the A-D) by simply reading the binary word present on I/O lines PA0 to PA7, then performing the appropriate branch instruction on the basis of the status of the "N" flag.

The CLEAR handshaking line is used by the PET to specify to the MP6812 the ANALOG INPUT channel that is to be multiplexed to the A-D converter. When the MP6812 detects a "low" state on its CLEAR line, it will keep the multiplexer switched to channel CH 0. Therefore, during the time that the PET wishes to sample only the SWEEPOUT signal (as when testing for the frequency of the RF signal from the sweep generator), PA6 is used to reset CLEAR "low". After the PET has detected that the sweep generator is at the proper frequency, PA6 is used to set CLEAR "high". The multiplexer will then advance sequentially to CH 1 (AMP) and CH 2 (PHASE) on successive strobe pulses from the PET. Once the AMP and PHASE data are stored in the PET, PA6 is used to reset CLEAR "low", and the PET then samples for the next desired frequency. The remaining handshaking line, PA5, is used by the PET to provide a pulse for externally triggering the sweep generator in the network analyzer system.

D. Evaluation of Accuracy and Speed of Hardware in the SDADP System

The primary performance criteria considered in selecting the Commodore PET and Analogic Model MP6812 were resolution, accuracy, and speed. The resolution and accuracy of the hardware are very important in determining the frequency, amplitude, and phase parameters which subsequently determine the preciseness of the computed dielectric

property values. The operating speed for the hardware is also important, particularly during the actual data acquisition process which is a dynamic process.

The resolution and accuracy of the system is dependent on the A-D converter in the MP6812. Because of the variability of the output voltage levels of the SWEEPOUT, AMP, and PHASE ports, the A-D was designed to handle voltages in the range of -10 to 10 volts. The A-D is a 12-bit device which means that the analog 20-volt range (-10 to 10 volts) can be divided into 4095 increments, where each increment (binary bit) is equivalent to 4.884 millivolts (mV). Since the inherent uncertainty of the A-D converter's output is plus or minus one half bit, the resolution of the A-D converter is ± 2.442 mV. The AMP and PHASE outputs have calibration factors of 50 mV/dB and 10 mV/degree, respectively. Therefore, in terms of decibels and degrees (the units used in measuring the complex reflection coefficient), the resolution of the amplitude data is ± 0.049 dB and the resolution of the phase data is ± 0.244 degrees. The dynamic range of the network analyzer is 70 dB in amplitude and 360 degrees in phase. Therefore, the resultant amplitude and phase resolutions of the A-D converter are 0.07% and 0.067%, respectively, of the analyzer's total dynamic range.

Computation of the resolution of the A-D with regard to frequency measurements is more complicated. This complication stems from the manner in which the SWEEPOUT voltage levels are related to the frequency of the signal being transmitted by the sweep generator. The SWEEPOUT voltage is always a 10-volt linear ramp function (with an initial level of 0 volt and a final level of 10 volts). Regardless of the particular sweep frequency band, the initial frequency in the sweep band will correspond to the 0-volt level of the SWEEPOUT signal, while the final frequency in the sweep band will always correspond to the 10-volt level. Therefore, the frequency resolution of the system depends on the total width of the frequency band being swept. For example, if the sweep band were 1800 MHz to 4200 MHz (which is a difference of 2400 MHz), the frequency resolution would be approximately ± 0.6 MHz. This is determined from the fact that one bit is equivalent to approximately

1.17 MHz, and the inherent uncertainty is plus or minus one half bit. Alternatively, if the sweep band were 1800 to 2400 MHz (which is a difference of 600 MHz), the frequency resolution would increase to within 0.15 MHz.

The speed of operation of the PET computer and MP6812 multiplexer and A-D converter was another important performance criterion. The SWEEPOUT, AMP, and PHASE signals are constantly changing as the frequency band is swept during the measurement process. Because all in-vivo probe impedance measurements are performed dynamically, the SDADP system must operate at a speed fast enough to perform any required measurement before any discernable frequency change occurs. This requirement is particularly true when the PET is sampling and testing the SWEEPOUT signal in search of a particular frequency. Normally, the length of a single frequency-sweep is 10 seconds for a frequency band covering approximately 2000 MHz. Therefore, frequency will be increasing at a rate of 0.0002 MHz/microsecond (where 1 microsecond = 10^{-6} seconds). The rate at which the SWEEPOUT signal can be acquired and sampled is once every 32 microseconds. This 32-microsecond period is comprised of the A-D conversion time plus the strobe time. As a result, the SDADP system is capable of sampling the frequency every 0.0064 MHz. Alternatively, during the time that it takes the binary SWEEPOUT signal to change by 1 bit, the PET computer could sample and test the SWEEPOUT value 150 times. In addition to testing the SWEEPOUT signal, once the desired frequency is located, the data acquisition hardware and microcomputer must be able to sample and store the SWEEPOUT, AMP, and PHASE signals before any significant frequency change occurs. The sequence of machine level instructions necessary for this task requires approximately 80 microseconds. Based on the computed rate of frequency change of 0.0002 MHz/microsecond during a sweep, the frequency change from the time the SWEEPOUT information is read and stored and the time that the PHASE information is read and stored is less than 0.02 MHz. This change is less than 0.001% of the total frequency band being swept. Therefore, measurement accuracy for

frequency, amplitude, and phase of the complex reflection coefficient measured by the probe is significantly improved using the microprocessor-based data acquisition system.

E. Software Development

As stated earlier in this section, a unique feature of the PET microcomputer is its ability to be programmed in either BASIC or directly in machine code. BASIC is a higher level language and has many useful functions (arithmetic, logical, I/O, etc.) in its instruction set that cannot easily be duplicated with machine level instructions. Although the machine level instructions are in a simpler assembly language format, which is much less powerful on a per instruction basis, the fact that the execution time of machine level instructions is much shorter than the corresponding BASIC instruction makes it advantageous to use machine language in certain applications where speed is required. As an example, consider the execution times of two equivalent instructions "POKE" (BASIC) and "STA" (machine level) for sending a byte (8 bits) of data through one of the PET's I/O ports. The execution time of the "POKE" instruction is 10 milliseconds, whereas the execution time of the "STA" instruction is only 0.004 millisecond. In this case, the machine language instruction is 2500 times faster than the BASIC instruction. The fact that the PET microcomputer can be programmed in a mixed-mode is an extremely useful feature. "Mixed-mode" programming means that software can be written to take advantage of both the powerful computing ability of the PET's BASIC instructions and the speed of the PET's machine level instructions. Therefore, in developing the software for the semi-automated data acquisition/data processing (SDADP) system, data acquisition routines were written primarily in machine code, whereas data processing routines were written primarily in BASIC.

Since the PET is the main controller in the SDADP system, its software must be capable of controlling a variety of functions. These functions include the following:

- o Provide operating instructions to personnel using the SDADP system,

- o Control operation of the network analyzer system and the MP6812 multiplexer/A-D converter during the data acquisition process,
- o Insure that all required setup information is specified and stored (e.g., endpoint frequencies, number of data points, identification of sample material, etc.),
- o Insure that all required measurements are performed (e.g., reference data and error correction data when requested),
- o Manage all intermediate data until they are needed for data processing,
- o Perform all required data processing operations (error correction, dielectric property computations, etc.), and
- o Store all computed results and relative information (e.g., dielectric properties, identification information, etc.) on cassette tape.

Because of the complexity and magnitude of these functions, development of the software for the SDADP system was an extensive effort. Consideration was given to factors such as whether BASIC or machine code was appropriate for a particular application and how interactive the system should be with a user. Also, memory allocation was a severe constraint since only 8K bytes of random access memory (RAM) were available for storing all program codes as well as intermediate and computed data.

In order to simplify the development and evaluation of the software, it was divided into four subroutines: Initialization, Data Acquisition, Error Correction, and Dielectric Property Computation. A flow chart that summarizes the software developed for the SDADP system is presented in Figure 9. The following descriptions summarize the purpose and functions of these subroutines.

1. Initialization Subroutine

One purpose of this subroutine is to read and store all pertinent initialization parameters. These include identification parameters such as the material being tested, the date, and the temperature in addition to specification parameters such as the frequency band and the information needed to compute the frequencies at which data are to be taken. The identification information is

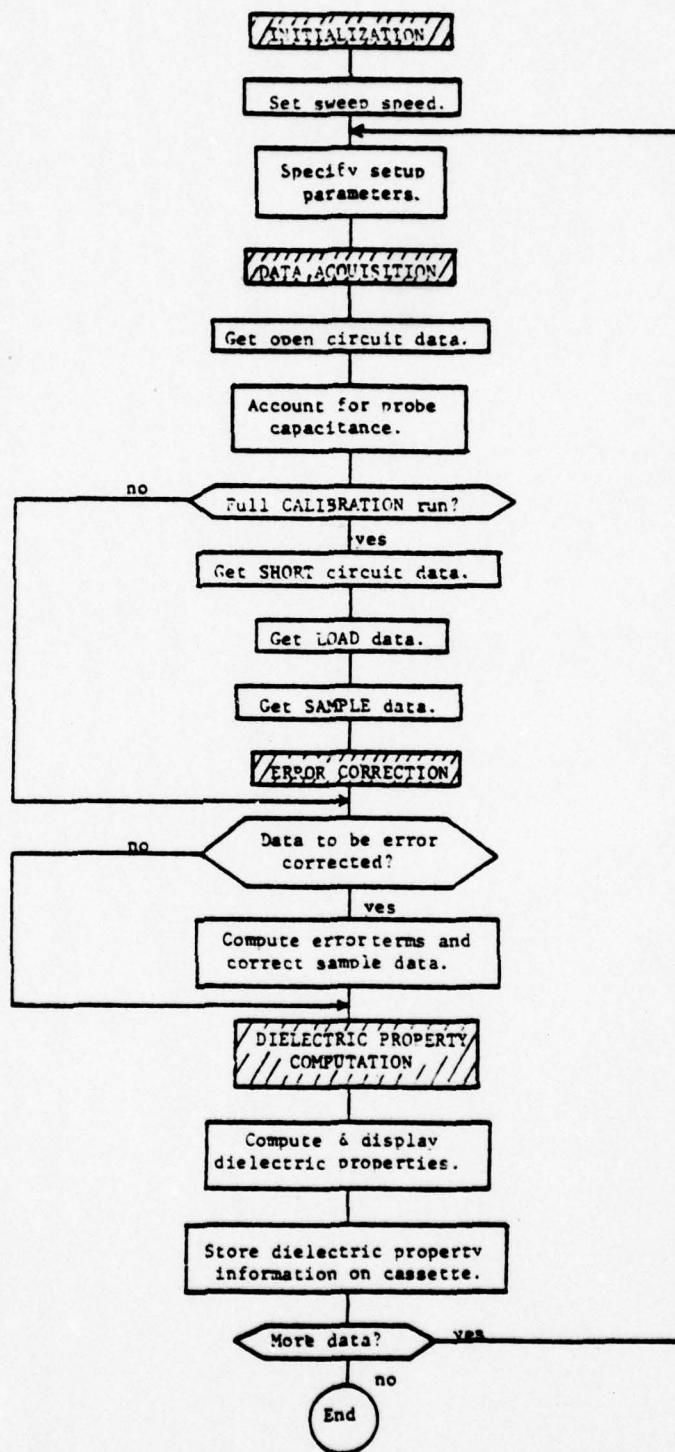


Figure 9. Overall flow chart of software routines for semi-automated data acquisition/data processing system.

straightforward, and it is used to document the final dielectric property output information, which is recorded on cassette tape.

One of the most important functions of this subroutine is to provide the information required to determine the relationship between frequency and the binary output of the MP6812. Because the PET must sample and test the SWEEPOUT port voltage until that voltage corresponds with the voltage level for the desired measurement frequency during the data acquisition process and because the PET can only read binary data, this information is provided through the Initialization Subroutine. Figure 10 depicts how this is accomplished. FA and FB are the endpoints of the sweep frequency band of interest. FS and FL are the first and last frequencies at which dielectric measurement data are to be acquired. BA, BB, BS, and BL are the corresponding binary numbers, respectively. FA, FB, FS, and FL are specified to the PET microcomputer by the system user. The PET will read BA and BB through its I/O port. The system then computes BS, BL and the binary voltages at which measurements are to be performed. With the exception of the instructions for reading BA and BB, the Initialization Subroutine is programmed in BASIC.

2. Data Acquisition Subroutine

The Data Acquisition subroutine controls the actual process of sampling the probe measurement data and storing them in memory. Its functions include the following:

- o Setting up the I/O ports on the PET microcomputer,
- o Triggering the sweep generator to initiate the measurement process,
- o Providing handshaking signals to the MP6812 for control of data sampling,
- o Computing the frequencies at which data are to be taken, and
- o Continuously testing SWEEPOUT and sampling and storing the frequency, amplitude, and phase parameters at the times corresponding to the desired measurement frequencies.

Because of the speed that is required, the Data Acquisition Subroutine is programmed primarily in machine code. In order to help conserve the

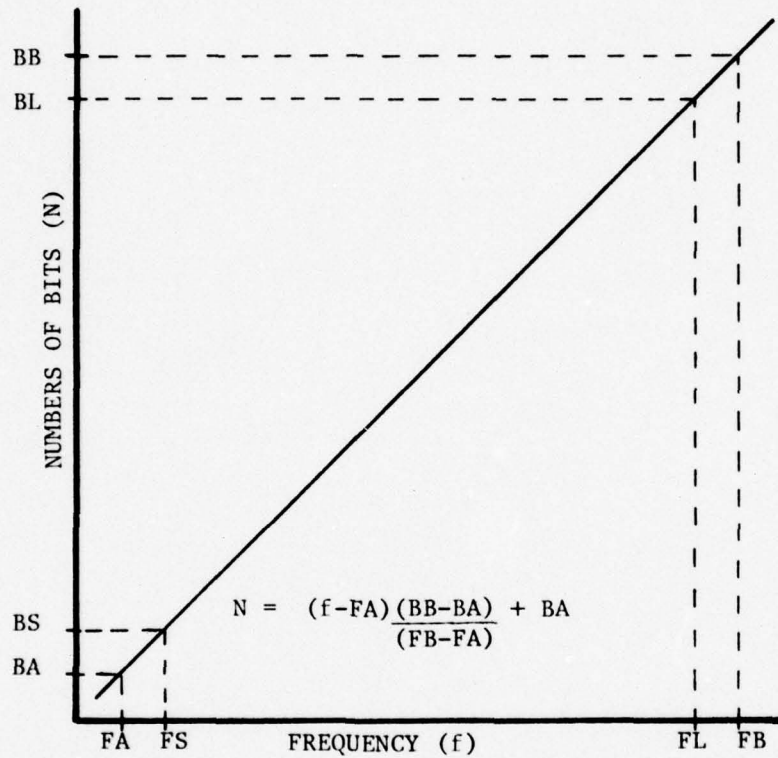


Figure 10. Theoretical linear relationship between frequency of signal from sweep generator and SWEEPOUT levels.

amount of memory used, the measured data (sampled during the data acquisition process) are stored in tables of two-byte integer words instead of in the floating point format used by the BASIC programming language. This technique preserves the accuracy of the data while reducing by a factor of four the amount of memory required for data storage.

3. Error Correction Subroutine

The purpose of this subroutine is to measure and store the frequency, amplitude, and phase parameters for various calibrated terminations (open circuit, short circuit, and matched loads). These data are then used to compute the error correction terms corresponding to directivity, source match, and frequency tracking errors, which are needed for correcting the measured in-vivo probe data. (The theoretical basis of the error correction process was discussed in Section II). Because of the complex computations that must be performed, this subroutine is primarily programmed in BASIC.

4. Dielectric Property Computation Subroutine

The primary purpose of this subroutine is to retrieve the in-vivo probe data from memory and to utilize them to compute the dielectric properties of the sample material. In addition, when requested by the user, this subroutine corrects the in-vivo probe data using the computed error correction data. The corrected measurement data are then used to compute the dielectric properties of the material. After the dielectric property information is computed, this subroutine displays the results and appropriate identification information on the CRT. If the user requests that these values be permanently stored, this subroutine will load the data onto a cassette data tape. Again, because of its data processing and computational requirements, this subroutine is also programmed in BASIC.

F. Preliminary Test Results

Although theoretical considerations indicated that the semi-automated data acquisition/data processing (SDADP) system would be capable of meeting all necessary performance criteria for determining

tissue dielectric properties, two experimental tests were performed in order to evaluate the system's actual performance. The purpose of the first test was to examine the ability of the SDADP system to accurately measure frequency. The purpose of the second test was to determine reliable data sampling rates for the SDADP system during the data acquisition process.

The first test was adapted from the Initialization Subroutine described previously, and is conducted as follows. First, the user is requested to enter the values of the endpoint frequencies of a desired sweep band (FA and FB in Figure 10) into the PET. The PET reads the corresponding values for the number of bits (BA and BB) from the MP6812 multiplexer/A-D Converter. These parameters are then used by the PET to determine the coefficients of an equation that theoretically describes the relationship between frequency and the SWEEPOUT signal. The PET then instructs the user to manually sweep (change frequency by hand) the generator over the entire frequency band from FA to FB. At several points during this manual sweep, the user is instructed to stop and use a frequency meter (or frequency counter) to measure the frequency of the RF output of the sweep generator. This information is then entered into the PET from the keyboard. The PET simultaneously reads the current SWEEPOUT level and uses it to compute and store a corresponding frequency value. If the dependent parameters of the equation are exactly correct, the equation perfectly describes the relationship between frequency and SWEEPOUT voltage. In this case, the computed frequency would exactly duplicate the frequencies measured with the frequency meter. After the entire frequency band from FA to FB is examined, the PET displays the frequency values measured with the frequency meter and the corresponding frequency values computed by the PET based on the SWEEPOUT voltage. (It should be noted that the frequency measuring accuracy of the SDADP system is dependent on the width of the frequency band being swept. Therefore, the results of these tests are computed in terms of the equivalent numbers of bits rather than in more conventional units such as megahertz.)

A typical result of the first test is presented in Table I. These data show that the frequency values computed by the PET are within plus or minus 3 bits of the frequencies measured with the frequency meter. Since the frequency range in this example corresponds to 2045 bits (i.e., $BB - BA = 2045$ bits), these test results show that the SDADP system can measure frequency within plus or minus 0.15 percent of the width of the frequency band being swept. For example, if the frequency band were 2000-MHz wide, the accuracy with which a desired frequency would be sampled would be plus or minus 3 MHz, whereas, if the frequency band were only 500-MHz wide, the sampling accuracy would be plus or minus 0.73 MHz. In general, obtaining accurate in-vivo probe measurements requires that the frequency be measured with approximately two percent of full scale accuracy. Therefore, the results of this test indicate that the relationship of SWEEPOUT voltage to measured frequency is nearly linear and that the PET microcomputer can utilize a linear parametric equation to accurately determine sampling frequency from SWEEPOUT data.

The second experimental test was adapted from the Initialization and Data Acquisition subroutines described previously, and it simulates the data acquisition process performed by the SDADP system. For performing this test, the three analog input channels (CH 0, CH 1, and CH 2 as indicated in Figure 8) of the MP6812 multiplexer/A-D converter were all connected to the SWEEPOUT signal port. During the test, the PET triggers the sweep generator to initiate the data acquisition process then monitors CH 0 in search of the frequencies at which data is to be sampled. When one of these frequencies is detected by the SDADP system, the PET sequentially samples and stores the data from CH 0, CH 1, and CH 2. This latter process requires exactly the same amount of time required by the SDADP system to sample and store the frequency, amplitude, and phase parameters during an actual in-vivo probe measurement. At the end of a complete frequency band sweep, the PET displays each of the frequencies sampled from CH 0, CH 1, and CH 2. If the values for each desired measurement frequency are nearly identical for all three channels, this indicates that the sweep rate is slow

TABLE I
RESULTS OF TEST TO DETERMINE THE ACCURACY
OF THE SDADP IN MEASURING FREQUENCY *

| Frequency Measured by Meter (F_1) | Frequency Measured by SDADP System (F_2) | Error $ F_2 - F_1 $ |
|--|---|------------------------|
| 173 | 173 | 0 |
| 343 | 343 | 0 |
| 513 | 513 | 0 |
| 683 | 683 | 0 |
| 854 | 853 | 1 |
| 1024 | 1024 | 0 |
| 1194 | 1195 | 1 |
| 1364 | 1365 | 1 |
| 1535 | 1532 | 3 |
| 1705 | 1703 | 2 |
| 1875 | 1875 | 0 |

* All frequency data are in units of bits

enough for frequency, amplitude, and phase data to be measured at exactly each desired frequency within the band.

Typical results from the second type of experimental test performed are presented in Table II. The sweep period for this test was ten seconds, which is the same period used for in-vivo probe measurements. The data are again presented in number of bits. The first column of data in this table is the specified frequency where the test data were to be measured. The second, third, and fourth columns of data are the actual frequencies (expressed in bits), measured through the CH 0, CH 1, and CH 2 inputs, respectively. Since the frequency values in each row of data in this table are nearly identical (worst case error is plus or minus one bit), the table clearly shows that the SDADP system is capable of operating at a rate high enough for accurate in-vivo probe measurement data acquisition.

TABLE II

RESULTS OF TEST TO EVALUATE THE OPERATING
SPEED OF THE DATA ACQUISITION PROCESS

| Specified Frequency * | Frequency Measured From CH0 | Frequency Measured From CH1 | Frequency Measured From CH2 |
|--------------------------|-----------------------------------|-----------------------------------|-----------------------------------|
| 56 | 55 | 55 | 55 |
| 245 | 244 | 244 | 244 |
| 340 | 239 | 339 | 339 |
| 434 | 433 | 433 | 433 |
| 528 | 527 | 527 | 528 |
| 623 | 622 | 622 | 622 |
| 717 | 717 | 717 | 717 |
| 812 | 812 | 811 | 811 |
| 906 | 905 | 906 | 906 |
| 1001 | 1000 | 1000 | 1000 |
| 1095 | 1095 | 1095 | 1095 |
| 1189 | 1188 | 1188 | 1188 |
| 1284 | 1284 | 1283 | 1283 |
| 1378 | 1378 | 1378 | 1378 |
| 1473 | 1472 | 1472 | 1472 |
| 1567 | 1566 | 1566 | 1567 |
| 1661 | 1660 | 1660 | 1660 |
| 1756 | 1755 | 1755 | 1755 |
| 1850 | 1850 | 1849 | 1850 |
| 1945 | 1944 | 1944 | 1944 |

* All frequency data are in units of bits

SECTION IV

SUMMARY OF EXPERIMENTAL RESULTS

During this three-phase research program, a large volume of in-vivo and in-vitro dielectric property information on various tissue types was accumulated. Extensive measurements have been performed on standard liquid dielectric materials in order to evaluate the accuracy and repeatability of the in-vivo measurement probe technique. Although the initial work utilizing the antenna modeling theorem concept was performed several years ago [18], it was during this current program that the technique and the measurement probe itself were developed to the point where accurate in-vivo measurements were made possible over a frequency range extending from 0.01 GHz to above 10.0 GHz [1,2,26]. In the course of this work, the parameters affecting probe performance were identified and optimized, the seemingly insurmountable problem of extending the technique to the microwave frequency range was solved, and a significant volume of basic data describing the in-vivo properties of several tissue types was acquired.

Many different types of in-vivo dielectric measurements were performed during this program. These included measurements on the following tissue types:

- o Muscle (dog and rat),
- o Fat (dog),
- o Brain (rat),
- o Kidney (rabbit and dog),
- o Whole blood (rat),
- o Granulocytes (human and rat), and
- o Platelets (human and rat).

Additionally, the probe dielectric measurements technique was used to examine the effects of drugs, particularly dimethylsulfoxide (Me_2SO), on tissue dielectric properties, and limited measurements of dielectric property changes in granulocytes and platelets due to temperature variations were performed. Preliminary measurements, using the probe technique, to detect changes in concentration of E. coli in water were also made.

The theoretical basis of the monopole probe dielectric measurement technique is discussed in the first Annual Technical Report [1]. Additional theoretical considerations and the results of extensive experimental investigations of the probe technique are described in the Second Annual Technical Report [2]. The in-vivo tissue dielectric property measurements performed during the second and third phases of this research program have provided dielectric data that were previously unavailable, some of which have been presented at scientific conferences [26,27].

In this section of the report, the most significant results of the experimental investigations for Phases I and II are presented together with the results of the work performed during Phase III. First, the results of sample size effects on measured dielectric properties of standard dielectric materials and the results of tests using the newly implemented microwave measurement error correction model are presented. This is followed by a discussion of the investigation of temperature changes and drug effects on the measured dielectric properties of blood components and renal tissue. Finally, a summary of the in-vivo tissue measurements which have been performed is presented.

A. Measurements of Standard Dielectric Materials

Each time a new measurement technique for obtaining laboratory data is developed, one of the first queries about the technique concerns its practicality and its accuracy. Such is also the case for the in-vivo probe dielectric measurements technique, particularly because of the great potential usefulness of this technique. Not only is the measurement procedure simple, but data may be obtained on a swept frequency basis from frequencies in the HF range (0.01 GHz) to frequencies well into the microwave region (10 GHz).

The probe measurement technique is practical because it permits obtaining in-vivo tissue dielectric property information not previously available and is useful for dielectric measurements of most liquids or semi-solids. To evaluate the accuracy of this measurement technique, extensive measurements of several standard liquid dielectric materials

were performed [1,2]. These measurements were performed over the 0.01 GHz to 10 GHz range, with the greatest emphasis placed on obtaining data for frequencies above 0.1 GHz. During the third phase of this research, efforts were directed primarily toward the evaluation of the physically limiting factors as well as factors associated with the inherent limitations of the measurement instrumentation. The particular factors investigated were the effects of sample volume on measurement accuracy and of microwave measurement test set/connection errors. A discussion of these factors follows.

1. Sample-Size Effects

The 0.89-cm and 0.49-cm long probes fabricated in the first year were useful over only a limited frequency range because the effective length of the probe was increased (by the square root of the dielectric constant) when it was inserted into a medium of high dielectric constant, which resulted in a change in terminal impedance that no longer was accurately described by the short monopole impedance expressions of Equation (2) (Section II). Even at frequencies where these probes were useful, the impedance was not completely reactive and therefore a radiated field existed. This radiated field resulted in a strong dependence of the probe dielectric measurement accuracy on the sample size. For probes which are long enough at the operating frequency to exhibit a radiated field pattern, the error in determining the relative permittivity and conductivity is significant. This error approaches zero only as the sample volume becomes infinitely large with respect to the EM penetration through the sample. For the early 0.49-cm long probe, the measured dielectric characteristics of saline changed 15 percent when the sample volume was increased twofold. By increasing the sample volume until no measurable change in dielectric properties occurred, the required sample volume was defined. The sample volume determined by the above procedure is one which is greater in size than the penetration depth of the EM energy at the operating frequency, and therefore, reflections at the sample boundary (which would cause errors in the measured dielectric properties) are minimized. A method for determining the error introduced in the measured antenna impedance for

small sample sizes when using a probe with a radiation resistance $R_r > 0$ is discussed in the First Annual Technical Report [1]. This error can be expressed quantitatively by an antenna reaction theorem [28].

During the investigations performed during the second and third phases of this research, studies showed that the problems associated with sample size could be alleviated by modifying the probe design in such a manner as to reduce the radiation resistance (R_r) essentially to zero. By substantially reducing the length of the measurement probe, it appears as an open circuit having a totally reactive impedance. Results of measurements performed with the 0.22-cm diameter probes illustrated in Figure 1 (Section II) are summarized in Tables III and IV. As seen from these measurement results, the computed dielectric properties of water and methanol vary less than one percent over the 0.1 - 10 GHz frequency range for volume changes between 15 ml and 250 ml. Therefore, the sample volume has virtually no effect upon the computed properties. It was experimentally determined that as long as the sample thickness was between one and two probe diameters, the measured results were accurate within the overall limitations of the probe technique.

Measurements of water samples of 50 ml and a single drop of water adhering to the end of the probe were also performed. Using a 0.22-cm diameter probe, the measured complex reflection coefficient changed less than 20 percent over the 0.1 - 10 GHz frequency range when a 50-ml sample was replaced by a drop of water. Similar measurements were performed using a 0.11-cm diameter probe which is approximately the diameter of an 18-gauge hypodermic needle. These latter measurements yielded accurate results for water at 2.0 GHz for sample volumes as small as a single drop of water. Although this small-diameter probe is still under development, it offers encouraging hope for deep-seated tissue dielectric measurements. Preliminary measurements using this small probe have been performed at frequencies up to 10 GHz. However, at frequencies above 4 GHz, the accuracy of the measurements performed using the 0.11-cm diameter probe were significantly degraded. It is anticipated that this is due to connector and adapter problems which

TABLE III
SAMPLE SIZE EFFECTS ON DIELECTRIC PROPERTIES
OF DEIONIZED WATER MEASURED WITH INFINITESIMAL PROBE

| f (GHz) | Relative Dielectric Constant (K') | | | | |
|---------|-----------------------------------|-------|--------|--------|--------|
| | 15 ml | 50 ml | 100 ml | 250 ml | 400 ml |
| 0.5 | 79.2 | 79.2 | 79.2 | 79.4 | 79.7 |
| 1.5 | 78.1 | 78.1 | 78.1 | 78.1 | 78.4 |
| 3.0 | 76.4 | 76.4 | 76.4 | 76.4 | 76.7 |
| 5.3 | 73.1 | 73.1 | 73.1 | 73.1 | 73.1 |
| 10.0 | 59.9 | 59.9 | 59.9 | 59.9 | 59.9 |

| CONDUCTIVITY σ (mmho/cm) | | | | | |
|---------------------------------|-------|-------|-------|-------|-------|
| 0.5 | 0.64 | 0.64 | 0.64 | 0.59 | 0.57 |
| 1.5 | 6.2 | 6.2 | 6.2 | 6.1 | 6.0 |
| 3.0 | 21.3 | 21.3 | 21.3 | 21.1 | 21.1 |
| 5.3 | 59.2 | 59.2 | 59.2 | 59.1 | 59.1 |
| 10.0 | 185.7 | 185.7 | 185.7 | 185.7 | 185.7 |

TABLE IV
SAMPLE SIZE EFFECTS ON DIELECTRIC PROPERTIES OF METHANOL
MEASURED WITH INFINITESIMAL PROBE

| RELATIVE DIELECTRIC CONSTANT (K') | | | | | |
|-----------------------------------|-------|-------|--------|--------|--------|
| f (GHz) | 15 ml | 50 ml | 100 ml | 250 ml | 400 ml |
| 0.5 | 33.1 | 33.1 | 33.1 | 33.1 | 33.1 |
| 1.0 | 29.8 | 29.8 | 29.8 | 29.8 | 30.0 |
| 3.0 | 18.5 | 18.5 | 18.5 | 18.5 | 18.7 |
| 10.0 | 7.2 | 7.2 | 7.2 | 7.2 | 7.2 |

| CONDUCTIVITY σ (mmho/cm) | | | | | |
|---------------------------------|------|------|------|------|------|
| 0.5 | 1.36 | 1.36 | 1.36 | 1.36 | 1.36 |
| 1.0 | 4.73 | 4.73 | 4.73 | 4.73 | 4.75 |
| 3.0 | 23.0 | 23.0 | 23.0 | 23.0 | 23.2 |
| 10.0 | 43.9 | 43.9 | 43.9 | 43.9 | 43.9 |

result from connecting such a small coaxial probe ultimately to an APC 7-mm connector. Although the 0.11 cm diameter probe is presently limited in its capability, further research and development should result in hypodermic needle-sized probes which yield accurate results for deep-seated tissues at frequencies as high as 10 GHz.

2. Error Correction Model

An analytical model for correcting the in-vivo probe measurements data for directivity, source match, and frequency tracking errors was presented in Section II. In this subsection, the implementation of the model and the examination of its effectiveness in correcting errors associated with the microwave measurement system are discussed. Examples of unprocessed, swept frequency measured reflection coefficient data (amplitude and phase) are shown in Figures 11 and 12. The upper curve in each case is the open circuit reference data. The lower curve represents the experimentally measured sample data for water at 23°C. From these data, the difference between the measured sample impedance and the open circuit impedance is used to compute the dielectric properties of the sample at desired frequencies within the sweep band. The semi-automated data acquisition/data processing (SDADP) system discussed in Section III eliminates the tedious process of reading data by hand from recorded curves such as those of Figures 11 and 12, thereby greatly reducing the time required for processing the measured data. However, regardless of the form in which the measured data are recorded, some method is needed to compensate for systemic measurement errors.

When data are recorded using the SDADP system, the Error Correction Subroutine residing in the PET microcomputer computes the directivity, source match, and frequency tracking errors at each frequency of interest and corrects the experimental sample data before the dielectric properties are computed. The same error correction may also be accomplished manually. Once the open circuit and sample impedance data are obtained in the form of a complex reflection coefficient (amplitude and phase) as shown in Figures 11 and 12, similar reflection coefficient data are obtained for known terminations (short circuit, open circuit,

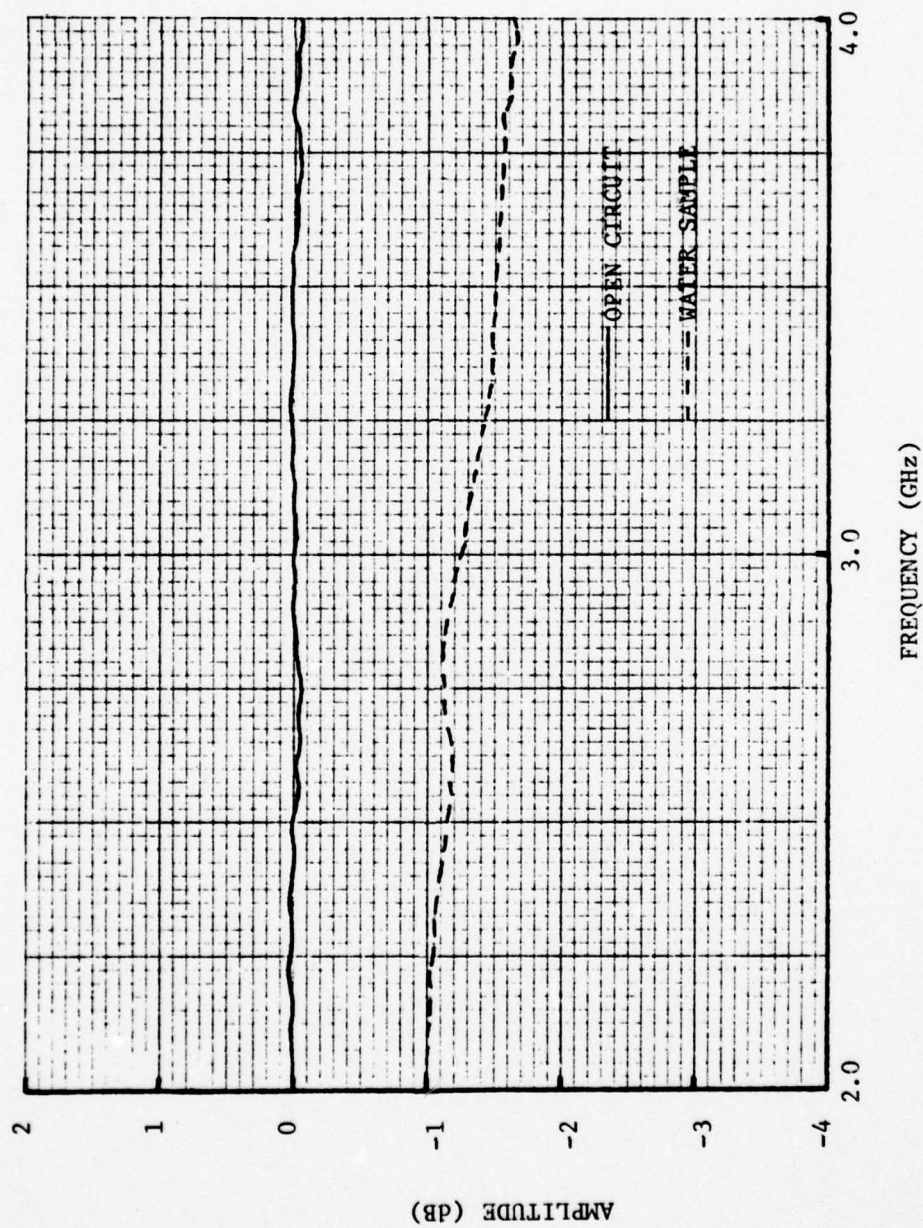


Figure 11. Unprocessed measured reflection coefficient amplitude data for deionized water at 23°C over the 2.0 - 4.0 GHz frequency range.

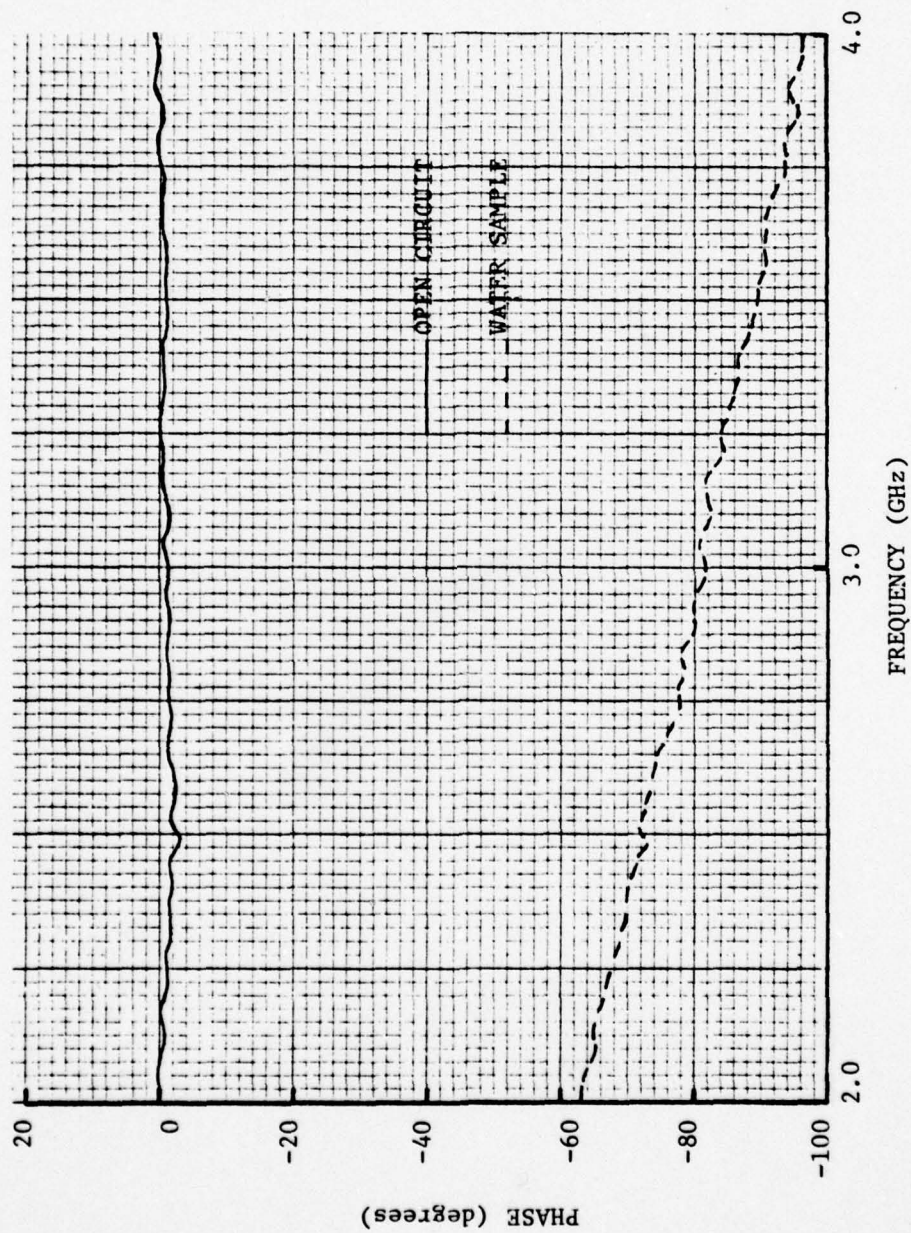


Figure 12. Unprocessed measured reflection coefficient phase data for deionized water at 23°C over the 2.0 - 4.0 GHz frequency range.

and matched loads) as illustrated by Figures 13 and 14. Figures 13 and 14 are the measured amplitude and the measured phase, respectively, of a short circuit termination, an open circuit termination, and a matched load (positioned at three different path lengths from the reference plane). This information is the same information which is stored in the memory of the PET microcomputer during a semi-automated data run. At each frequency of interest, the corresponding amplitude and phase data for each termination are read from the recordings. The matched load data are used to compute an "error circle." A vector from the origin of a plane representing the complex reflection coefficient to the center of that error circle is the directivity error E_{11} , which is computed using Equation (8). This error is primarily associated with the directional couplers of the reflectometer (Figure 2). The open circuit and short circuit data are then used to compute the source match error (E_{22}) and the frequency tracking error ($E_{21}E_{12}$) terms in Equation (8). These results and the measured reflection coefficient data (S_{11m}) from Figures 11 and 12 are then used to compute the actual reflection coefficient, S_{11a} , from Equation (9).

Two computer algorithms exist for computing the error correction terms. One is written in BASIC for the PET microcomputer, and the other is written in FORTRAN for the Control Data Cyber 74 computer. An example printout of the computed error terms and the corrected reflection coefficient data for the water data from Figures 11 and 12 using the FORTRAN program is shown in Figure 15. The dielectric properties are then computed using these corrected reflection coefficient (S_{11a}) data. The computed relative dielectric constant and conductivity of the "corrected" and "uncorrected" water dielectric data are shown in Figures 16 and 17, respectively. In both cases, these data are plotted against an "envelope" which defines the range of normal dielectric property values for water as characterized by standard reference sources [15,29-31] and our previous laboratory measurements [2]. It is noted that accounting for the systemic measurement errors significantly improves the accuracy of the computed results. Table V shows the dielectric constant and conductivity of water computed from

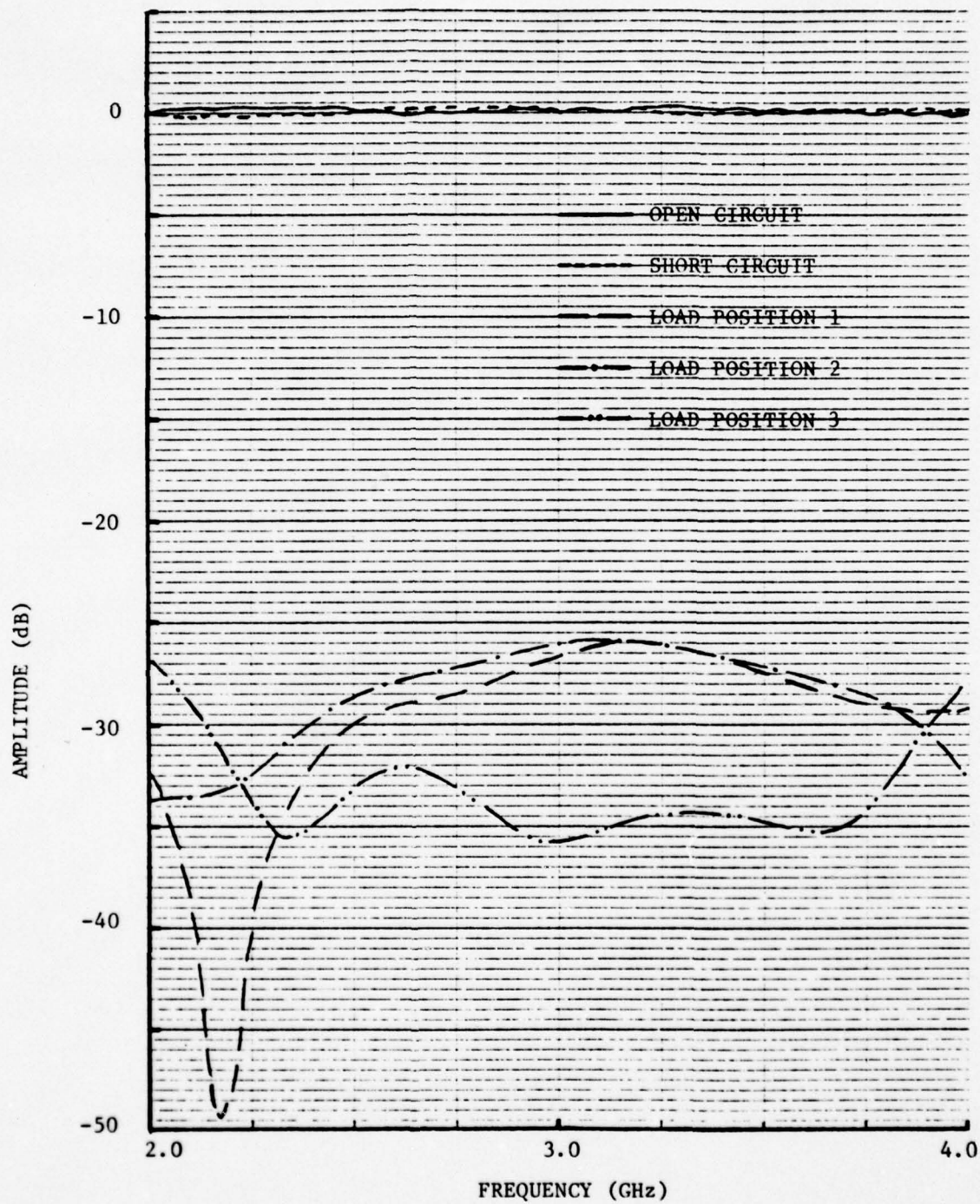


Figure 13. Measured reflection coefficient amplitude data for open circuit, short circuit, and three matched load terminations over the 2.0 - 4.0 GHz frequency range.

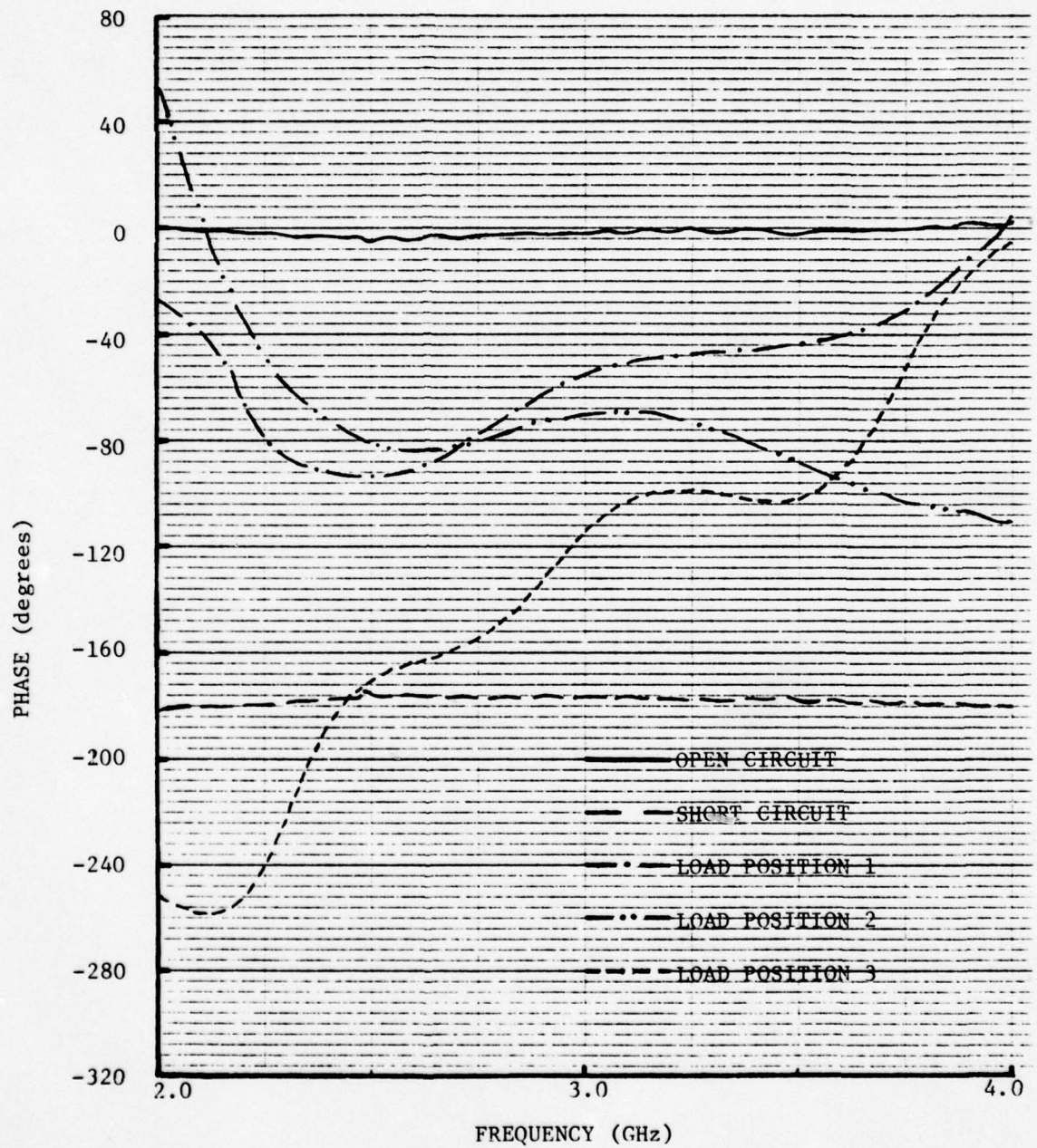


Figure 14. Measured reflection coefficient phase data for open circuit, short circuit, and three matched load terminations over the 2.0 - 4.0 GHz frequency range.


```

" INPUT OPEN-CIRCUIT PROBE CAPACITANCE *10**14" 1.22
INPUT FREQUENCY(1) (IN GHz)
1 2.25 3.5 3.75 3.85 3.5 3.75 4.
FREQUENCY (1) 3.000 GHz
INPUT AMPLITUDE (DB), PHASE (DEG) FOR LOAD
1 1 -38.843 -258.775
2 1 -31.108 -269.999
3 1 -38.345 -32.788
" INPUT SHORT-CIRCUIT AMPLITUDE (DB), PHASE (DEG)" 1 -2.430 -200.683
" INPUT OPEN-CIRCUIT AMPLITUDE (DB), PHASE (DEG)" 1 -2.297 -19.804

FREQUENCY (1) 3.000 GHz
INPUT AMPLITUDE (DB), PHASE (DEG) FOR LOAD
1 1 -30.835 -75.265
2 1 -40.466 -134.999
3 1 -30.317 -88.679
" INPUT SHORT-CIRCUIT AMPLITUDE (DB), PHASE (DEG)" 1 -2.253 -195.732
" INPUT OPEN-CIRCUIT AMPLITUDE (DB), PHASE (DEG)" 1 -2.386 -22.445

FREQUENCY (1) 4.000 GHz
INPUT AMPLITUDE (DB), PHASE (DEG) FOR LOAD
1 1 -33.442 -16.503
2 1 -31.940 -26.406
3 1 -37.020 -120.267
" INPUT SHORT-CIRCUIT AMPLITUDE (DB), PHASE (DEG)" 1 -2.209 -199.363
" INPUT OPEN-CIRCUIT AMPLITUDE (DB), PHASE (DEG)" 1 -2.474 -17.32

FREQUENCY SOURCE MATCH ERROR FREQUENCY TRACKING ERROR DIRECTIVE ERROR
2.00 -.32510E-02 -.52627E-02 .71681E+00 -.25913E+00 .12534E-01 .12029E-01
2.25 .10307E-01 -.29525E-01 .72133E+00 -.25864E+00 .71172E-02 .19235E-02
2.50 .44632E-02 -.20663E-01 .72366E+00 -.24406E+00 .82572E-02 -.87059E-02
2.75 -.99379E-02 -.27938E-01 .72372E+00 -.24615E+00 -.87732E-02 -.13293E-01
3.00 -.13699E-01 -.24240E-01 .72574E+00 -.24229E+00 -.12098E-02 -.18234E-01
3.25 .91770E-02 -.55240E-02 .72940E+00 -.23804E+00 .24658E-02 -.1953E-01
3.50 -.74490E-02 -.19923E-02 .72996E+00 -.23940E+00 .75687E-03 -.19046E-01
3.75 -.21792E-01 .15018E-01 .72532E+00 -.23682E+00 .13249E-02 -.22935E-01
4.00 -.29012E-01 .38373E-01 .72754E+00 -.23150E+00 .63667E-02 -.10209E-01

ENTER -1 FOR MORE CALIBRATION, 0 FOR DATA RUN, 1 TO STOP.
0
INPUT AMPLITUDE (DB) AND PHASE (DEG) OF TEST
FOR FREQUENCY " 2.1 1 -3.225 -92.848
"FOR FREQUENCY " 2.25 1 -3.269 -99.119
"FOR FREQUENCY " 2.5 1 -3.534 -94.400
"FOR FREQUENCY " 2.75 1 -3.534 -98.031
"FOR FREQUENCY " 3.1 1 -3.622 -101.332
"FOR FREQUENCY " 3.25 1 -3.622 -104.962
"FOR FREQUENCY " 3.5 1 -3.843 -108.923
"FOR FREQUENCY " 3.75 1 -4.108 -112.554
"FOR FREQUENCY " 4.1 1 -4.153 -115.525

GHz AMPLITUDE PHASE
2.000 -.68476E+00 -.64170E+02
2.250 -.74459E+00 -.68938E+02
2.500 -.86438E+00 -.74045E+02
2.750 -.11591E+01 -.78834E+02
3.000 -.13499E+01 -.83609E+02
3.250 -.15285E+01 -.87103E+02
3.500 -.17339E+01 -.91734E+02
3.750 -.21677E+01 -.96330E+02
4.000 -.21999E+01 -.99792E+02

```

Figure 15. Printout of computed error correction terms and corrected water reflection coefficient data from FORTRAN program.

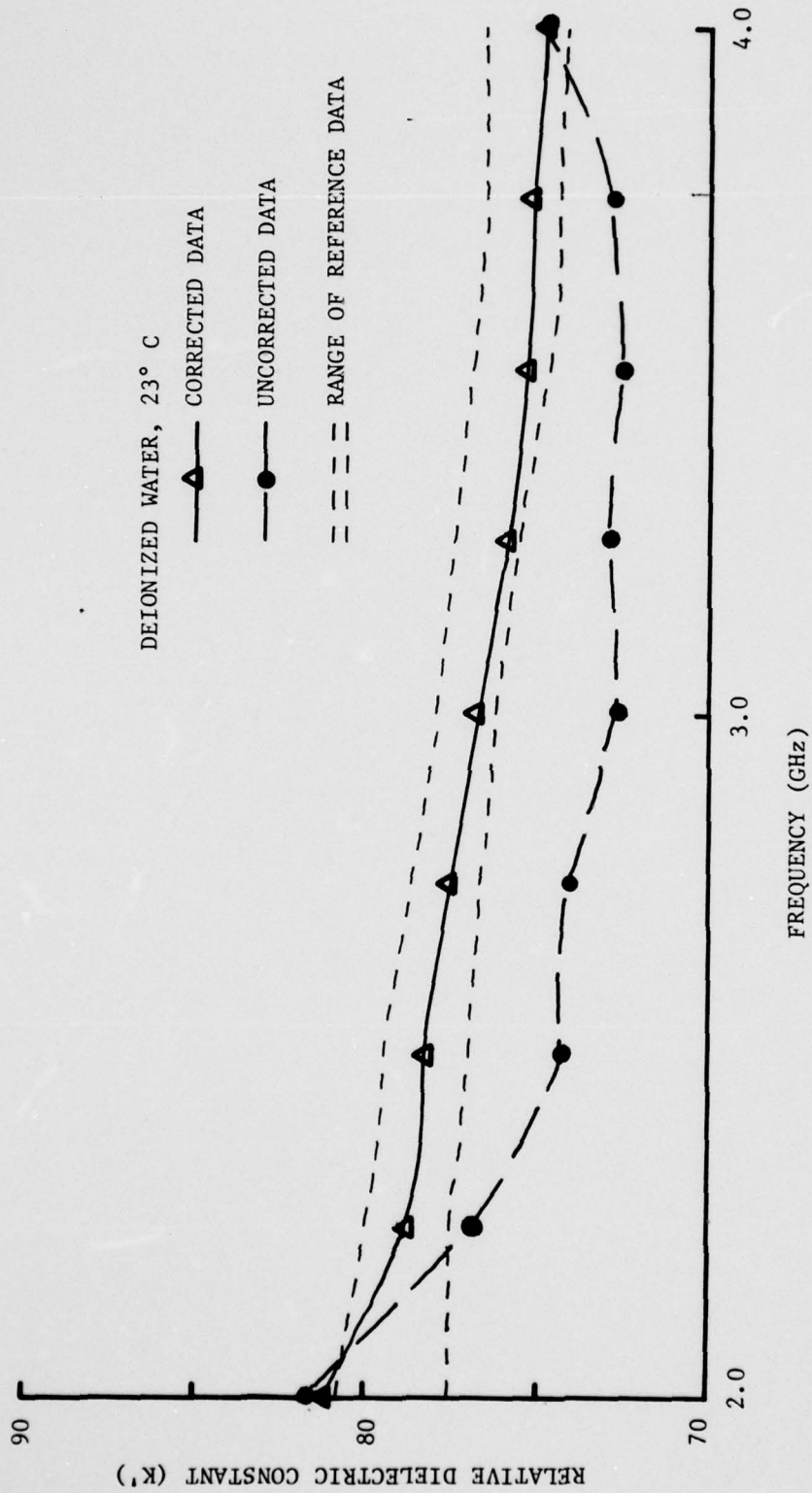


Figure 16. Relative dielectric constant of deionized water computed from corrected and uncorrected probe measurements compared to the range of dielectric constant data from reference sources.

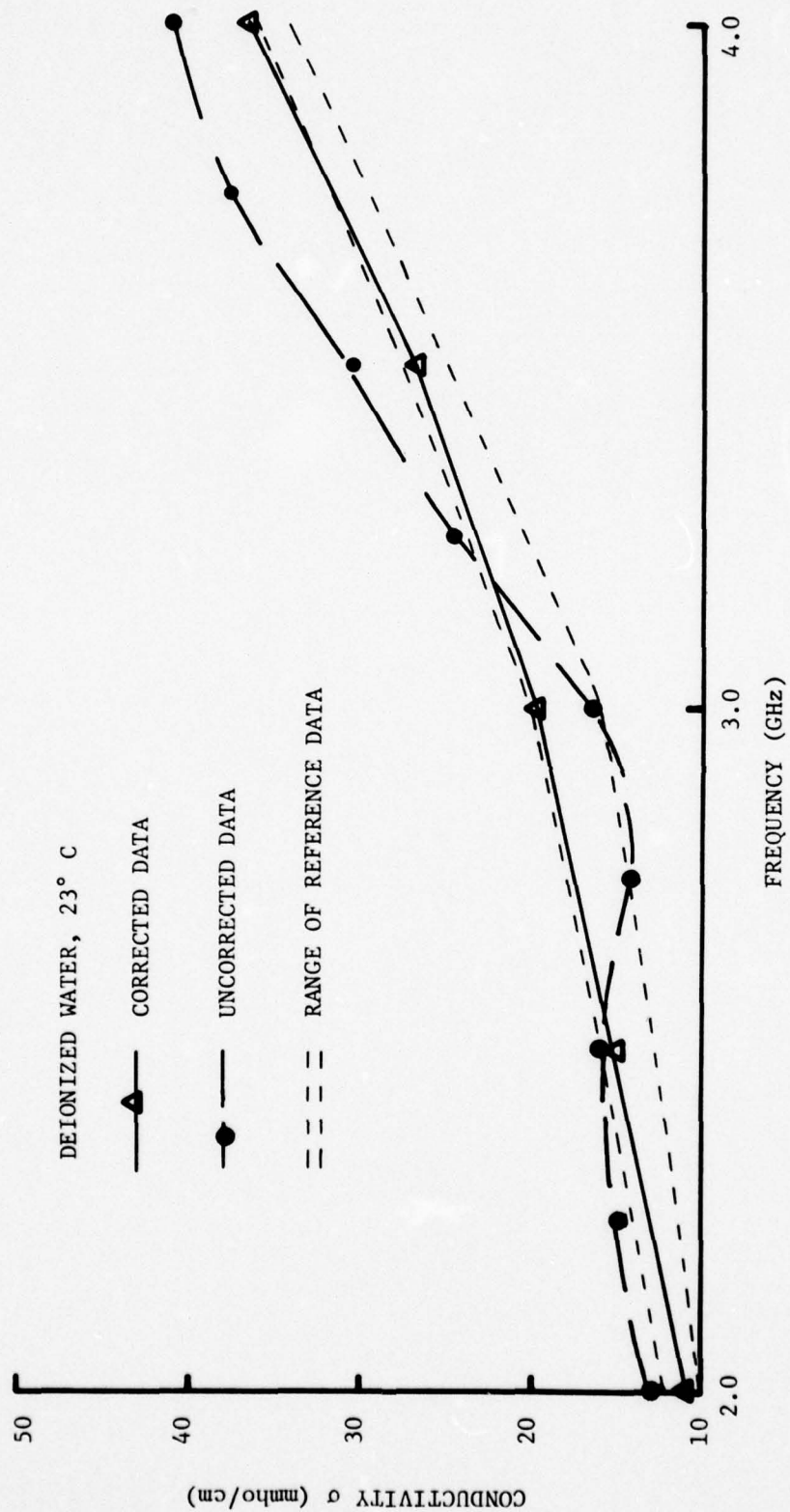


Figure 17. Conductivity of deionized water computed from corrected and uncorrected probe measurements compared to the range of conductivity data from reference sources.

TABLE V
RELATIVE DIELECTRIC CONSTANT AND CONDUCTIVITY (mmho/cm)
OF WATER COMPUTED FROM CORRECTED MEASUREMENTS

| Frequency (GHz) | | 1500 | 1852 | 2500 | 2610 | 2874 | 3000 | 3254 | 3571 | 3750 | 4000 |
|--------------------------------|----------|------|------|------|------|------|------|------|------|------|------|
| Data Source | | | | | | | | | | | |
| NBS | K' | * | 89.7 | * | * | 78.6 | 77.4 | 77.8 | 74.0 | * | * |
| | σ | * | 10.5 | * | * | 19.3 | 21.8 | 25.1 | 28.4 | * | * |
| Von Hippel | K' | * | * | * | * | * | 76.7 | * | * | * | * |
| | σ | * | * | * | * | * | 20.2 | * | * | * | * |
| Pottel | K' | * | * | * | 76.9 | * | * | * | * | 75.6 | * |
| | σ | * | * | * | 14.2 | * | * | * | * | 28.7 | * |
| Cook | K' | * | * | * | * | * | 77.7 | * | * | * | * |
| | σ | * | * | * | * | * | 21.7 | * | * | * | * |
| Georgia Tech | K' | 78.4 | 78.2 | 77.4 | 77.2 | 76.9 | 76.5 | 76.3 | 75.6 | 75.4 | 75.1 |
| | σ | 6.17 | 9.16 | 15.6 | 16.3 | 19.6 | 20.3 | 24.7 | 28.1 | 31.8 | 46.2 |
| * Indicates data not reported. | | | | | | | | | | | |

probe measurements which had been corrected for systemic measurement errors compared to reference data available from reliable sources such as the National Bureau of Standards [29] and from several individual investigators [15,30,31]. The corrected water data obtained using the infinitesimal probe are well within the bounds determined by the several sources of reference data. In fact, the variability of the data measured with the in-vivo probe is considerably less than the variability of the reference data.

B. Investigation of Temperature and Drug Effects on Measured Dielectric Properties

Detailed knowledge of the effects of perfusate solutions, cryoprotectant concentration, and temperature on tissue dielectric properties is extremely important in cryopreservation applications where electromagnetic energy is used for thawing. Because of this importance, the in-vivo probe has been investigated as a method for obtaining accurate dielectric data on changes in tissue dielectric properties due to cryoprotectant and temperature effects. Physical stress causing deformations in the teflon dielectric portion of the probe is induced when the probe is placed in contact with extremely cold materials which alters the probe's calibration in an undeterminable manner. A special hermetically sealed probe was developed which alleviated this problem. It has been tested through measurements of deionized water over a wide range of temperatures, and it has been used to measure the electrical properties of platelets, granulocytes, and kidney tissue over the temperature range from -40°C to $+20^{\circ}\text{C}$ with good results. These results are summarized in the following paragraphs.

The dielectric properties of rat and human platelets were determined as a function of temperature in a medium composed of Ringers Citrate Dextrose (RCD) and plasma both with and without a cryoprotective drug (Me_2SO). The purpose of these measurements was to determine the effects of a 6% Me_2SO concentration on (1) the dielectric properties of rat and human platelets in the frozen and thawed states and (2) the alteration of the phase change temperature of the platelets in RCD-

plasma. Measurements were performed both during freezing and during thawing, and the temperature of the platelets concentrate was continuously monitored via both a very small thermistor probe and an alcohol thermometer.

Before making measurements on the solution of rat platelets, the solution was cooled slowly to a temperature of -40°C . At -40°C , the relative dielectric constant was 5 in the medium without Me_2SO , and 7 in the medium with 6% Me_2SO . As the temperature was increased, almost no change in the relative dielectric constant was measured for the cells in the medium without Me_2SO until the phase transition occurred at 0°C . Following the phase transition, the dielectric constant increased to approximately 75, which represents an order of magnitude change between the frozen and thawed states. Similar changes occurred in conductivity. The platelets in the medium with 6% Me_2SO also underwent major changes in relative dielectric constant and conductivity through the phase change, but (1) the phase change occurred at a lower temperature and (2) the increase in relative dielectric constant and conductivity was more gradual up to the temperature where the actual phase change occurs. These results are represented graphically in Figures 18 and 19. Note that the phase change temperature for rat platelets in 6% Me_2SO is about -8°C , whereas the phase change temperature for rat platelets without the added cryoprotective drug is 0°C . The loss tangent as a function of temperature for rat platelets with and without Me_2SO is shown in Figure 20. Note that the presence of the polar Me_2SO increases the peak in the loss tangent nearly twofold.

Similar dielectric property data for human platelets are displayed graphically in Figures 21 to 23. Again, order-of-magnitude changes are seen in the relative dielectric constant and conductivity during the phase transition from solid to liquid. The loss tangent plotted in Figure 23 also peaks at a greater value when 6% Me_2SO is present in the medium than when Me_2SO is not present, although the difference is not as great as in rat cells.

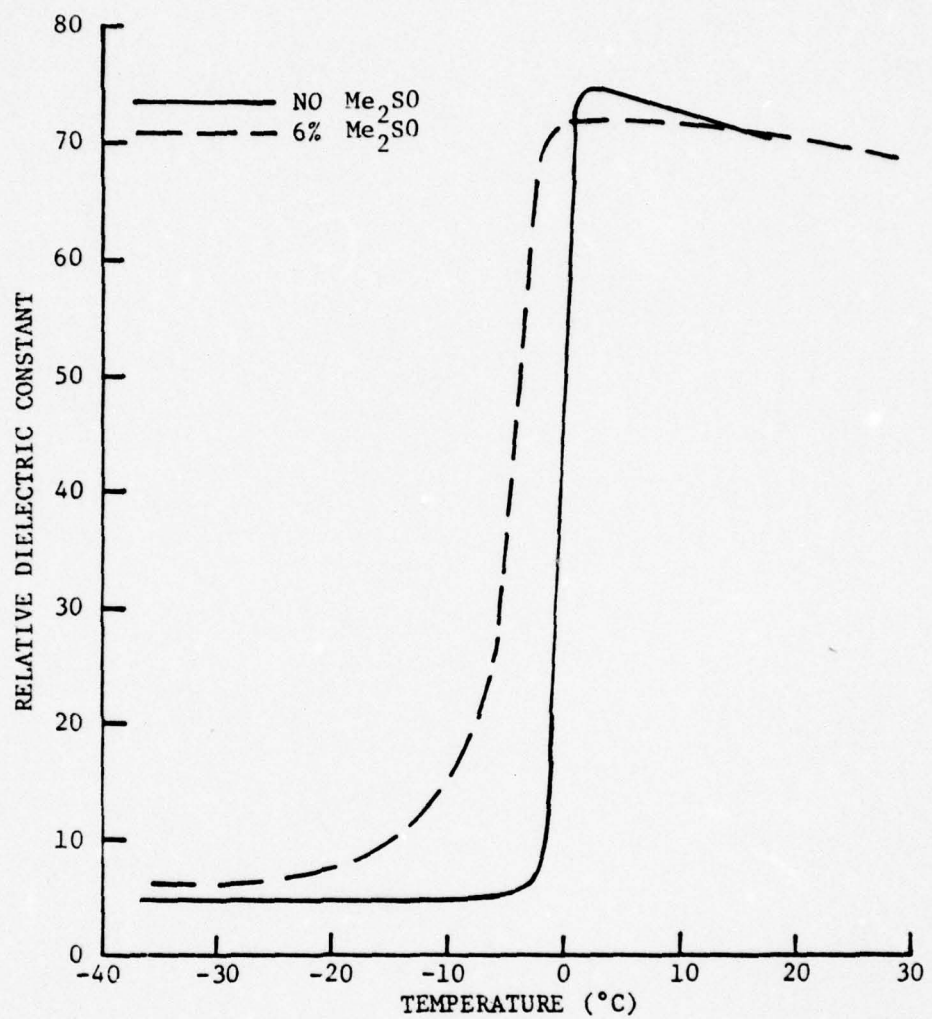


Figure 18. Measured Relative Dielectric Constant of Rat Platelets in 20% Plasma-RCD

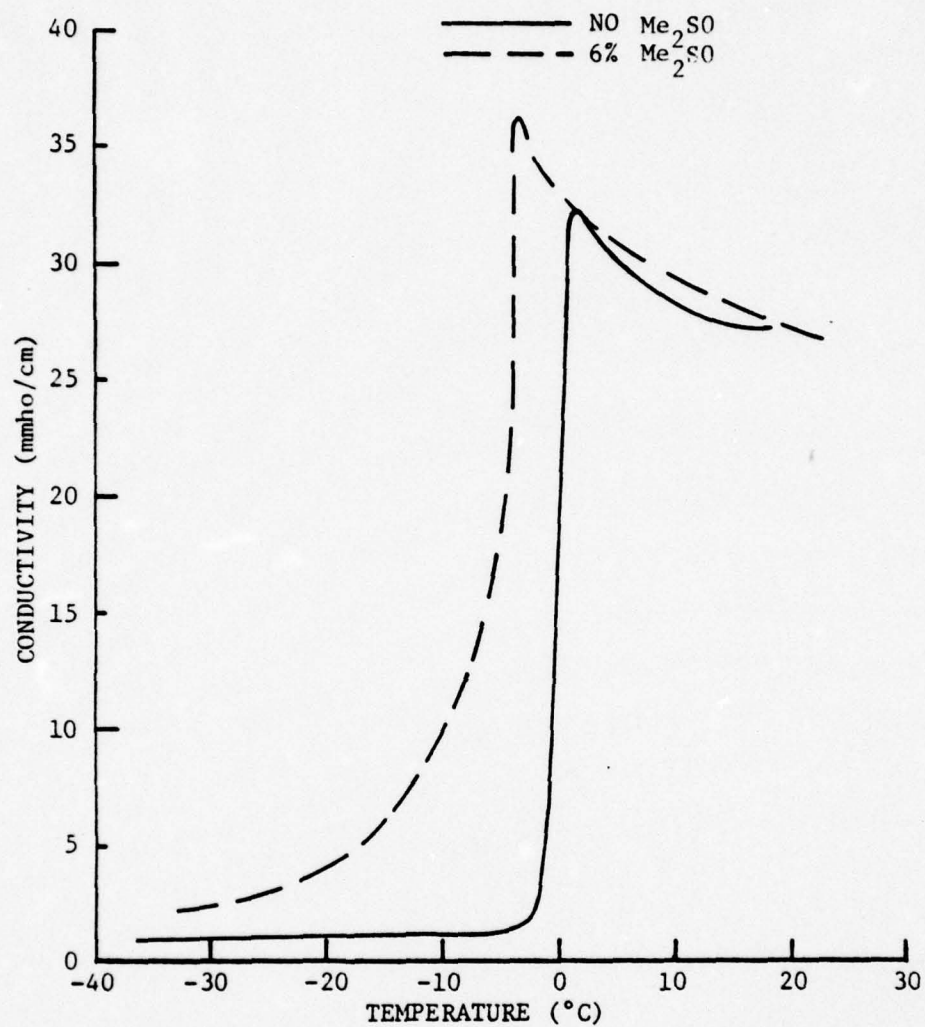


Figure 19. Measured Conductivity of Rat Platelets in 20% Plasma-RCD.

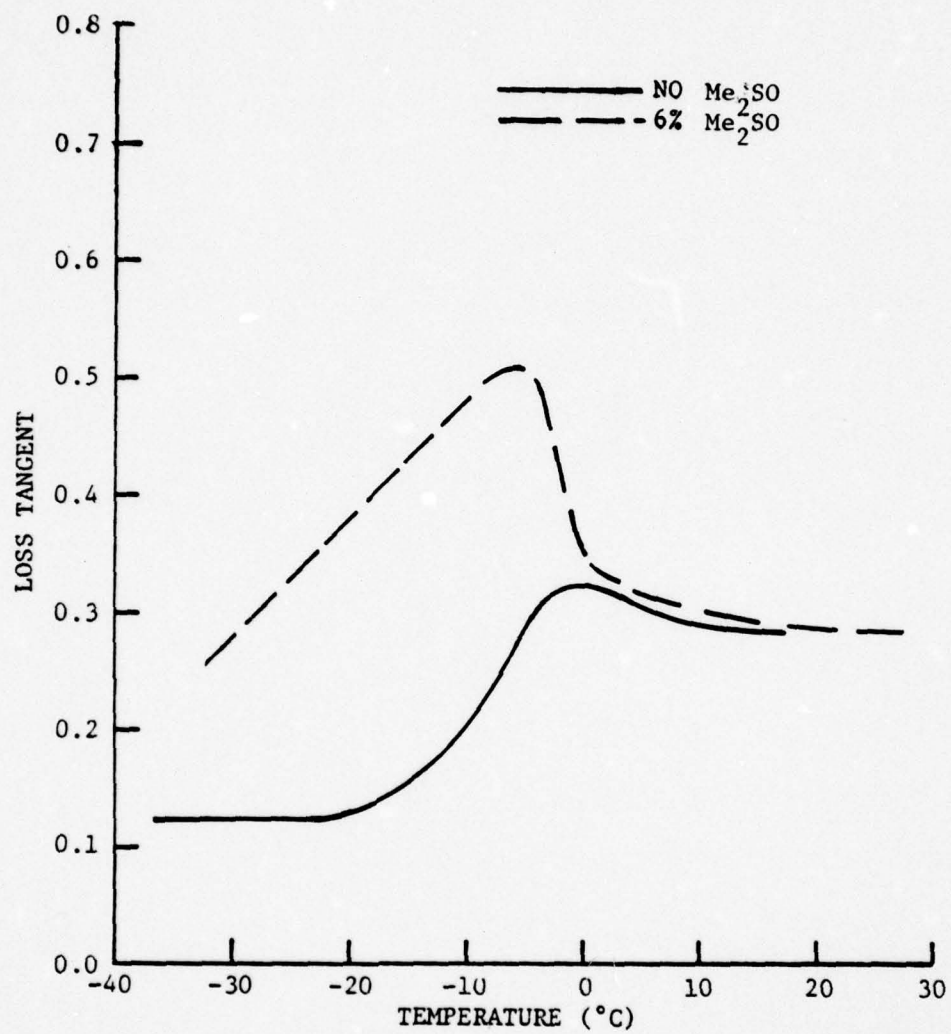


Figure 20. Loss Tangent of Rat Platelets in 20% Plasma-RCD

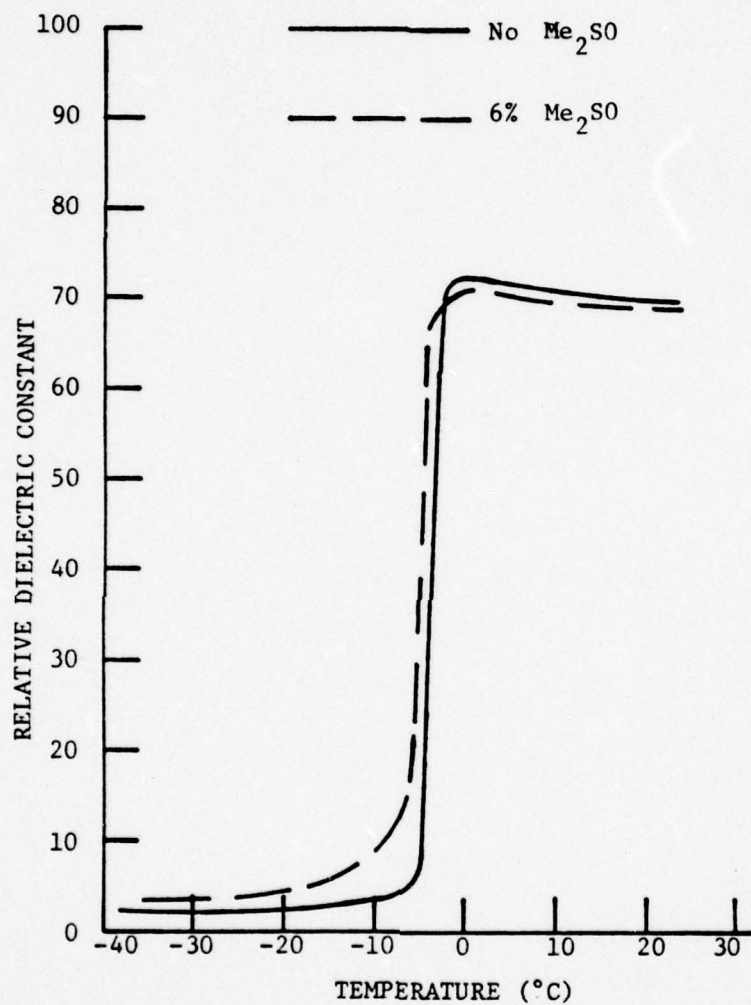


Figure 21. Measured Relative Dielectric Constant of Human Platelets in 20% Plasma-RCD.

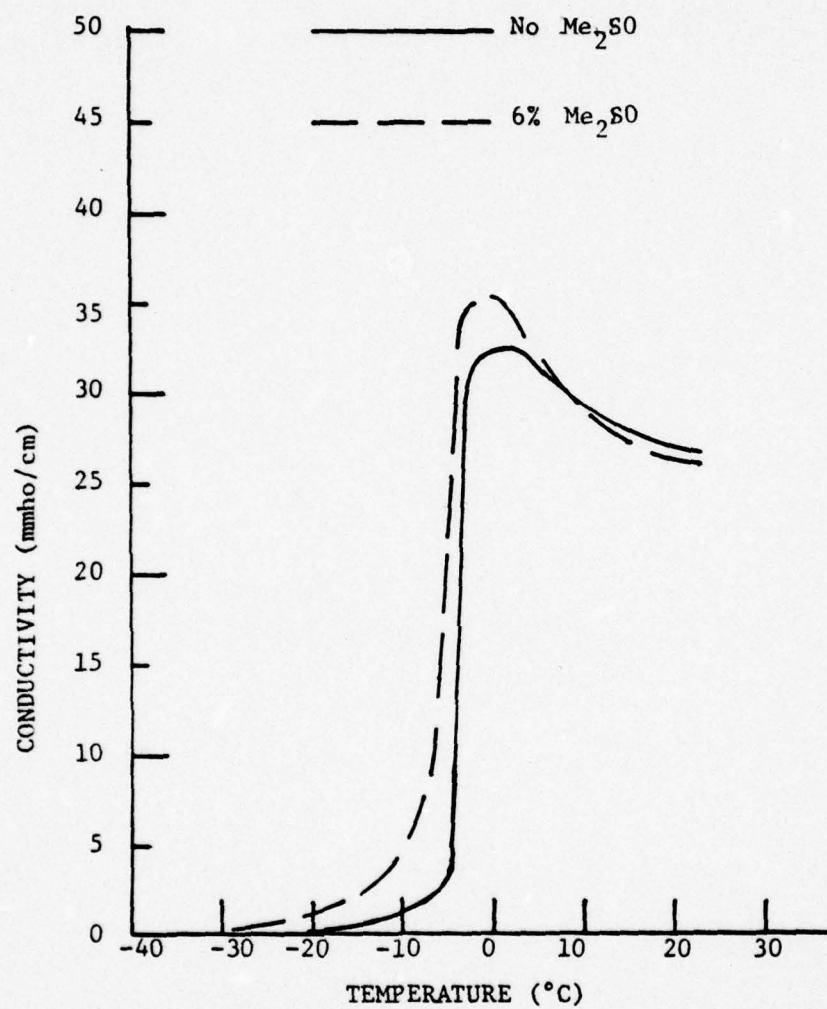


Figure 22. Measured Conductivity of Human Platelets in 20% Plasma-RCD.

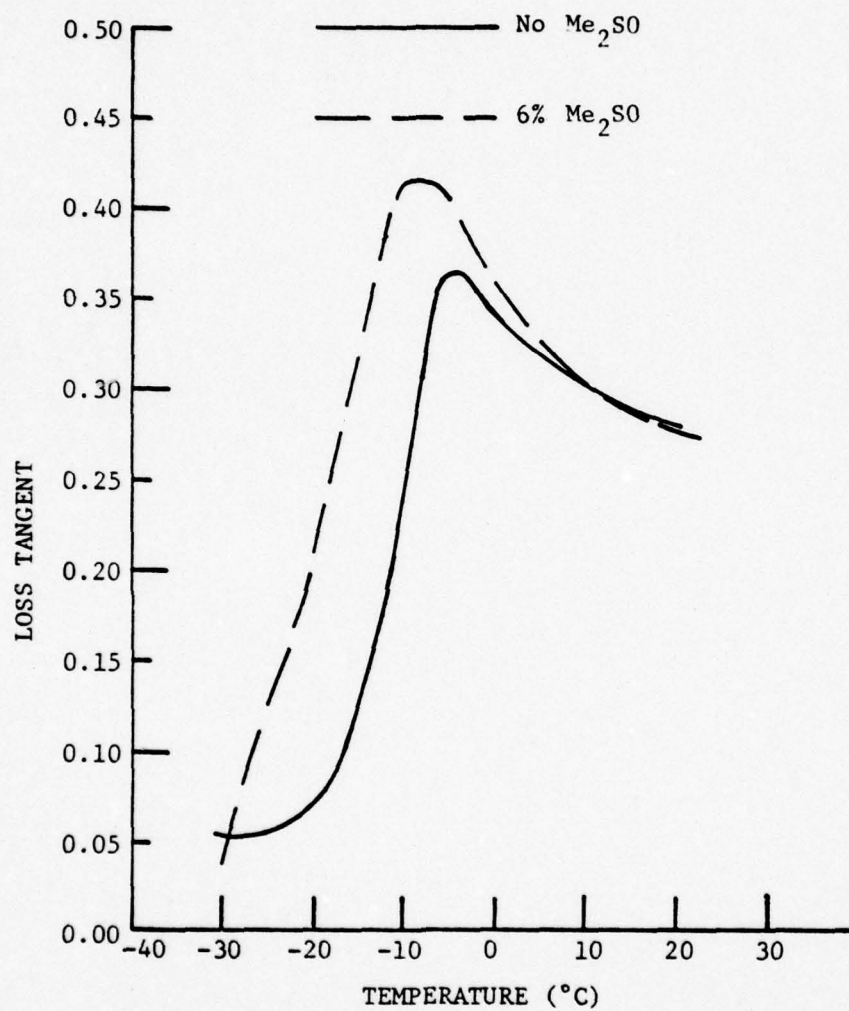


Figure 23. Loss Tangent of Human Platelets in 20% Plasma-RCD.

The dielectric properties of rat granulocytes in an equal concentration of gelatin suspension have been determined as a function of temperature both alone and in combination with a cryoprotectant concentration of 6% Me_2SO . Similar measurements have also been performed for human granulocytes in a medium containing autologous serum, 0.02 ml of 10,000-unit Heparin, 0.1 ml of 10% EDTA, and 10 mg Cortisol both with and without Me_2SO . These measurements were performed as part of a research effort to develop effective EM illumination systems for rapid, uniform thawing of cryopreserved granulocytes. The measurements were performed using short-circuited transmission line techniques and using the hermetically-sealed infinitesimal monopole probe. These results have been reported previously [32,33] and will not be repeated here.

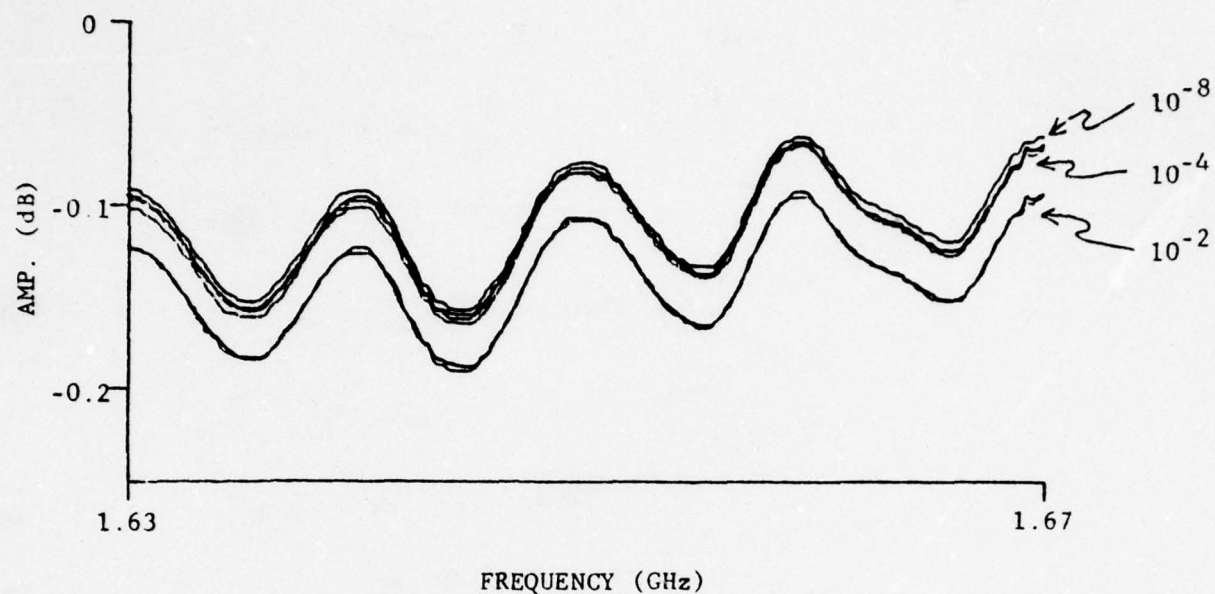
Probe measurements of the dielectric properties of both frozen and thawed kidney tissue perfused with a $\text{K}^+-\text{Mg}^{++}$ rich perfusate containing different concentrations of the cryoprotectant drug Me_2SO indicate that the presence of drugs containing polar molecules significantly affect the tissue dielectric properties. Results of thawed canine kidney tissue measurements over the 0.1-GHz to 10-GHz frequency range indicate differences in both dielectric constant and conductivity due to the presence of the cryoprotectant drug as listed in Table VI. Measurements of frozen and thawed kidney tissue at 2450 MHz indicate that the cryoprotectant drug has its most significant effect on the conductivity in the frozen state. The conductivity of perfused kidney tissue without Me_2SO is a factor of seven less than that of renal tissue perfused with a 10 percent (1.4 molar) drug concentration, which is approximately 0.07 mmho/cm with Me_2SO . At 2450 MHz, increases as great as 30 percent occur in the relative dielectric constant of frozen kidney tissue perfused with a cryoprotectant drug. Similar effects of Me_2SO on renal tissue were also measured at 918 MHz. However, the magnitude of the effect of 10 percent Me_2SO on the conductivity of frozen canine kidney tissue at 918 MHz was noticeably reduced, with approximately a factor of three increase being measured.

TABLE VI
SUMMARY OF Me₂SO EFFECTS ON THE DIELECTRIC
CHARACTERISTICS OF CANINE KIDNEY CORTEX

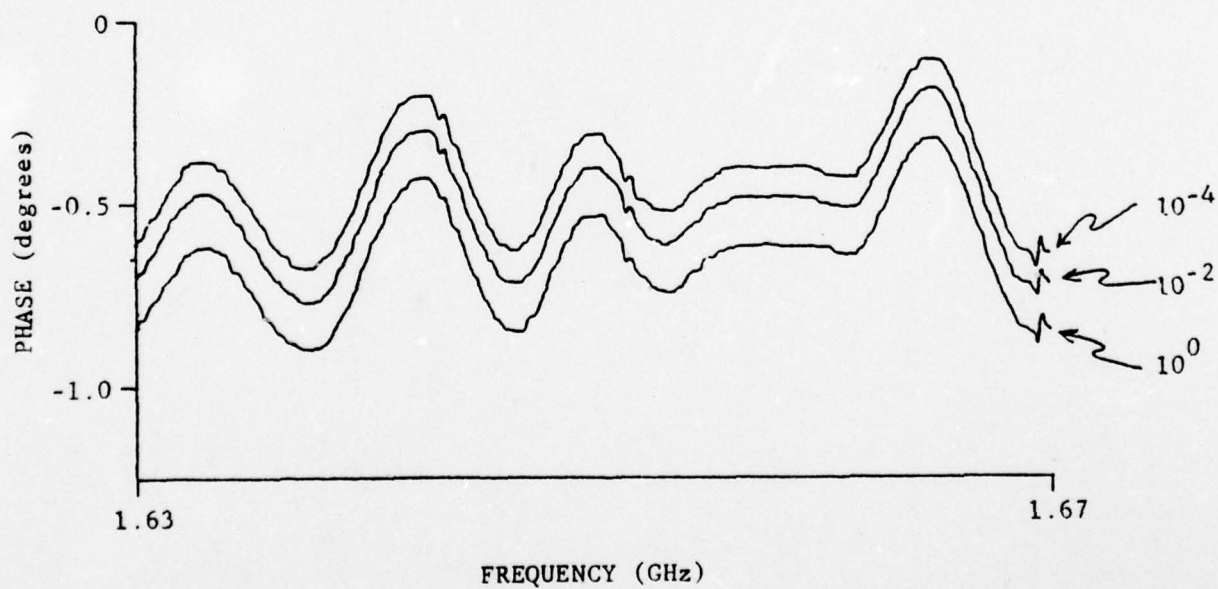
| RELATIVE DIELECTRIC CONSTANT (K') | | |
|-----------------------------------|---------------------------------|----------------------------------|
| F (GHz) | PERFUSED, NO Me ₂ SO | PERFUSED, 10% Me ₂ SO |
| 0.2 | 65.7 | 65.1 |
| 0.4 | 60.0 | 56.9 |
| 0.6 | 53.5 | 58.2 |
| 0.8 | 51.8 | 57.4 |
| 1.0 | 50.6 | 57.0 |
| 2.0 | 47.6 | 58.4 |
| 4.0 | 43.6 | 48.9 |
| 6.0 | 41.4 | 46.0 |
| 8.0 | 38.9 | 43.3 |
| 10.0 | | |
| CONDUCTIVITY σ (mmho/cm) | | |
| 0.2 | 7.3 | 7.3 |
| 0.4 | 8.0 | 8.0 |
| 0.6 | 8.5 | 9.0 |
| 0.8 | 9.5 | 11.0 |
| 1.0 | 10.7 | 12.0 |
| 2.0 | 15.9 | 19.4 |
| 4.0 | 29.9 | 34.4 |
| 6.0 | 50.3 | 58.4 |
| 8.0 | 75.5 | 91.7 |
| 10.0 | 101.5 | 123.0 |

A limited number of preliminary measurements were also performed to investigate whether the in-vivo probe measurement technique, with the present instrumentation, had the necessary sensitivity to measure extremely small changes in dielectric characteristics of different media. To evaluate the sensitivity of the present probe and associated equipment, measurements of E. coli bacteria of various concentrations in distilled water were performed. Starting with an initial concentration of 10^8 cells/ml of water, serial dilutions were prepared as follows: a 10^0 power dilution had 10^8 cells/ml of water, a 10^{-4} dilution contained 10^4 bacterial cells/ml of water, and a 10^{-8} dilution contained no bacteria. Measurements were performed using a 0.22-cm diameter infinitesimal probe over several narrow swept frequency bands, and the results of the 1.63 to 1.67-GHz band and the 3.98 to 4.00-GHz band are presented in Figures 24 and 25, respectively. Shown in these figures are unprocessed reflection coefficient measurements at several different concentrations. Figure 25(b) shows the phase of two serial dilutions relative to pure distilled water. The swept measurements of the 10^{-2} and 10^{-4} dilutions were performed twice as seen in the figure.

Although the measured changes involving the E. coli concentrations are quite small, these differences in the reflection coefficient are discernable as a function of bacterial concentration. Other measurements performed to detect bacterial concentration differences in a complex nutrient media were not as successful, with most measured changes in reflection coefficient being at or slightly above the system noise level. This difference in bacterial concentration detection ability for the two different media is attributed to the fact that the complex media already contained cellular material and bound water, thus making the detection of another cellular substance more difficult. On the other hand, the distilled water medium contained only the bacteria. It may well be possible to improve the detection of foreign material in known media (or to detect configurational changes in biochemical compounds which result in an alteration of the dipole moment of the

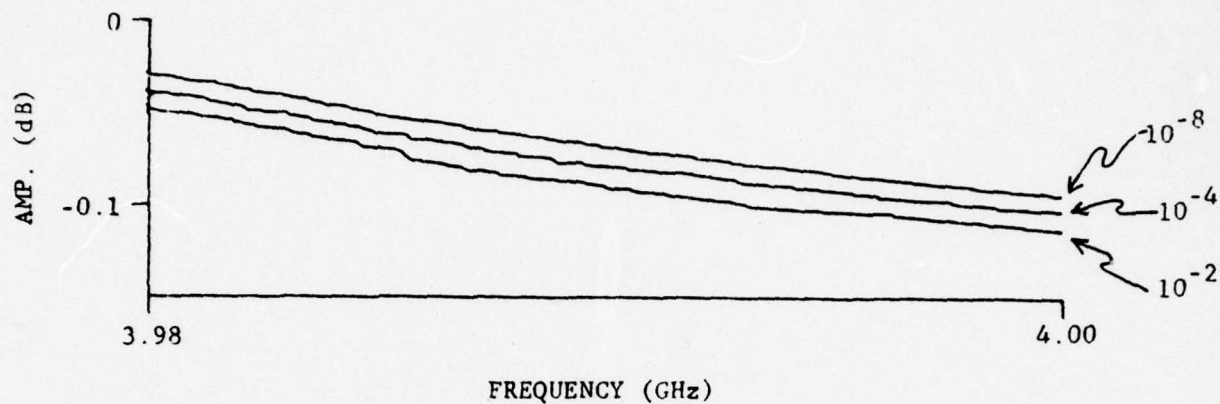


(a) Amplitude

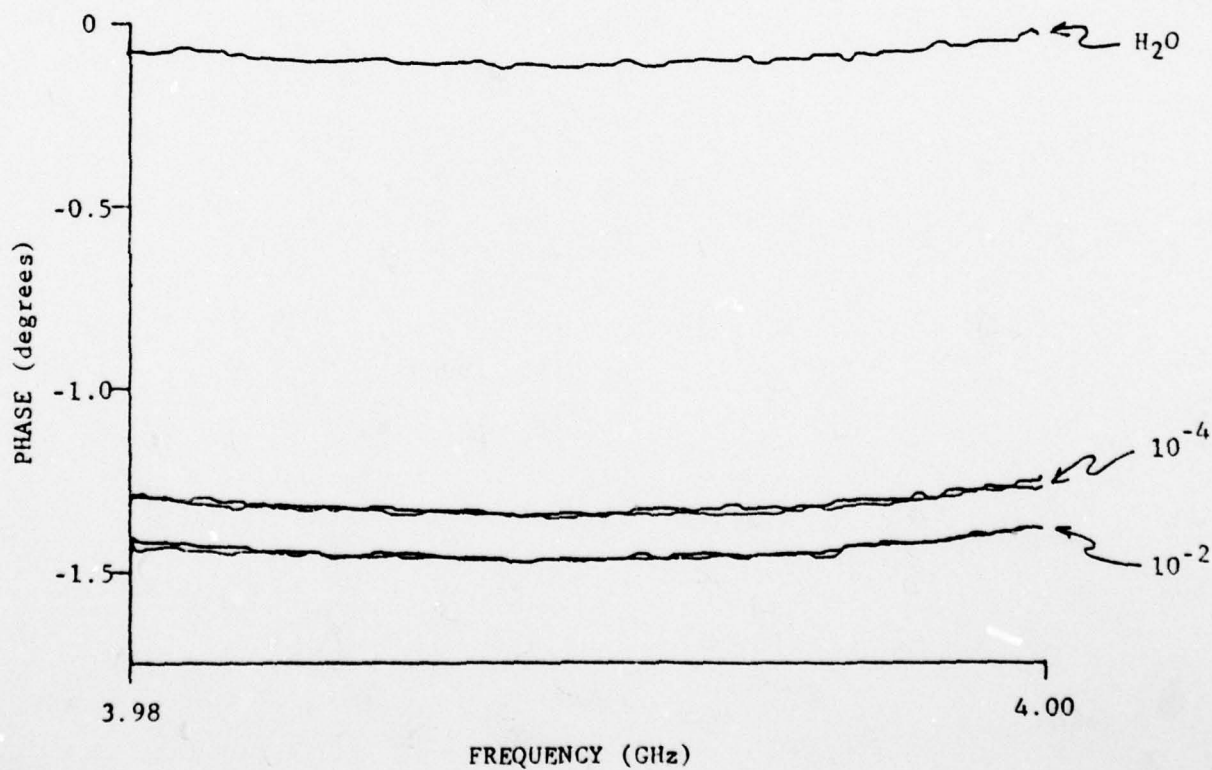


(b) Phase

Figure 24. Measured reflection coefficient, (a) amplitude and (b) phase, of serially diluted concentrations of *E. coli* bacteria in distilled water over the 1.63 - 1.67 GHz frequency range.



(a) Amplitude



(b) Phase

Figure 25. Measured reflection coefficient, (a) amplitude and (b) phase, of serially diluted concentrations of *E. coli* bacteria in distilled water over the 3.98 - 4.00 GHz frequency range.

compound) by further developing the data processing techniques. Methods such as data integration, spectral analysis, and auto- and cross-correlation computation could be used to further improve the signal-to-noise ratio of the network analyzer measurement system.

C. Summary of In-Vivo Tissue Measurements

In this subsection, the results of the various in-vivo tissue dielectric measurements performed during the period of this grant are summarized. Many of the results of in-vivo measurements of dog and rat tissues are presented in detail in the second Annual Technical Report [2]. The data presented here are a composite of measured data accumulated during Phases II and III of this research program. These data include results of (1) canine muscle, fat, and kidney measurements and (2) rat muscle, brain, and whole blood measurements.

A number of factors have been identified which affect the accuracy and repeatability of in-vivo tissue dielectric measurements. The most significant of these factors are associated with tissue/probe contact. Two additional factors which were found to influence the results obtained from in-vivo tissue measurements were temperature and probe positioning. All of the factors identified during this research which affect the accuracy and/or repeatability of the in-vivo are listed below:

- (1) tissue dehydration at the measurement area resulting in actual changes in tissue properties,
- (2) accumulation of dried tissue fluids on the contact surface of the in-vivo probe which effectively insulate the probe from the tissue,
- (3) probe contact pressure variations,
- (4) improper positioning of the probe on the tissue resulting in poor repeatability,
- (5) changes in tissue temperature resulting in small changes in dielectric properties, and
- (6) actual tissue inhomogeneity in the measurement area.

Steps were taken to minimize each of the above factors which constitute potential error sources during the performance of the in-vivo dielectric measurements. Tissue dehydration was minimized in the rat

muscle measurements by covering the measurement area with the skin tissue which had been surgically removed. A similar technique was used for the canine muscle tissue measurements. Tissue dehydration during in-vivo measurements performed within the chest cavity of the dog was insignificant; also the chest cavity was covered between measurements. Dried fluid accumulation at the tip of the measurement probe was prevented by thoroughly cleansing the probe following each measurement sequence. The probe was dipped in metal cleaner and then wiped thoroughly with methanol. Probe contact pressure variations were not a problem so long as complete contact was maintained between the surface of the probe and the tissue. The measured reflection coefficient data were, however, quite sensitive to positioning of the probe on the tissue under study. Changes as great as 20 percent were observed measurements of the same tissue if care was not taken to position the probe in the exact same measurement location for each measurement repetition. Temperature of the tissues was monitored using a miniature thermistor probe placed on the tissue in an area adjacent to the measurement area, but not close enough to be within the fringing field of the dielectric measurement probe. When a decrease in body temperature due to the anesthesia was great enough to be of consequence in the tissue measurement region, the heat from a laboratory lamp was used to maintain the tissue being measured at a constant temperature. Finally, during in-vivo measurements it is important to select a measurement area of all one tissue type in order to avoid variations in the measured results due to inhomogeneity of the sample.

The results of all the in-vivo canine and rat tissue measurements are summarized in Figures 26 to 31. The relative dielectric constant and conductivity of in-vivo rat and canine muscle tissue compared to in-vitro muscle data from Schwan [34] in Figures 26 and 27. The uncertainty in the measured data is expressed as the standard-error-of-the-mean (SEM) and is indicated in the figures by the error bars. The differences in the in-vivo experimental data are attributed both to the actual differences which could exist between the

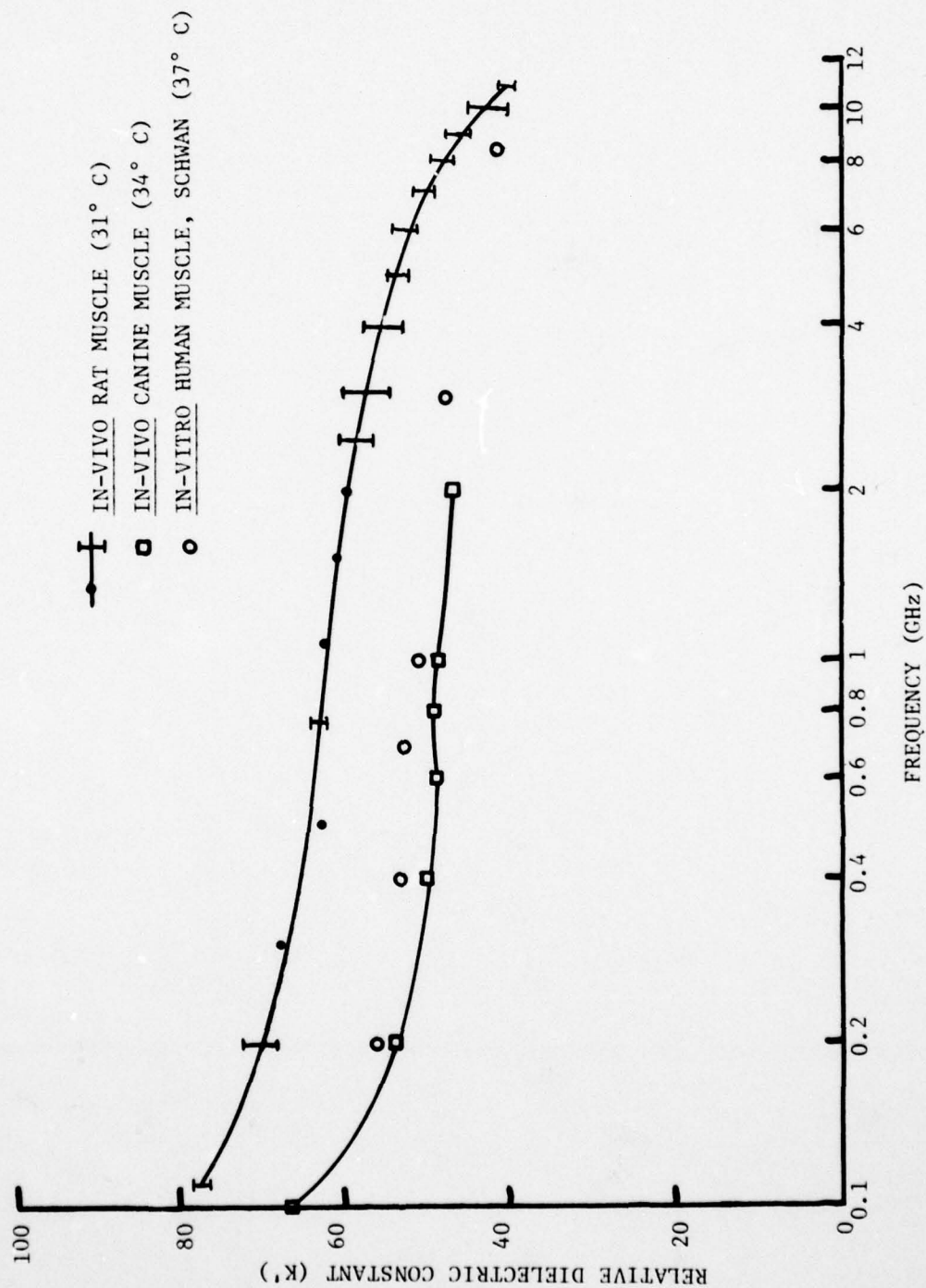


Figure 26. Experimentally determined relative dielectric constant of in-vivo rat muscle and canine muscle compared to reference data [34].

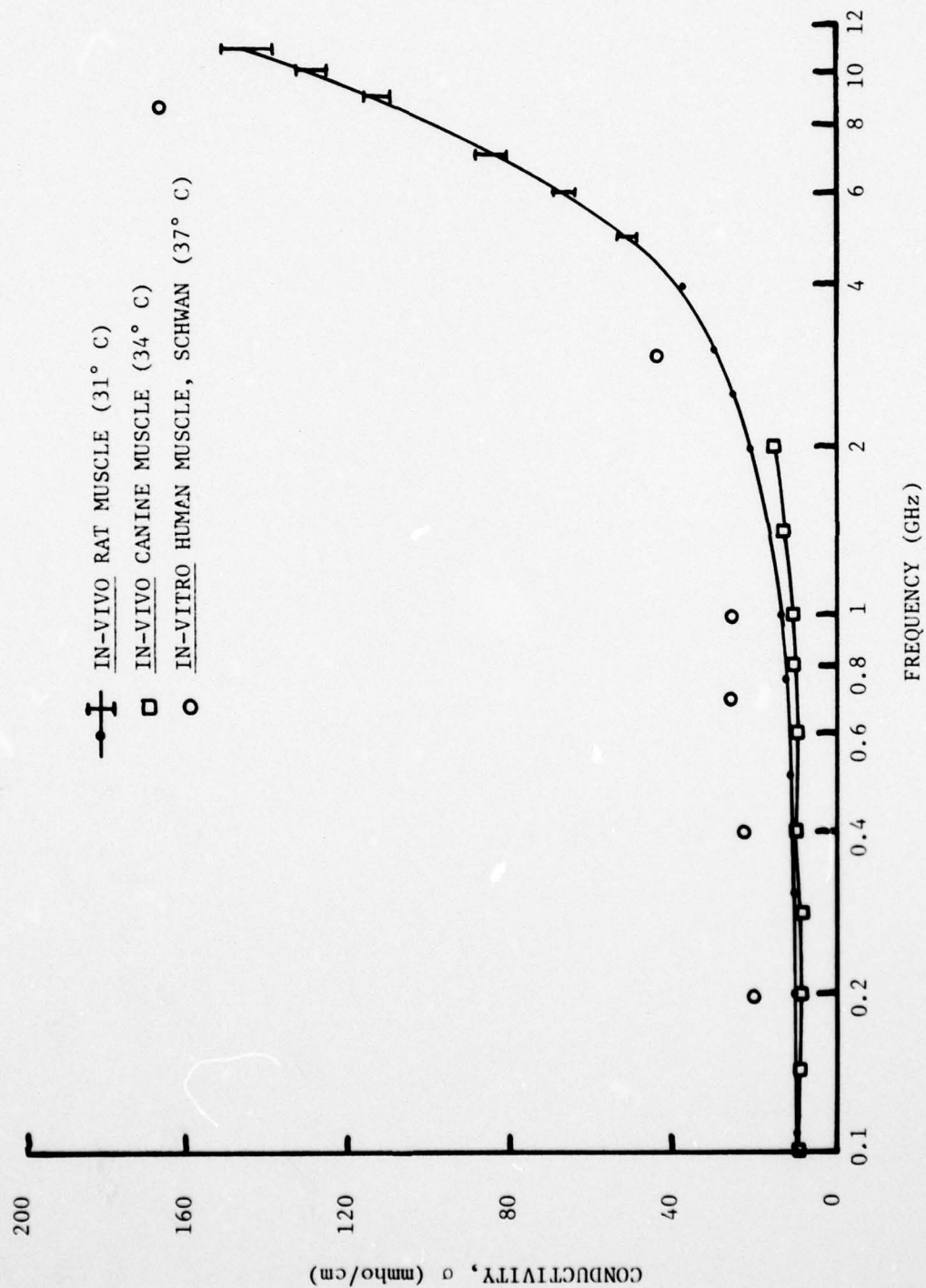


Figure 27. Experimentally determined conductivity of in-vivo rat muscle and canine muscle compared to reference data [34].

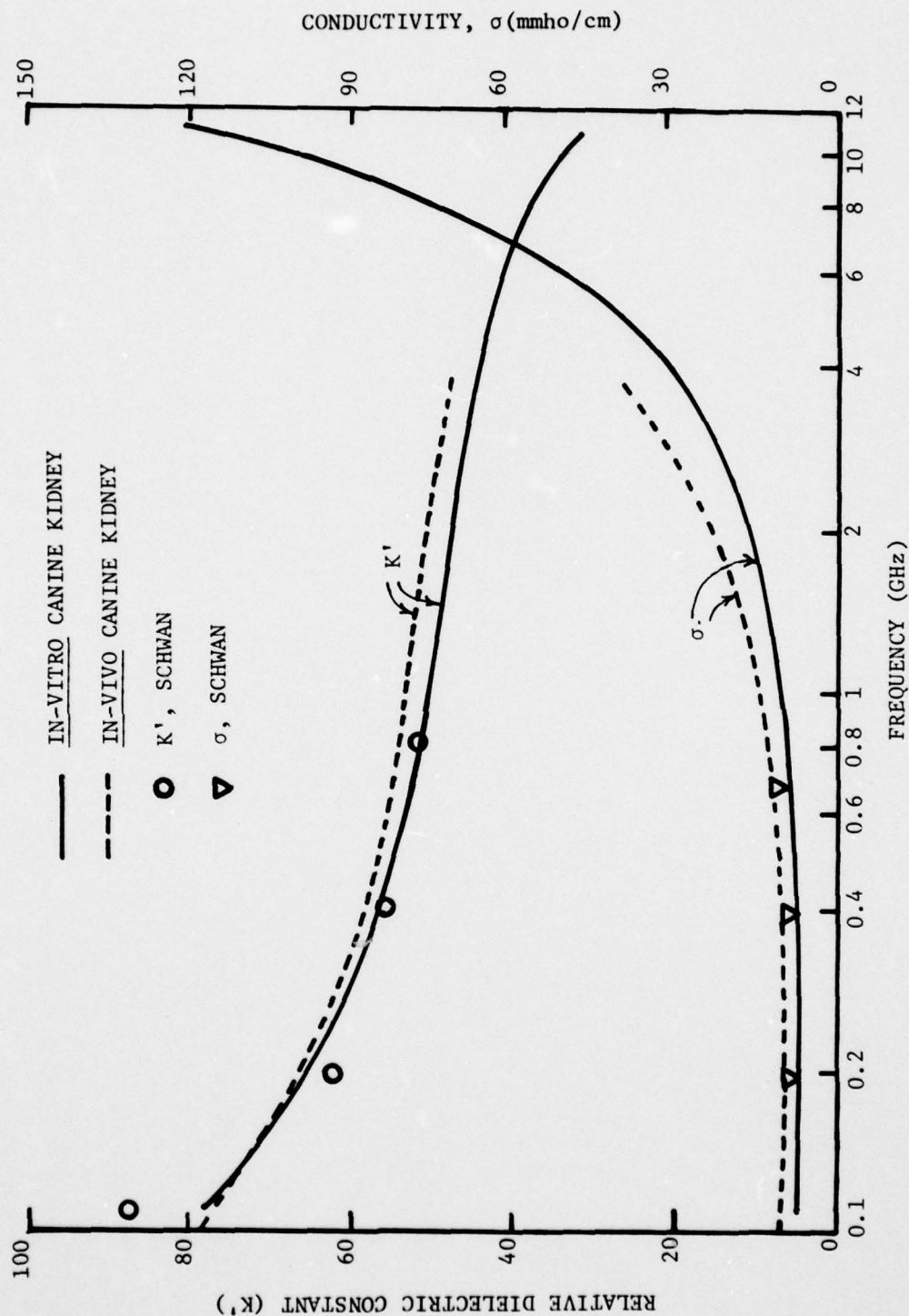


Figure 28. Experimentally determined relative dielectric constant and conductivity of in-vivo and in-vitro canine kidney cortex compared to reference data [34].

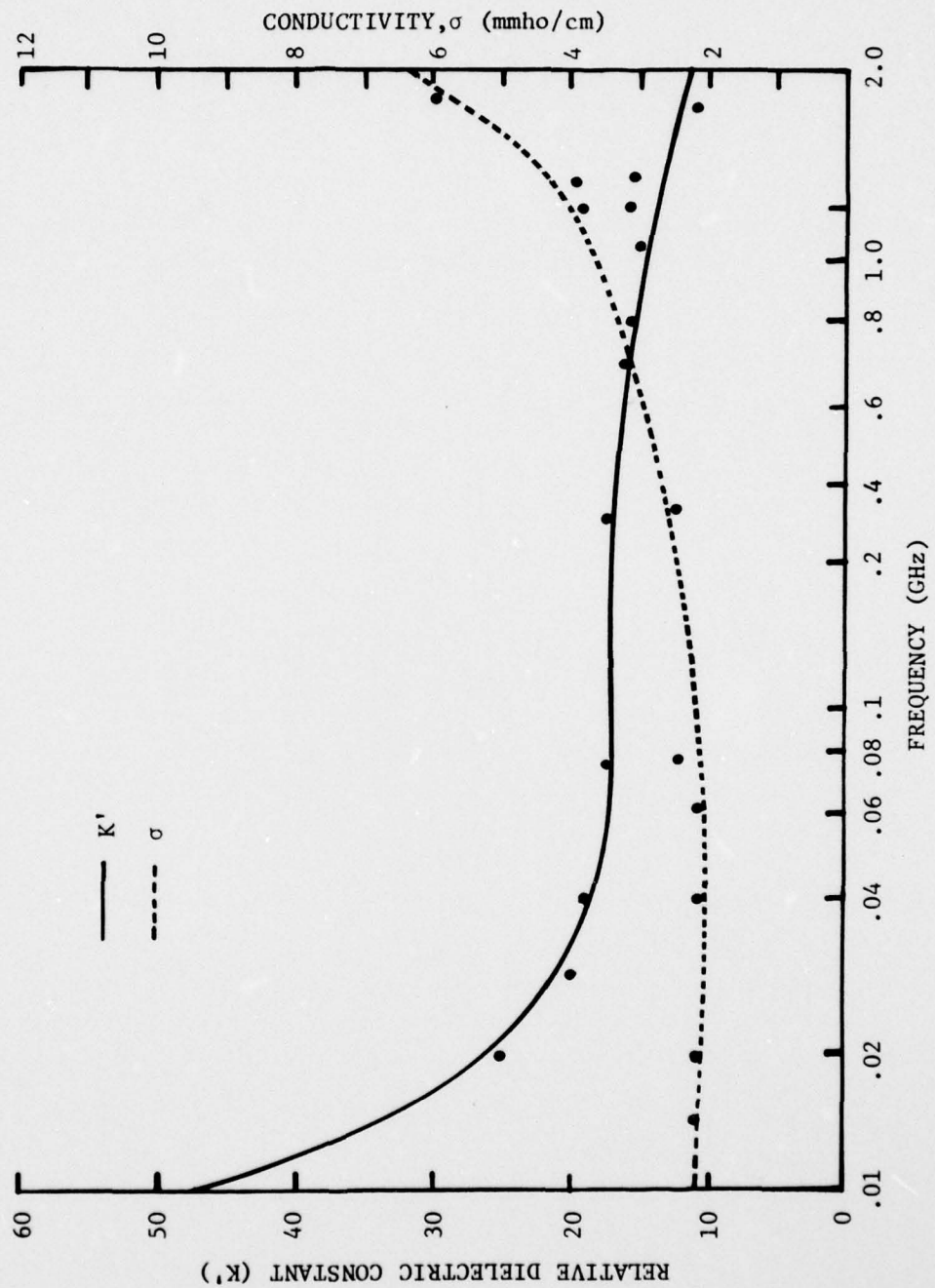


Figure 29. Experimentally determined relative dielectric constant and conductivity of *in-vivo* canine fat tissue at 37°C.

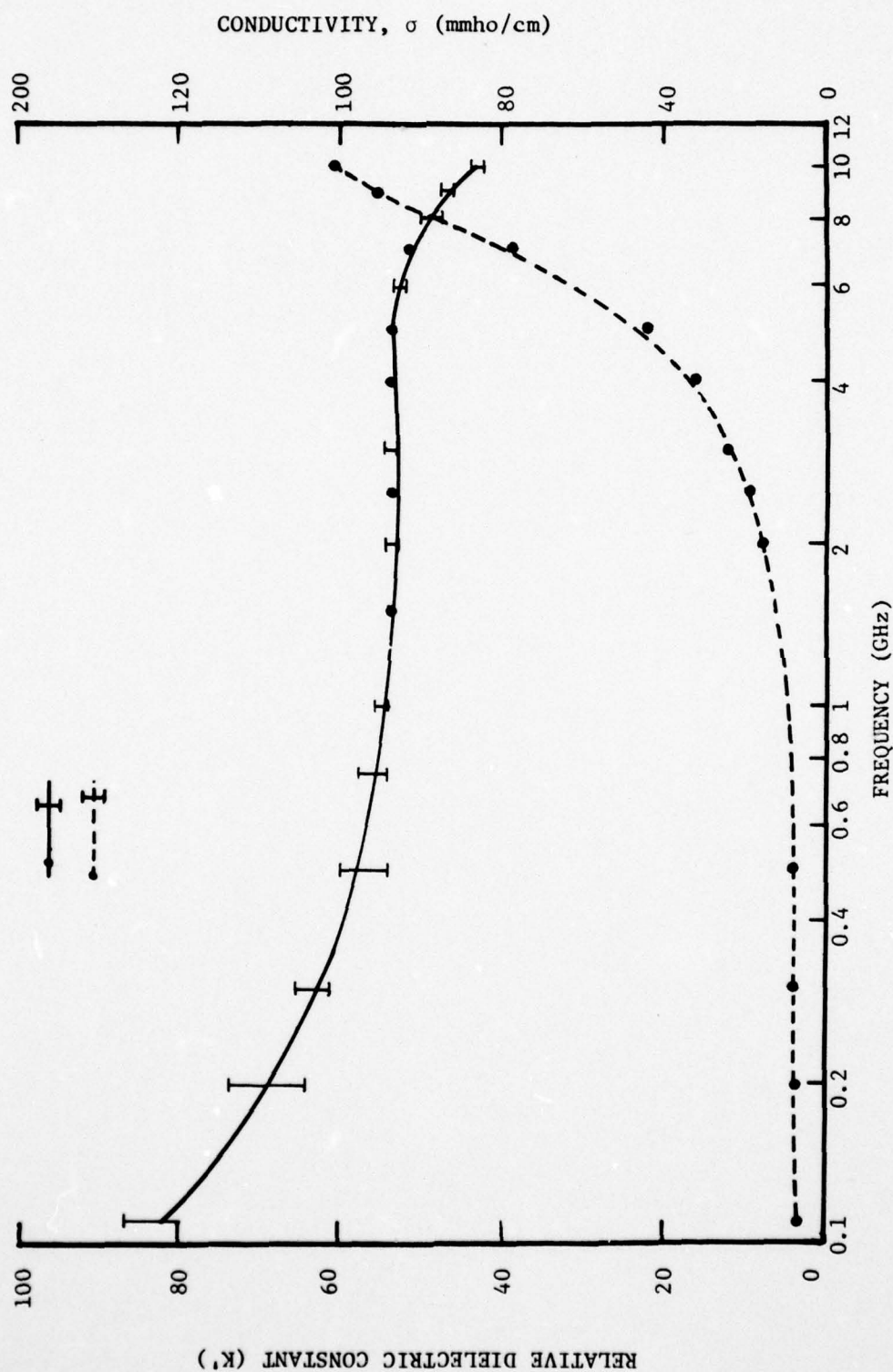


Figure 30. Experimentally determined relative dielectric constant and conductivity of *in-vivo* rat brain at 32°C.

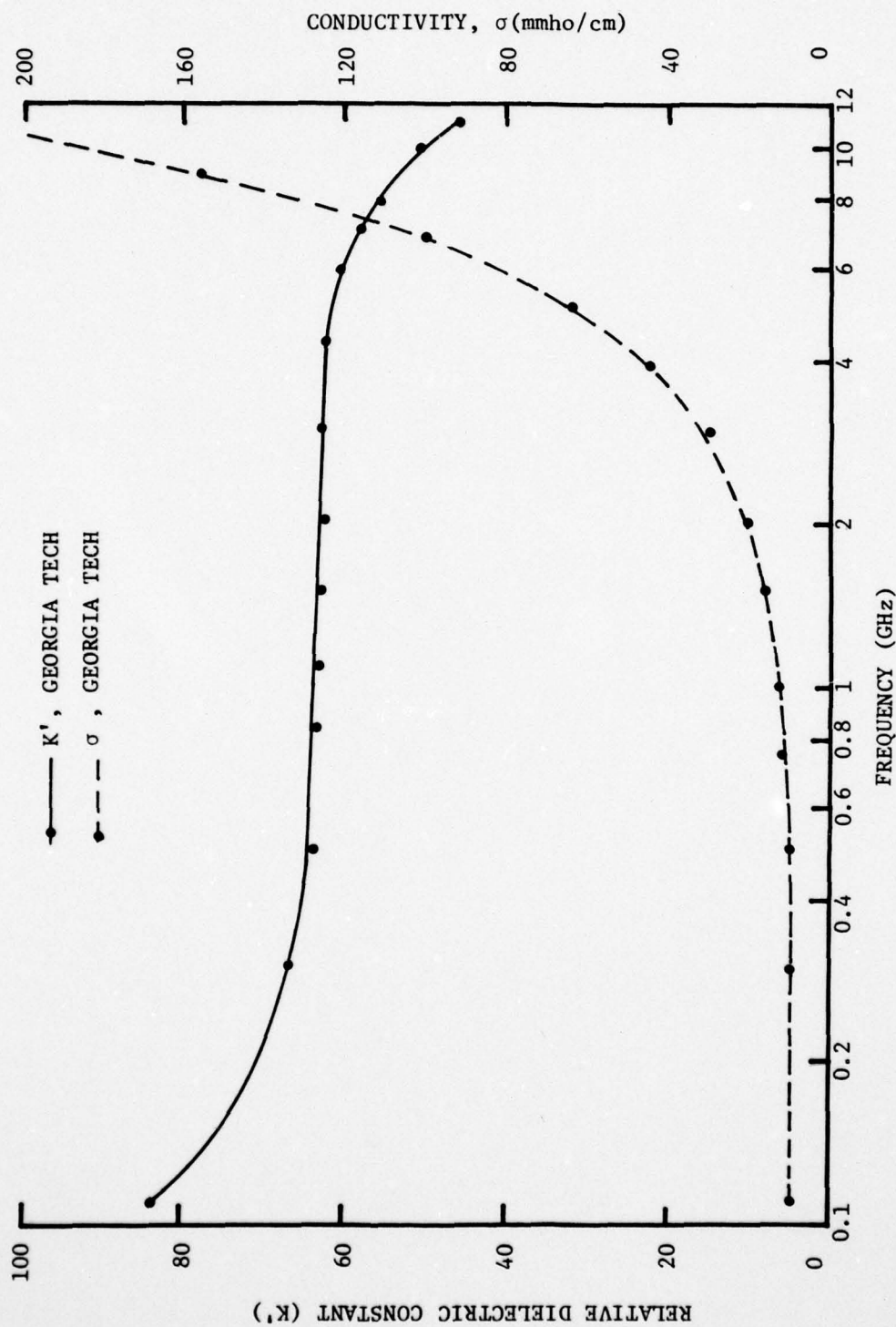


Figure 31. Experimentally determined relative dielectric constant and conductivity of rat blood at 23°C.

different tissue samples and to the difference in tissue sample temperature. The differences in the results of the in-vitro measurements of human autopsy material and the in-vivo results could be due to water content, temperature, or actual physiological differences which may exist between in-situ and in-vitro tissues. Measurement results of in-vivo and in-vitro canine kidney cortical tissue are presented in Figure 28. Again, these results are compared to in-vitro data from Schwan. Note that although the in-vitro data obtained from probe measurements are in close agreement with Schwan's data, the in-vivo data are different from both sets of in-vitro data. The results of measurements performed on canine fat, rat brain, and rat blood are shown in Figures 29, 30, and 31, respectively. The canine fat tissue measurements are compared to results for low water content tissues reported by Johnson and Guy [8].

The in-vivo tissue measurements performed during the course of this research program have provided informative results which point toward the need for further and more extensive investigations of the factors which affect the dielectric properties of biomaterials. Of particular interest is the quantization of the observed differences, although small, between the dielectric characteristics of living and dead tissues. Further research is needed to determine if a physiological basis for measured differences exists and whether that basis could possibly be manifested in the tissue dielectric characteristics. Further improvements in the probe measurement technique are needed to improve its sensitivity and reduce measurement variability. Many of these improvements would simply be associated with the measurement protocol itself, while others would require additional development. Once the necessary improvements are implemented, many questions concerning biomaterial dielectric property differences and changes could be answered more fully.

SECTION V

CONCLUSIONS

The research efforts performed during this three-phase program have been successfully completed. Two different in-vivo probe techniques and their associated instrumentation were studied, the accuracy and repeatability of these techniques were evaluated, and a semi-automated data acquisition/data processing system was developed. One technique considered involved needle-like monopole probes of different lengths, and the second technique involved a dual-probe (two closely-spaced probes with extended center conductors) configuration.

An infinitesimal monopole measurement probe was developed which is capable of accurately measuring the dielectric properties measurements of small sample volumes ($\approx 0.2 \text{ cm}^3$) over a frequency range extending from below 0.1 GHz to above 10 GHz. A number of infinitesimal monopole probes, both with and without small circular ground planes attached, was fabricated and experimentally evaluated. These included 0.41-cm, 0.22-cm, and 0.11-cm diameter probes. Of these, the 0.22-cm diameter probes were most extensively studied and were found to yield accurate results from 0.1 GHz to above 10GHz. The probe's measurement accuracy was determined through measurements of standard liquid dielectric materials including deionized water, methanol, ethylene glycol, 0.1 molar saline, and 0.3 molar saline. Although accurate results were obtained up to above 10 GHz, it may be possible to extend the upper frequency bound even further by including a real term in the antenna impedance expression to account for the increasing radiation conductance of the probe with increasing frequency and by accounting for transmission line losses.

In-vivo dielectric property measurements were made on a number of tissue types in dogs, rats, and mice. The types of tissues measured were canine muscle, canine kidney, canine fat, rat muscle, rat blood, rat brain, and mouse muscle. Additionally, measurements addressing the effects of temperature and drugs on dielectric properties were

performed. Specifically, the effects of dimethylsulfoxide (Me_2SO) on the dielectric properties and on the phase-transition temperature of canine kidney tissue, human and rat platelets, and human and rat granulocytes were investigated. The presence of 1.4 M Me_2SO increases the conductivity of kidney tissue significantly and lowers the phase-transition temperature of both kidney tissue and platelets. The in-vivo dielectric data compiled during the course of this research program represent, in many cases, the only in-vivo dielectric information in existence on many of these tissues.

The investigations of the monopole probe measurement technique also showed that a number of factors influence the measurement accuracy at microwave frequencies. The primary factors are systemic microwave measurement errors and sample preparation/probe positioning. Systemic measurement errors include directivity, source match, and frequency tracking errors. In order to minimize these errors, the measurement instrumentation was upgraded in such areas as improved coupler directivity in the reflectometer and improved cables. Also, a measurement error correction model was developed which permitted calibration of the system using known terminations (short circuit, open circuit, and matched loads). The error model thus permitted compensation for the remaining systemic measurement errors. An ability to perform swept frequency measurements was also developed which made it possible to obtain continuous dielectric property information as a function of frequency.

During the third phase of these research investigations, a semi-automated data acquisition/data processing (SDADP) system was developed which permitted rapid and accurate data acquisition and computation of the dielectric properties. The SDADP system significantly increased the overall capability of the probe technique by significantly reducing the human involvement in the measurement process, and therefore, the possibility of error associated with reading the data manually from recordings and typing the data into the computer. Previously, measurements were repeated and rechecked to reduce the possibility of human error. Presently, the data acquisition and data processing time

are greatly reduced because of the microprocessor-based data acquisition system reads the data, corrects the measured data, and computes the dielectric properties. All of these tasks are performed in a manner of seconds as opposed to hours when done manually.

The dual probe measurement technique considered during the Phase I investigations utilizes two very closely-spaced, needle-like probes. One of the probes transmits a very low power signal while the other probe acts as a tightly-coupled receiving antenna. One dual-probe has been designed, fabricated, and tested in the microwave frequency range. Results of measurements performed in the 2.5 to 3.0-GHz range indicate that the technique is useful for performing microwave dielectric measurements. However, the inherent accuracy of this technique may not be as good as that of the monopole probe. Although an alternate measurement technique to the monopole probe is not needed to perform accurate tissue dielectric measurements, it may still be useful to further investigate the dual-probe technique because this technique may be well-suited for direct measurement of power absorption.

The in-vivo dielectric property measurement system (infinitesimal monopole probe, measurement instrumentation, and SDADP system), measurement procedures, and data presented in this report represent an important advancement in the ability to define the dielectric characteristics of living tissue. The most significant advantages of the in-vivo probe technique over any heretofore available dielectric property measurement techniques are (1) the ability to perform measurements in-vivo for a wide range of sample volumes, (2) the ability to obtain continuous electrical property data over a wide range of frequencies (0.1 GHz - 10 GHz) via swept frequency measurements, (3) the capability to perform measurements very rapidly, and (4) a very simple and flexible measurement procedure with respect to other techniques. With development of data recording and processing techniques, this ability to accurately determine the dielectric properties of tissues in-vivo has lead to a capability for determining power absorption in tissues. These capabilities could be used in dosimetry determinations for aiding in the establishment of a radiation level with respect to

AD-A065 164

GEORGIA INST OF TECH ATLANTA ENGINEERING EXPERIMENT --ETC F/G 6/18
IN-VIVO DETERMINATION OF ENERGY ABSORPTION IN BIOLOGICAL TISSUE--ETC(U)
JAN 79 E C BURDETTE, F L CAIN, J SEALS DAAG29-75-G-0182

UNCLASSIFIED

ARO-13231.1-L

NL

2 OF 2
ADA
065164



END
DATE
FILMED

4 - 79
DDC

personnel safety and in the planning of treatments for applications of EM hyperthermia to cancer treatment. Further, this measurement technique represents a potentially useful diagnostic tool for detecting the occurrence of certain physiological processes, for differentiating between normal and diseased tissue, or for elucidating deficits due to drugs.

SECTION VI

RECOMMENDATIONS

The results and conclusions of the investigations performed during this three-phase research program indicate that the further development of the in-vivo electrical property measurement probe would be extremely useful in applications and investigations of EM interaction with living systems. The next logical step forward would be to extend the probe capability to further the state-of-the-art in dielectric property and dosimetry analysis. However, in order to reach these goals, additional research is necessary.

A number of additional tasks needs to be addressed if the full potential of the probe measurement capability is to be realized. Some of the potential applications of the in-vivo measurement probe include establishment of a desperately needed data base, use of these data in scaling both dielectric and physical characteristics of subjects used in radiation hazard research to more accurately relate to the human case, use in designing effective applicators for EM hyperthermia treatment of cancer, and development of this in-vivo measurement technique as a diagnostic tool. An important step toward the realization of these applications would be to perform the following suggested tasks:

- o Study the feasibility of performing in-vivo dielectric measurements on human subjects using the infinitesimal monopole probe,
- o Perform extensive in-vivo electrical property measurements on animal subjects used in radiation hazards studies and on human subjects,
- o Utilize these in-vivo dielectric properties in the development of more accurate methods for dosimetry analysis,
- o Fully develop the dual-probe technique for direct absorption measurements,
- o Further improve the accuracy and sensitivity of the monopole measurement probe for use as a diagnostic tool to measure changes in physiological processes, and
- o Fully document differences between living and non-living tissue dielectric properties.

SECTION VII

REFERENCES

1. Ecker, H.A., E.C. Burdette, F.L. Cain, and J. Seals, "In-Vivo Determination of Energy Absorption in Biological Tissue," Annual Technical Report, Project A-1755, U.S. Army Research Office Grant No. DAAG29-75-G-0182, July 1976.
2. Cain, F.L., E.C. Burdette, and J. Seals, "In-Vivo Determination of Energy Absorption in Biological Tissue", Annual Technical Report, Project A-1755, U.S. Army Research Office Grant No. DAAG29-75-G-0182, July 1977.
3. Proceedings of the International Symposium on Cancer Therapy by Hypothermia and Radiation, Washington, D.C., April 28-30, 1975 sponsored by the National Cancer Institute, Grant #1 R13 CA 17526.
4. Ecker, H.A., E.C. Burdette, and F.L. Cain, "Simultaneous Microwave and High Frequency Thawing of Cryogenically Preserved Canine Kidneys," Record of the 1976 IEEE International Symposium on Electromagnetic Compatibility, Washington, D.C., July 1976, pp. 226-230.
5. LeVeen, H.H., S. Wapnick, V. Piccone, G. Falk, and N. Ahmed, "Tumor Eradication by Radiofrequency Therapy: Response in 21 Patients," JAMA, Vol. 235, No. 20, May 17, pp. 2198-2200.
6. Burdette, E.C., and A.M. Karow, "Kidney Model for Study of Electromagnetic Thawing," Cryobiology - International Journal of Low Temperature Biology and Medicine, Vol. 15, No. 2, April 1978, pp. 142-151.
7. Burns, C.P., E.C. Burdette, and V.P. Popovic, "Electromagnetic Thawing of Frozen Granulocytes," Proceedings of the Microwave Power Symposium, 1975, pp. 30-36.
8. Johnson, C.C., and A.W. Guy, "Nonionizing Electromagnetic Wave Effects in Biological Materials and Systems," Proceedings of the IEEE, Vol. 60, No. 6, June 1972, pp. 694-695.
9. Michaelson, S.M., "Human Exposure to Nonionizing Radiant Energy - Potential Hazards and Safety Standards," Proceedings of the IEEE, Vol. 60, No. 4, April 1972.
10. Burdette, E.C. and M.L. Studwell, "Evaluation of Cryogenic Temperature Sensors for Use in Electromagnetic Fields," Record of 1976 IEEE International Symposium on Electromagnetic Compatibility, Washington, D.C., July 1976.

11. Johnson, C.C., et al., "Liquid Crystal Fiberoptic Temperature Probe for the Measurement of Electromagnetic Power Absorption in Tissue," Digest of the 1974 IEEE MTT International Microwave Symposium, pp. 32-34.
12. Christensen, D.A., "An Optical Etalon Temperature Probe for Biomedical Applications," Proceedings of the 28th Annual Conference on Engineering in Medicine and Biology, Vol. 17, p. 249.
13. Cain, F.L., E.C. Burdette, and J.J. Wang, "Bioengineering - EM Hyperthermia," Final Engineering Report, Project E-200-913, June 1977.
14. Tinga, W.R., and S.O. Nelson, "Dielectric Properties of Materials for Microwave Processing - Tabulated," Journal of Microwave Power, 8(1), 1973, pp. 24-25.
15. Von Hippel, Arthur R., Dielectric Materials and Applications, MIT Press, 1954, pp. 47-122.
16. Von Hippel, Arthur R., Dielectrics and Waves, MIT Press, 1954, pp. 23-91.
17. Spector, William S., Handbook of Biological Data, W.B. Saunders Company, pp. 291.
18. Burns, C.P. and R.L. Magin, "In-Vivo Measurements of Electrical Properties of Biological Tissue," Proceedings of the 1972 Microwave Hazards Measurements and Dosimetry Workshop, June 1972.
19. Tanabe, Eiji and William T. Joines, "A Nondestructive Method for Measuring the Complex Permittivity of Dielectric Materials at Microwave Frequencies Using an Open Line Resonator," IEEE Transactions on Instrumentation and Measurement, Vol. IM-25, No. 3, September 1976, pp. 222-226.
20. Deschamps, Georges A., "Impedance of an Antenna in a Conducting Medium," IRE Transactions on Antennas and Propagation, September 1962, pp. 648-650.
21. Jordon, E.C. and K.G. Balmain, Electromagnetic Waves and Radiating Systems, Prentice-Hall, Inc., Englewood Cliffs, New Jersey, 1968, pp. 323-326.
22. Tai, C.T., "Characteristics of Linear Antenna Elements," Antenna Engineering Handbook, Chapter 3, H. Jasik, Editor, McGraw-Hill, 1961, p.2.
23. Waveguide Handbook, Ed. N. Marcuvitz, Dover Publications, Inc., New York, 1951, pp. 213-216.

24. Brown, George H. and O.M. Woodward, Jr., "Experimentally Determined Impedance Characteristics of Cylindrical Antennas," Proceedings of the IRE, April 1975, pp. 257-262.
25. Semi-Automated Measurements Using the 8410B Microwave Network Analyzer and the 9825A Desk-Top Computer, Hewlett-Packard Application Note 221, March 1977.
26. Burdette, E.C., and J. Seals, "A Technique for Determining the Electrical Properties of Living Tissues at VHF Through Microwave Frequencies," Proceedings of the 1977 IEEE Region Three Conference and Exhibit, April 1977, pp. 120-123.
27. Burdette, E.C., and J. Seals, J.C. Toler, and F.L. Cain, "Preliminary In-Vivo Probe Measurements of Electrical Properties of Tumors in Mice," Digest of the 1977 IEEE MTT-S International Microwave Symposium, San Diego, CA, June 1977, pp. 344-348.
28. Richmond, J.H., "A Reaction Theorem and its Application to Antenna Impedance Calculations," IRE Transactions on Antennas and Propagation, November 1961, pp. 515-520.
29. Buckley, F. and A.A. Maryott, "Tables of Dielectric Dispersion Data for Pure Liquids and Dilute Solutions," National Bureau of Standards Circular 589, November 1958.
30. Cook, H.F., "A Comparison of the Dielectric Behavior of Pure Water and Human Blood at Microwave Frequencies," British Journal of Applied Physics, Vol. 3, August 1952, pp. 249-255.
31. Hasted, J.B., Water: A Comprehensive Treatise (The Physics of Physical Chemistry of Water), Ed., F. Franks, Plenum Press, New York - London, Volume 2, 1972, pp. 255-305.
32. Burdette, E.C., "Freezing and Electromagnetic Thawing of Frozen Granulocytes," Final Technical Report, Project A-1654, NIH Contract No. NO1-HB-42950 to Emory University, P.O. Box 6614, February 1978.
33. Burns, C.P., E.C. Burdette, and V.P. Popovic, "Electromagnetic Thawing of Frozen Granulocytes," Proceedings of the 1975 Microwave Power Symposium, May 1975, pp. 30-35.
34. Schwan, H.P., "Electrical Properties of Tissues and Cells," Advances in Biological and Medical Physics, Vol. V, J.H. Lawrence and C.A. Tobias, Editors, Academic Press, 1964, pp. 291-425.